Bioactive Poly(Lactic-co-Glycolic Acid)-Calcium Phosphate Scaffolds for Bone Tissue Regeneration

Jenni Rebecca Popp

Dissertation Submitted to the Faculty of the
Virginia Polytechnic Institute and State University
In fulfillment of the requirements for the degree of

Doctor of Philosophy
In
Biomedical Engineering

Committee Members:

Aaron S. Goldstein, Co-Chairman
Brian J. Love, Co-Chairman
William R. Huckle
Yong W. Lee
M. Nichole Rylander

March 27, 2009
Blacksburg, Virginia

Keywords: Amorphous Calcium Phosphate, Hydroxyapatite, Osteoblast Differentiation, Zinc, Microspheres

Bioactive Poly(Lactic-co-Glycolic Acid)-Calcium Phosphate Scaffolds for Bone Tissue Regeneration

Jenni R. Popp

Abstract

Bone is currently the second most transplanted tissue, second only to blood. However, significant hurdles including graft supply and implant failure continue to plague researchers and clinicians. Currently, standard clinical procedures include autologous and allogeneic grafting. Autologous grafts may achieve functional repair; yet, they are available in limited supply and are associated with donor site morbidity. Allogeneic grafts are available in greater supply, but have a higher risk of infection. To overcome the disadvantages of current grafts, tissue engineering has become a major focus for the regeneration of bone. The goal of tissue engineering is to use a multidisciplinary approach to create biomimetic constructs that stimulate osteogenic regeneration to heal bone defects and restore tissue function.

Biodegradable scaffolds are used in tissue engineering strategies as an interim template for tissue regeneration. The scaffold architecture provides mechanical support for cell attachment and tissue regeneration. Biocompatible poly(lactic-co-glycolic acid) (PLGA) has been processed through a number of techniques to create porous 3D architectures. Hydroxyapatite (HAP) and tricalcium phosphate have been used in conjunction with polymer scaffolds due to their osteoconductivity and biocompatibility, but they often lack osteoinductivity and are resistant to biodegradation. Conversely, amorphous calcium phosphate (ACP) is a mineral that solubilizes under aqueous conditions, releasing calcium and phosphate ions, which have been postulated to enhance osteoblast differentiation and mineralization. Controlled dissolution can be achieved by stabilizing ACP with divalent cations such as zinc or copper. Furthermore, incorporation of such osteogenic ACPs within a biodegradable PLGA scaffold could enhance the osteoconductivity of the scaffold while providing calcium and phosphate ions to differentiating osteoprogenitor cells, thereby stimulating osteogenesis when implanted *in vivo*.

In this research, the effect of zinc on the differentiation of osteoprogenitor cells was investigated. Zinc supplementation of the culture media had no stimulatory effect on cell proliferation or differentiation. ACPs were synthesized using zirconium (ZrACP) and zinc (ZnACP) as stabilizers to achieve sustained ion release. Elevated concentrations suggested sustained ion release over the course of 96 hours and enhanced solubility of ZrACP and ZnACP. X-ray diffraction analysis showed a conversion of ZrACP to a semi-crystalline material after 96 hours, but ZnACP showed no conversion after 96 hours.

Composite scaffolds were fabricated by incorporating HAP, zirconium-stabilized ACP (ZrACP), or zinc-stabilized ACP (ZnACP) into a sintered PLGA microsphere matrix and then characterized to determine the effect of the minerals on the *in vitro* differentiation of MC3T3-E1 cells. Scanning electron microscopy revealed a porous microsphere matrix with calcium phosphate powders distributed on the surface of the microspheres. Measurements of mechanical properties indicated that incorporation of 0.5 wt% calcium phosphates resulted in a 30% decrease in compressive modulus. When cells were cultured in the scaffolds, composite ACP scaffolds stimulated proliferation and ALP activity, while HAP scaffolds stimulated osteoblast gene expression. Overall, the results of this work indicate the addition of calcium phosphate minerals to PLGA scaffolds supported cell growth and stimulated osteogenic differentiation, making the scaffolds a promising alternative for bone tissue regeneration.

Acknowledgements

This research would not have been accomplished without the assistance from several individuals at Virginia Tech. First, I would like to thank my advisors, Dr. Brian Love and Dr. Aaron Goldstein, for their support and guidance throughout my graduate career. I am grateful to Dr. Yong Woo Lee for the use of his laboratory equipment and his service on my graduate committee. I am also grateful to Dr. William Huckle for his advice and assistance with quantitative RT-PCR and primer design and his willingness to serve on my graduate committee. I would also like to thank Dr. Nichole Rylander for serving on my graduate committee. I am grateful Stephen McCartney and John McIntosh for their invaluable advice and assistance with scanning electron microscopy.

I am especially grateful to fellow graduate students and labmates Kristin McKeon, Katherine Kavlock, Lindsay Sharp, and Chris Bashur for their support and assistance inside the lab and out. I would like to thank Bryce Whited for taking the time to teach me the nuances of mammalian cell culture and a number of biochemical assays. I would also like to thank Kate Laflin for her enthusiasm and hard work on scaffold fabrication. I would like to thank my family for their endless love, support, and encouragement: Jon and Sandy Bickford, Mike Popp, Casey Popp, and Deane and Loretta Norwood. Most importantly, I am indebted to my fiancé, Jason Franz, for his unconditional love and support throughout the ups and downs of my graduate research. I would like to thank my oldest friend, Kathryn Laustsen, for helping maintain my sanity on a daily basis and for her constant support. Finally, I would like to acknowledge my late grandmother, Eileen Greenwood Popp, for the inspiration to become an engineer and pursue a graduate degree.

This work was funded by the David W. & Lillian Francis Fellowship and the Institute for Critical Technology and Applied Science at Virginia Tech.

Table of Contents

List of Figures

List of Figures, continued

List of Tables

Chapter 1: Introduction

1.1. Clinical Significance

Bone substitutes are a common therapy for the treatment of bone defects that result from trauma, disease, and congenital abnormalities [1]. Bone grafts are commonly required in orthopedic trauma surgery to replace function and facilitate healing of musculoskeletal injuries [2]. In 2005, more than 500,000 bone graft procedures were performed in the United States and greater than 2.2 million worldwide [1].

Three types of commonly used grafts include: autologous, allogeneic, and xenogenic grafts. Autologous grafts are transplanted directly to the wound site from a healthy area of a patient such as the iliac crest, femur, or tibia [3]. Autologous grafts are the current standard for treating bone defects because they provide osteogenic cells as well as osteoconductive and osteoinductive properties needed to facilitate bone healing [4, 5]. Autografts can be harvested from numerous locations including the iliac crest, distal femur, proximal tibia, and distal radius. The iliac crest is the most common source because of the amount of bone available and the relative ease of harvest. However, autografts are not without disadvantages including donor site morbidity at the graft removal site and a limited supply of tissue available for harvest.

Allogeneic grafts are an alternative to autologous grafts and account for approximately one-third of all bone grafts used in North America [2]. Allogeneic grafts are tissue grafts which are taken from a cadaver or a living donor. Therefore, they are available in much higher quantities and they lack the donor site morbidity associated with autologous grafts. However, the use of allogeneic grafts risks bacterial or viral infection. To combat this problem, allogeneic grafts are frequently processed before implantation rather than using fresh allogeneic grafts. As a result of sterilization, allogeneic grafts may lose significant osteoinductive properties [2].

The least common type of bone graft is the xenogenic graft, which is obtained from a non-human species. Xenogenic grafts often have problems with immune rejection and it may be difficult to a find matching donor. However, xenogenic grafts are an excellent source of tissues that are in low supply from human donors.

Tissue engineering aims to overcome the disadvantages of current grafts. Tissue engineered constructs may be created to be available in an off-the-shelf capacity to account for high demand. The incorporation of bioactive factors and osteoprogenitor cells into a synthetic graft has the potential to further accelerate wound healing. Additionally, biodegradable

constructs can be tailored to fit the desired wound, integrate into native tissue and eliminate the need for graft removal or further therapeutic intervention. Therefore, engineered bone tissue has the potential to overcome the disadvantages of current grafts making it an attractive alternative for osseous regeneration. Current challenges in bone tissue engineering are in the development of suitable scaffold materials to improve osteoblast adhesion, proliferation, and differentiation.

1.2. Bone Biology

An overall understanding of bone structure and function is necessary for determining strategies for the regeneration of bone by tissue engineering. Bone tissue performs several basic functions in the body, including soft tissue support and skeletal muscle attachment. Bones such as the ribs and the cranium provide essential protection for vital organs. On the molecular level, calcium and phosphorus homeostasis is maintained by stores within the bone tissue; while bone marrow, within the central cavity of long bones, is a source of blood cell production [6, 7]. A thorough understanding of such functions provides insights into the structure and function of desired graft materials.

1.2.1. Composition, structure, and organization of bone

The extracellular matrix of bone is composed of an organic matrix of collagenous and non-collagenous proteins which is strengthened by a mineralized, inorganic matrix composed of calcium and phosphate in the form of carbonated hydroxyapatite (HAP) [8]. Approximately 60% of bone mass is composed of mineral, 30% collagenous matrix, and 10% water [9]. Collagen is the major component of the bone matrix, composing 95% of the organic portion of the matrix. Minerals accumulate in the spaces between collagen fibers where they crystallize and harden. The salts then deposit and crystallize on the surface of the collagen fibers. This combination of collagen fibers and minerals gives bone its characteristic tensile strength and hardness, respectively. The remaining 5% of the organic matrix is composed of proteoglycans and non-collagenous matrix proteins such as osteocalcin, osteopontin, osteonectin, and bone sialoprotein [6, 7].

Bone tissue is organized into two specific types; each serving a specific function (Fig. 1.1). Cortical (compact) bone provides more effective mechanical support and protection, while trabecular (cancellous) bone is involved in metabolic functions such as calcium homeostasis [10]. Compact bone forms the outer layer of all bones and the majority of the shaft, or diaphysis, of long bones and consists of densely packed collagen fibrils that form concentric lamellae. At

the center of the lamellae is the Haversian canal which contains major blood vessels. Between the lamellae are small spaces containing osteocytes called lacunae. From the lacunae, canaliculi radiate outward in all directions. The canaliculi connect lacunae with one another and the Haversian canals to transport waste, oxygen and nutrients. Each Haversian canal, with its surrounding lamellae, lacunae, osteocytes, and canaliculi, forms an osteon which is about 200 μm in diameter and 10 to 20 mm long [9].

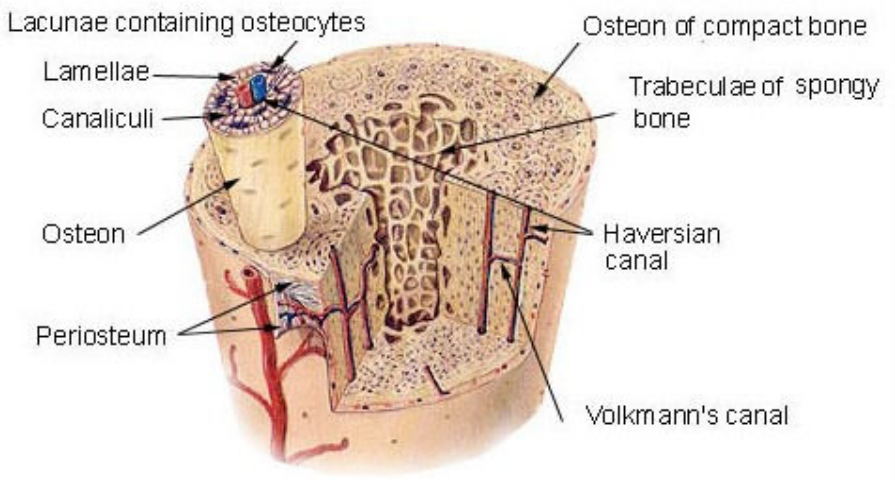

Figure 1.1. Organization of Bone. US National Cancer Institute's Surveillance, Epidemiology, and End Results Program. 2000, Accessed February 27, 2009. http://training.seer.cancer.gov/module_anatomy/images/illu_compact_spongy_bone.jpg [fair use]

Trabecular bone is a more loosely organized, spongy structure. It does not contain osteons like those seen in cortical bone. The bone structure is highly porous, with 75-95% of the bone volume being interconnected pores filled with bone marrow [9]. The lamellae are arranged in a more irregular pattern of thin plates of bone called trabeculae. Similar to compact bone, the trabeculae contain lacunae with radiating canaliculi. Trabecular bone forms the majority of flat and irregularly shaped bones and the ends, or epiphyses, of long bones [7].

1.2.2. Mechanical Properties of Bone

Bone is a heterogeneous tissue and therefore has varying mechanical strengths depending on anatomical location [11, 12]. Furthermore, strength properties vary widely with age and loading direction [13]. The mechanical properties of bone reflect the microstructure of the tissue. Within bone tissue, hydroxyapatite crystals are deposited within an ordered, overlapping

arrangement of collagen fibers [7]. The collagen fibers provide tensile strength, while the hydroxyapatite crystals provide compressive strength.

A review by Athanasiou et al [9] shows that the strength of compact bone varies between the longitudinal and transverse direction. The strength of compact bone in the longitudinal direction has been measured between 78.8 and 151 MPa in tension and between 131 and 224 MPa in compression. However, compact bone is much weaker perpendicular to the long axis (51-56 MPa in tension and 106-133 MPa in compression). Further, the elastic moduli of compact bone, in both tension and compression, are 17-20 GPa in the longitudinal direction and 6-13 GPa in the transverse direction.

In contrast to compact bone, trabecular bone is a highly porous structure without an arrangement of Haversian systems in the longitudinal direction. As a result, trabecular bone does not have the significant strength properties that are characteristic of compact bone. The strength and modulus of trabecular bone range from 2-5 MPa and 90-400 MPa, respectively [9].

1.2.3. Formation of Bone

Bones are formed through two distinct processes of ossification: endochondral ossification and intramembranous ossification. Both processes produce mature bones with similar composition. Both mechanisms involve the replacement of pre-existing connective tissue with bone [7].

1.2.3.1. Endochondral Ossification

Endochondral ossification gives rise to the long bones of the skeleton by a process involving the calcification of cartilage. In this process, mesenchymal cells differentiate into chondroblasts which produce a hyaline cartilage matrix template that is gradually replaced by bone [6, 7]. A membrane called the perichondrium then forms around the cartilage.

In forming long bones, the cartilage model grows in length and thickness by chondrocyte cell division and cartilage matrix deposition. Chondrocytes in the middle of the cartilage template increase in size as the cartilage template grows. Some of the hypertrophied cells burst, releasing their contents and changing the pH of the local environment. This change induces calcification of the cartilage. Calcification reduces the nutrient supply to the chondrocytes causing them to die and leave behind empty lacunae.

During the calcification process, a nutrient artery penetrates the bone, permitting osteoprogenitor cell migration into the perichondrium where they differentiate into osteoblasts. The osteoblasts form a thin layer of compact bone under the perichondrium called the periosteal bone collar. This later becomes the periosteum.

Within the middle of the cartilage template, the periosteal bud, containing osteoblasts, osteoclasts, red bone marrow, and capillaries, develops. The infiltration of the capillaries induces the growth of the primary ossification center; the region where bone will replace most of the cartilage. Osteoblasts then deposit bone matrix over the calcified cartilage to form trabeculae. The ossification center enlarges toward the ends of the bone and osteoclasts resorb the newly formed trabeculae leaving a marrow cavity at the core. The marrow cavity fills with red bone marrow and primary ossification proceeds inward.

The shaft of long bones (diaphysis), initially composed of hyaline cartilage, is gradually replaced with compact bone. When blood vessels enter the end of the long bone (epiphysis), a second ossification center forms. Bone formation at the second ossification center occurs similar to that in the main ossification center. However, the spongy bone is not replaced by compact bone at the site of secondary ossification and hyaline cartilage remains on the surface of the epiphysis to act as the cartilage at the articular surface of the bone. Secondary ossification proceeds outward from the center of the epiphysis toward the outer surface of the bone.

1.2.3.2. Intramembranous Ossification

Intramembranous ossification gives rise to the flat bones of the skeleton such as the cranium. In contrast to endochondral ossification, intramembranous ossification forms bone without a cartilaginous intermediate [6, 7].

Mesenchymal cells are recruited to the site where bone will develop and differentiate into osteoprogenitor cells and then later into osteoblasts. The osteoblasts secrete organic matrix until they are completely encompassed. The osteoblasts undergo another transformation into osteocytes and matrix secretion stops. The osteocytes are now located in the lacunae and extend their processes into canaliculi. Minerals are then deposited within the matrix, which then becomes calcified.

Trabeculae develop as the bone matrix forms. They then fuse with each other to form the latticework of trabecular bone. Vascularized connective tissue, which eventually differentiates into red bone marrow, is contained within the spaces between the trabeculae. Vascularized

mesenchyme condenses on the outside of bone where it eventually forms the periosteum. The surface layers of trabecular bone are eventually replaced with compact bone, but the center remains spongy.

1.2.4. Remodeling of Bone

Numerous cell types are present within bone tissue and work in concert to maintain healthy bone tissue and perform the necessary functions of bone. Four main types of cells responsible for the remodeling of bone are osteoprogenitor cells, osteoblasts, osteoclasts, and osteocytes [6, 7].

Osteoprogenitor cells are unspecialized cells derived from mesenchyme that can differentiate into osteoblasts. They are located inside the periosteum, in the endosteum, and in Haversian canals. Upon fracture, osteoprogenitors are activated to differentiate into osteoblasts that will heal the fracture.

Osteoblasts are the main cell type responsible for forming bone tissue and are derived from mesenchymal stem cells. They are found on the surface of bone and in bone cavities. They express phenotypic markers such as alkaline phosphatase and osteocalcin. As new bone layers are formed by the osteoblast, the cells become trapped and turn into osteocytes.

Osteocytes are the most abundant cell type in bone tissue and are involved in calcium homeostasis [10]. They are derived from osteoblasts and are found in the lacunae of the mineralized matrix [12]. They become encased in the mineralized matrix as bone forms.

Osteoclasts are phagocytic, multinuclear cells derived from hematopoietic stem cells [10] and are responsible for dissolving mineral and degrading the organic matrix of bone. The osteoclasts secrete proteolytic enzymes and several acids to digest or dissolve the organic matrix. The cells also phagocytose small particles of bone matrix and release them into the blood.

Bone remodeling is a life-long, coupled process of bone formation by osteoblasts and bone resorption by osteoclasts. The purpose of the remodeling process is to replace old, brittle bone tissue, with newer and more viable bone tissue. This process is important for the support of dynamically changing loads and the renewal of old, brittle organic matrix. In healthy bone, osteoclasts resorb a small portion of bone and then make way for the osteoblasts to form new bone. The new bone is formed in layers of lamellae to create concentric circles. New bone formation continues until the forming lamellae reach blood vessels contained within the Haversian canals [7].

A delicate balance exists between bone resorption by osteoclasts and bone formation by osteoblasts. When this process becomes uncoupled to favor net bone formation or net bone resorption in disease or with age, bones may become extremely brittle or osteolytic lesions may form. If too much mineral is deposited or too much bone forms, bumps or spurs form that may interfere with joint function [6, 7].

1.2.5. Fracture Healing

The human body undergoes a natural process of osseous repair when a bone is injured. Upon fracture, the blood vessels at the fracture site are also broken. In bone tissue, blood vessels include those of the periosteum, the marrow (medullary) cavity, and the osteons. The blood clots to form a fracture hematoma, halting the flow of blood [14]. As a result, bone and periosteal cells in the area die. Capillaries grow into the hematoma while phagocytes and osteoclasts begin to digest and metabolize damaged tissue. Connective tissue, called granulation tissue, forms in the fracture, and secretes a fluid that kills bacteria while providing a framework for new bone growth. This region is also called a callus region.

Fibroblasts and osteoprogenitor cells begin to invade the granulation tissue. The fibroblasts produce collagen and the osteoprogenitor cells differentiate into chondroblasts where this is no vasculature. The chondroblasts then produce fibrocartilage and transform the granulation tissue into a fibrocartilaginous callus that bridges the bone gap.

Osteoprogenitor cells in the vascularized environment differentiate into osteoblasts and begin to form trabeculae. The trabeculae join the fracture ends and the fibrocartilage is converted to trabecular bone to form a bony callus. Finally, remodeling of the bony callus occurs to remove any dead tissue and compact bone forms on the outer edges of the fracture [7].

1.2.6. Bone Related Diseases

A number of diseases and disorders of bone tissue are related to development, infection, calcium and mineral homeostasis, or the delicate balance between bone formation and bone resorption [15]. Some of these diseases include osteoporosis, osteogenesis imperfecta, Paget's disease, and multiple myeloma.

Osteoporosis is the most common bone disease in adults [7]. In osteoporosis, bone formation is diminished due to an abnormally low osteoblast activity, and more rarely an increase in osteoclast activity. As a result, the organic matrix of bone is severely reduced,

leaving bones extremely brittle. Osteoporosis has multiple common causes including decreased loading of bones over time, malnutrition, and old age.

Osteogenesis imperfecta is a disorder caused by a deficiency in the synthesis of type one collagen [15]. The disease is genetic and is characterized by mutations in the genes that code for the α1 and α2 chains of collagen. The disease can range in severity. Patients with the least severe form of the disease are able to synthesis normal collagen, but in decreased amounts. In the more severe form of the disease the abnormal peptide chains are not able to form the collagen helix resulting in extremely brittle bone.

Paget's disease, like osteoporosis, is related to the process of bone remodeling [6]. However, Paget's disease is characterized by a highly accelerated rate of both resorption and formation which results in irregular hardening and softening of the bones. The net effect of the disease is an increase in bone mass, but the resulting tissue is disordered and mechanically unstable [15].

Multiple myeloma is a cancer of the plasma cells in red bone marrow [6]. In addition to the formation of a tumor cell mass, myeloma usually produces osteolytic lesions and causes severe bone pain [16]. The lesions are caused by an increase in bone resorption due to increased osteoclast formation and activity in the vicinity of myeloma cells [16]. In a histological study comparing multiple myeloma patients with and without osteolytic bone lesions, Bataille et al [17] found that patients with bone lesions had a major uncoupling of the normal bone remodeling process. However, patients without osteolytic bone lesions had balanced bone remodeling with an increase in both bone resorption and formation. Others have shown reductions in markers of bone formation and increases in markers of bone resorption in multiple myeloma patients with bone lesions [18].

1.3. Bone Tissue Engineering Model

Bone injuries that result from trauma, disease, or congenital defects often require surgical intervention to restore normal function. Limitations associated with current bone grafts create a need for a novel source of bone graft. Tissue engineering applies principles of science and engineering to repair tissues, and strategies that have been proposed involve using biomaterials, cells, and growth factors alone or in combination [19]. Strategies aimed at restoring tissue function through tissue engineering include acellular matrices or matrices with cells. Additionally, matrices may or may not contain growth factors or other bioactive molecules to

further accelerate tissue healing. Ultimately, the goal of tissue engineering is to restore function to a damaged tissue by implanting a tissue engineered construct into the defect site that will facilitate the natural healing process. Strategies for tissue regeneration involve: (1) a scaffold for osteoconduction, (2) bioactive molecules for osteoinduction, (3) and osteoprogenitor cells to actively repair the wound site.

The role of the matrix or scaffold is to accelerate bone regeneration by providing an osteoconductive template onto which osteoprogenitor cells can migrate and deposit extracellular matrix. The scaffold should be designed to initially withstand the mechanical load of the surrounding tissue and degrade at a rate that matches the formation of new tissue. Over time, the biodegradable scaffold is envisioned to degrade as osteoprogenitor cells penetrate the scaffold and deposit extracellular matrix. It is envisioned that the newly formed tissue will gradually support the mechanical load of the bone until the scaffold is completely resorbed.

To further enhance healing by the osteoconductive scaffold, osteoinductive factors may be added to the construct. Bone morphogenetic proteins, part of the TGF-β superfamily, are the most commonly studied osteogenic cytokines [20]. Currently, two recombinant human bone morphogenetic proteins (rhBMPs) are available for clinical use in healing bone injuries, rhBMP-2 and rhBMP-7 [2].

Lastly, osteoprogenitor cells can be added to the scaffold and cultured ex vivo before implantation. Osteoprogenitor cells can be derived from heterologous, allogeneic, or autologous tissue and from multiple tissues in the body. Then, under the appropriate conditions, osteoprogenitor cells differentiate into osteoblasts that deposit a mineralized matrix. When the construct is implanted, it is envisioned that native osteoprogenitor cells respond to the secretion of growth factors and are recruited into the graft site.

1.3.1. Osteoprogenitor Cells

The addition of osteoprogenitor cells to an osteoconductive scaffold may increase the osteogenic potential of the scaffold and promote healing. For tissue engineering applications, osteoprogenitor cells should be easily isolated from a plentiful source. The cells should then be capable of expanding in large quantities and differentiating into the osteoblastic lineage.

1.3.1.1. Sources of Osteoprogenitor Cells

Mesenchymal stem cells (MSCs) are multipotent stem cells that are present in many adult tissues and are responsible for the body's ability to naturally remodel and repair damaged tissues [21, 22]. Morphologically, undifferentiated MSCs have a spindle shape that resemble fibroblasts and have the ability to differentiate into multiple lineages, including bone, cartilage, muscle, and fat [23-25]. MSCs have been isolated from numerous tissues including bone marrow, amniotic fluid, muscle, adipose, and synovial tissues and have great potential for tissue engineering strategies [24]. However, some of these sources have inherent disadvantages, including difficulty of extraction, differentiation potential, and loss of stem cells with age. Researchers are continuously searching for additional sources of highly potent stem cells. A few of this stem cell sources are summarized below.

1.3.1.1.1. Bone Marrow Stromal Cells (BMSCs)

The constant remodeling of skeletal tissue suggests the presence of cells that have retained the capacity to proliferate and differentiate within the bone marrow. Several studies have demonstrated the capacity of bone marrow derived stem cells to differentiate into fibroblasts, osteoblasts, chondroblasts, and adipocytes [26, 27]. These multipotent adult stem cells are commonly called bone marrow stromal cells (BMSCs) or bone marrow derived mesenchymal stem cells (BMMSCs).

Bone marrow stromal cells have been isolated from the femurs and tibias of rats [28]. After isolation, the mesenchymal stem cells can be separated from the total stem cell population based on the ability to adhere to tissue culture polystyrene. These stem cells proliferate rapidly and express markers of osteoblast differentiation when cultured in the presence of dexamethasone, ascorbic acid, and β-glycerophosphate.

1.3.1.1.2. Adipose Derived Stem Cells (ADSCs)

Adipose tissue is a highly complex tissue that consists of many types of cells. The stromal-vascular cell fraction of the adipose tissue, obtained after collagenase digestion, has been found to contain multipotent adipose tissue-derived stromal cells [29]. The harvest of adipose tissue is a simple surgical procedure that is often performed for cosmetic purposes. The tissue can be obtained in large quantities by surgical resection, tumescent lipoaspiration, or ultrasound-assisted lipoaspiration. ADSCs can then be easily isolated from the tissue by an enzyme

digestion and have the potential to differentiate into bone, cartilage, tendon, skeletal muscle and fat under the appropriate conditions. In one study, rat ADSCs treated with growth and differentiation factor-5 (GDF-5) demonstrated significantly greater mineralization and expression of Cbfa1, ALP, and OCN genes than untreated controls [30].

In addition, ADSCs maintain differentiation potential after cryopreservation. Therefore, ADSCs represent an ideal source of multipotent stem cells due to the large quantities of adipose tissue available, ease of tissue harvest, and the low potential for donor site morbidity [30, 31]. However, it must be noted that a number of factors, including donor age, type of tissue, location of tissue, and culturing conditions influence the proliferation and differentiation capacity of ADSCs [29].

1.3.1.1.3. Amniotic Fluid Stem Cells(AFSCs)

Cells from amniotic fluid are commonly used for prenatal diagnosis of fetal abnormalities. The population of cells in amniotic fluid is a heterogeneous cell population derived from the developing fetus, even in normal fetal development [32]. Recently, amniotic fluid and the amniotic epithelium have been shown to contain stem cells capable of multilineage differentiation [32, 33]. Tsai et al developed a novel two-stage culture protocol for isolation of multipotent mesenchymal stem cells from human amniotic fluid [33]. The differentiation potential of the AFSCs was shown to include mesodermic (osteogenic, adipogenic) and ectodermic (neuronal differentiation) cell types. In addition, AFSCs expressed Oct-4 mRNA and protein, commonly expressed by embryonic stem cells and embryonic germ cells as well as a number of additional markers associated with mesenchymal or neuronal cells [34]. Furthermore, cells obtained from routine diagnostic amniocentesis were induced to differentiate along six lineages (osteogenic, adipogenic, myogenic, endothelial, neurogenic, and hepatic) comprising all three germ layers. As a result, these studies demonstrated the pluripotent nature of AFSCs and their potential for tissue regeneration.

AFSCs may be an easily obtainable stem cell source, available in significant quantities from normal diagnostic amniocentesis. Although more investigation is necessary for further characterization of AFSCs, they may also be a source of fetal pluripotent stem cells without the ethical concerns associated with human embryonic stem cells.

1.3.1.1.4. Dental Pulp Stem Cells(DPSCs)

Within the center of a tooth is a cavity containing nerves and blood vessels called dental pulp. The pulp is rich in progenitor cells that give rise to odontoblasts and ameloblasts which deposit the mineralized matrices of dentin and enamel, respectively [35]. These progenitor cells, termed dental pulp stem cells (DPSCs), have the ability to regenerate damaged dentin in vivo. Multiple studies have demonstrated that DPSCs isolated from human impacted third molars possess the characteristic stem cell properties such as self renewal and a high proliferation rate [35-38]. In addition, it is thought that dental pulp might be a source of multipotent stem cells, similar to those found in bone marrow [38-41]. Microarray analysis of human DPSCs and BMSCs showed similar gene expression profiles for the two cell types, suggesting that the pathways for bone and tooth development may be similar regardless of their distinct origins during embryogenesis [42]. Laino et al demonstrated that stem cells derived from human exfoliated deciduous teeth are able to develop and mineralized bone-like tissue in vitro as shown by ALP activity, alizarin red S staining, and immunofluorescent staining of bone markers [37]. Papaccio et al demonstrated the ability of cryopreserved DPSCs to retain osteoblast differentiation capacity and form mineralized matrix after long-term cryopreservation [40]. Recently, DPSCs from adult humans have been cultured to express markers of osteogenic differentiation such as bone sialoprotein (BSP), alkaline phosphatase (ALP), and osteocalcin (OCN) [37, 38, 43, 44].

Furthermore, human dental pulp extracts have been cultured in vitro and transplanted into immunocompromised mice using hydroxyapatite/tricalcium phosphate powder as a carrier [45]. After 7 weeks following transplantation, woven bone was observed on the surface of the carrier. Newly formed bone continued to remodel 15 weeks after transplantation, showing osteoblasts lining the bone surfaces and osteocytes trapped within the newly formed bone. DPSCs cultured in vitro expressed mRNA for type I collagen, fibronectin, and osteocalcin, but not dentin sialophosphoprotein, a marker specific to odontoblasts. This *in vitro* profile of the DPSCs, in conjunction with the in vivo assessment of the transplants, demonstrates the ability of the DPSCs to selectively produce bone and not dentin. Therefore, stem cells derived from dental pulp may be an attractive, bankable source for future tissue regeneration [40, 46, 47].

1.3.1.2. Stages of Osteoblast Differentiation

Upon induction, osteoprogenitor cells undergo three distinct stages of osteoblast development and differentiation *in vitro*: proliferation, matrix synthesis and maturation, and matrix mineralization [48-52] (Fig. 1.2). Proliferation of osteoprogenitor cells is characterized by extensive growth, spreading, as well as morphological changes and minimal, early alkaline phosphatase (ALP) expression [49]. During this stage, type I collagen mRNA is highly expressed, paralleling high rate of DNA synthesis. However, the formation of a collagenous extracellular matrix during this time is minimal. Toward the end of the proliferation phase, cell numbers reach a plateau around day 10 or 12 and DNA synthesis subsequently ceases [51].

The proliferation phase is followed by an intermediate phase between days 12 and 18, which is characterized by a decrease in cell proliferation and an increase in ALP gene expression and enzyme activity. An increase in collagen matrix deposition immediately follows the decrease in cell proliferation as well as the appearance of low levels of noncollagenous ECM proteins such as osteocalcin and bone sialoprotein [49].

In the final stage of osteoblast differentiation, between days 16 and 20, type I collagen (COLI) gene expression continues to decline. ALP gene expression and protein activity begin to decline while matrix deposition is maximal. This stage is also characterized by matrix mineralization which is evidenced by an increase in calcium deposition that continues through four weeks of culture to form a bone-like tissue consisting of multilayers of cells in an ordered, mineralized collagen matrix [50, 51]. Upon matrix mineralization and bony nodule formation, an increase and subsequent decrease in ALP activity is followed by the increased expression of osteopontin (OPN), bone sialoprotein (BSP), osteocalcin (OCN) [48].

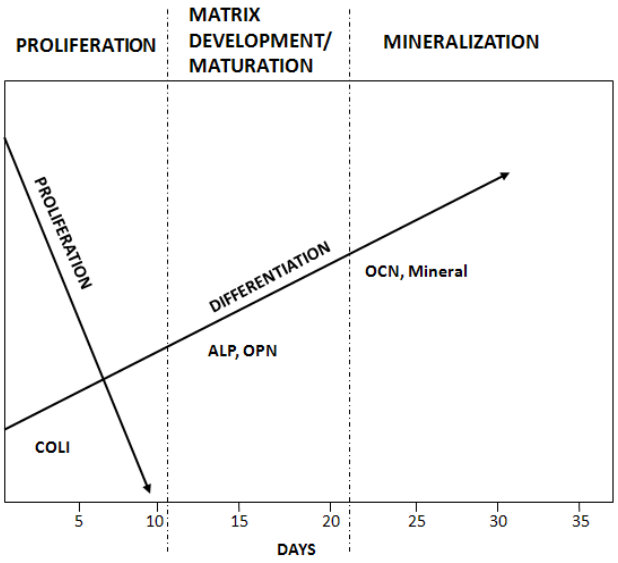

Figure 1.2. Model of the relationship between proliferation and differentiation during rat osteoblast developmental sequence. Redrawn from T. A. Owen, M. Aronow, V. Shalhoub, L. M. Barone, L. Wilming, M. S. Tassinari, M. B. Kennedy, S. Pockwinse, J. B. Lian, and G. S. Stein, "Progressive development of the rat osteoblast phenotype in vitro: reciprocal relationships in expression of genes associated with osteoblast proliferation and differentiation during formation of the bone extracellular matrix," *J Cell Physiol,* vol. 143, pp. 420-30, Jun 1990. [fair use]

Several studies have suggested the importance of collagen for mineralization of the ECM [50, 51]. Collagen deposition in the extracellular matrix is highly dependent on the supplementation of the culture medium with ascorbic acid [50]. Ascorbic acid is required by the cells to hydroxylate proline and lysine residues during collagen synthesis. Rat calvarial osteoblasts cultured in the absence of ascorbic acid were unable to produce a collagenous ECM and mineralization did not occur [51]. When cultured in the presence of 50 µg/mL ascorbic acid, rat calvarial osteoblasts produced both collagenous and mineralized matrix, suggesting both ascorbic acid and a collagen ECM are required for mineralization.

1.3.2. Biomaterial Scaffolds

Biomaterial scaffolds are used in tissue engineering to facilitate tissue regeneration by providing a temporary framework for new tissue growth. Materials are often selected for their biocompatibility and biodegradability which avoids the need for future surgical removal [19]. In addition, materials are often chosen to mimic chemical, morphological, and strength properties of the surrounding tissue.

The architecture of the fabricated scaffold should mimic the natural architecture of the native tissue as closely as possible. The surface of the scaffold must allow for cellular attachment and migration. The scaffold must also contain interconnected pores for cell infiltration, nutrient delivery, and waste removal. Interconnectivity and pore diameter must be sufficient for osteoblast passage. Bone formation requires a minimum pore size of 100 μm, with an optimum pore size of 300 to 500 μm [2, 53].

It is also crucial that the scaffold have sufficient mechanical stiffness to withstand implantation and support integration with the native tissue. Studies have shown that scaffold mechanical stiffness directs the differentiation of stem cells and can be tuned for the desired tissue [54]. Matrices with stiffness resembling brain, muscle, and bone tissue induced differentiation of human MSCs to those lineages, respectively [54].

The surface morphology of materials can have a great effect on the function of osteoblasts. Composite materials of HAP and soluble calcium phosphate with greater roughness than HAP promoted greater MC3T3-E1 cell adhesion [55]. Webster et al investigated the functions of osteoblasts on nanophase (grain sizes less than 100 nm) alumina, titania, and HAP [56]. Osteoblast proliferation, ALP activity, and calcium deposition were significantly greater on nanophase ceramics than conventional ceramics. Further studies were conducted to elucidate the mechanisms of select osteoblast adhesion on nanophase versus conventionally formulated ceramics. It was found that nanophase ceramics adsorbed greater concentrations of vitronectin and conventional ceramics adsorbed greater concentrations of laminin [57]. This correlates with the enhanced adhesion of osteoblasts on nanophase ceramics and of endothelial cells on conventional ceramics [57]. Liu et al investigated the function of osteoblasts on nanophase titania/PLGA composites with nanometer surface roughness [58]. Sonication was used to alter the dispersion of titania in the PLGA and control the surface roughness of the composite. Composites with nanometer roughness had greater cell density, collagen content, ALP activity, and calcium deposition than smoother surfaces [58].

Two major classes of materials used for tissue engineering are natural biomaterials and synthetic biomaterials. Natural biomaterials include organic materials such as collagen, fibrin, hyaluronic acid, and calcium phosphates derived from coral. Synthetic biomaterials include polymers such as polyglycolic acid, polylactic acid, polycaprolactone and ceramics such as hydroxyapatite, tricalcium phosphate, and amorphous calcium phosphate.

1.3.2.1. Natural Biomaterials

Natural biomaterials are commonly used because of their inherent biocompatibility and similarities to the extracellular matrix. Collagen is a major component of the extracellular matrix of hard tissues and is commonly used to facilitate cell adhesion and proliferation. It is the most abundant structure in the human body and can easily be isolated from both human and animal tissues [59]. Collagen can then be used to create a variety of scaffold geometries and the degradation rate can be tailored by altering protein density and crosslinking of the collagen fibers [59]. However, collagen alone provides little structural support for a scaffold [1]. Therefore, collagen may be best utilized as a component of a composite scaffold.

Hyaluronan, a simple glycosaminoglycan, has been used as a scaffold material for cartilage tissue engineering and wound healing applications [10, 60]. Hyaluronan can be processed to form a biodegradable hydrogel by crosslinking individual polymer chains. Crosslinking of the gel can be achieved by photopolymerization with glycidyl methacrylate, which reacts covalently with hyaluronic acid [60]. The rate of degradation is decreased after crosslinking, allowing time for new tissue growth and healing.

Alginates are polysaccharides derived from seaweed. They are block copolymers that are usually processed as cross-linked gels in the presence of divalent cations such as calcium [61]. Alginates can be processed into any number of shapes and cells can be directly mixed with the aqueous alginate mixture prior to crosslinking. However, degradation rates can be low and uncontrollable [61].

Chitosan, derived from the shells of crustaceans, is commonly used for tissue engineering applications because of the similarities to natural human glycosaminoglycans [10]. Chitosan, a partially deacetylated derivative of chitin, is a copolymer of N-acetyl-D-glucosamine and D-glucosamine [62]. The natural polymer, usually fabricated as a hydrogel, has numerous advantages including biocompatibility, biodegradablility, and nonantigenicity. Scaffold properties are affected by the deacetylation of chitosan and ultimately affect cell adhesion, proliferation, and scaffold biodegradability.

Demineralized bone matrix is processed through the acidic decalcification of cortical bone [2]. After processing, the matrix is used as an osteoconductive scaffold that has the trabecular structure of the original bone tissue [1]. In addition, the demineralized bone matrix may retain some of the growth factors not destroyed by acid demineralization and thus have some osteoinductive potential.

1.3.2.2. Synthetic Biomaterials

Examples of synthetic polymers are calcium phosphates, poly(glycolic acid) (PGA), poly(L-lactic acid) (PLLA), and their copolymer poly(lactic-co-glycolic acid) (PLGA). Each has unique assets and has the ability to be altered to achieve specific properties for the desired tissue application.

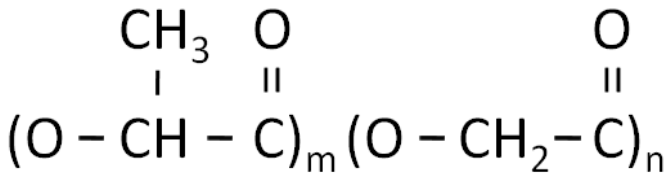

Figure 1.3. Chemical structure of PLGA copolymer

Synthetic polymers such as PLLA, PGA, and their copolymer, poly(lactic co-glycolic acid) (PLGA), have been approved by the US Food and Drug Administration for use in humans and are available commercially for various applications [61]. Generally, PGA alone begins to degrade in less than a month [63], which could result in collapse of the graft when implanted in a bony defect. In contrast, PLLA doesn't begin to degrade until after 9 months [63], inhibiting sufficient ingrowth of new tissue. Therefore, PLGA is used to create polymer scaffolds with an intermediate degradation rate, on the order of one to two months, to maintain strength while allowing ingrowth of new tissue. In addition, PLGA has been shown to support the attachment and proliferation of a number of cell types, including osteoblast-like MC3T3-E1 cells [19, 64]. The copolymer degrades by chemical hydrolysis into lactic acid and glycolic acid byproducts which are non-toxic and naturally removed from the body. The degradation rate and mechanical properties of PLGA can be tuned by altering the copolymer ratio and molecular weight of each component, making the copolymer ideal for multiple tissue engineering purposes. Studies have shown that ratios of 75:25 or 85:15 PLGA are most appropriate for bone healing which requires approximately 6 weeks [19].

1.3.2.3. Calcium Phosphate Ceramics

1.3.2.3.1. Types of Calcium Phosphate Ceramics

Calcium phosphates are of interest in tissue engineering because of their natural occurrence in skeletal and dental tissues. They are available in a number of forms including particles, blocks, coatings, and injectable cements. Calcium phosphate minerals such as

hydroxyapatite (HAP) [$Ca_{10}(PO_4)_6(OH)_2$; Ca/P = 1.67] [65] and β-tricalcium phosphate (β-TCP) [$Ca_3(PO_4)_2$; Ca/P = 1.5] [65] have been studied extensively as fillers for bone defects and scaffolds for engineered bone tissue [66] and have been approved by the FDA for use as bone substitutes in humans [67]. The advantage of these calcium phosphate ceramics in osseous reconstruction and regeneration is their biocompatibility, osteoconductivity and, similarity to natural bone [68, 69]. Some types of calcium phosphates and their formulas are shown in Table 1.1.

Table 1.1 Types of Calcium Phosphates

CALCIUM PHOSPHATE	FORMULA	Ca/P RATIO	REFERENCE
Hydroxyapatite	$Ca_{10}(PO_4)_6(OH)_2$	1.67	[65]
Tricalcium Phosphate	$Ca_3(PO_4)_2$	1.5	[65]
Octacalcium Phosphate	$Ca_8(PO_4)_4(HPO_4)_2{\cdot}5H_2O$	1.33	[70]
Amorphous Calcium Phosphate	$Ca_3(PO_4)_2{\cdot}3H_2O$	1.5	[71, 72]

1.3.2.3.2. Hydroxyapatite

Apatites are calcium phosphate minerals with the formula $Ca_{10}(PO_4)_6X$, where X can be $(OH)_2$, F_2, or Cl_2 to form hydroxyapatite (HAP), fluorapatite, and chlorapatite. Bone mineral is composed mainly of a form of hydroxyapatite called carbonated hydroxyapatite in which many of the hydroxyl groups are substituted with carbonate groups [8]. Because of the similarities to natural bone, synthetic hydroxyapatite ($Ca_{10}(PO_4)_6(OH)_2$) has been studied extensively as a filler for bone defects and scaffolds for engineered bone tissue [2]. Synthetic HAP is osteoconductive and supports osteoblast attachment and spreading; however it lacks osteoinductive properties and is resistant to biodegradation [55, 73]. The degradation rate of HAP sintered at high temperatures is said to be 0.1 mg/year in subcutaneous tissue [74]. The slow rate of degradation is thought to be attributed to calcium to phosphate ratio or crystal structure [65, 69, 75]. This resistance to degradation can be a desirable property for the coating of metal prosthetics to improve fixation. However, this may be a limitation for tissue grafts intended for bone regeneration within a defect.

1.3.2.3.3. Tricalcium Phosphate

Tricalcium phosphate exists in two different phases that differ in their crystal structure: α-TCP and β-TCP [70]. Because of their differences in crystallinity, they have different resorption properties. α-TCP, which is created by sintering β-TCP at greater than 1170 °C, is more soluble. β-TCP has the ideal chemical formula $Ca_3(PO_4)_2$ and has a calcium phosphate ratio of 1.5. The effect of β-TCP graft materials on osteoblast differentiation and bone formation has been evaluated *in vitro* and *in vivo*. Dong et al demonstrated enhanced bone formation when a pure porous β-TCP graft and bone marrow derived osteoprogenitor cells were implanted subcutaneously in a rat model [76]. The β-TCP grafts were combined with osteoprogenitor cells and incubated for two weeks in osteogenic medium, before implantation. Composites incubated in medium prior to implantation demonstrated higher ALP activity and OCN content than unconditioned grafts. β-TCP scaffolds (Vitoss (Orthovita, Inc, Malvern, PA)) have also been approved by the FDA for use in bone defects [77]. The scaffold is composed of small crystals of β-TCP formed into a scaffold containing micro- and macropores and has shown significant bone formation **in vivo**.

1.3.2.3.4. Amorphous Calcium Phosphate

Amorphous calcium phosphate (ACP) [Ca/P = 1.5] is a soluble, bioactive ceramic that lacks the long range order characteristic of crystalline substances [72]. Under aqueous conditions, ACP rapidly converts to a poorly crystalline apatite structure [71]. During this conversion, Ca^{2+} and PO_4^{3-} ions are transiently released into the surrounding environment. Although a limitation of ACPs has been their rapid dissolution, divalent cations such as Zn^{2+} and Cu^{2+}, which are essential for normal cell function, have been shown to slow the rate of ACP conversion to HAP [78, 79]. Stabilized amorphous calcium phosphates may be attractive alternatives as they have been shown to transiently stimulate osteoblastic differentiation as they release calcium and phosphate ions and raise the local pH [80]. Interestingly, the process of ACP conversion may serve as mechanism for delivery of osteoinductive divalent cations.

1.3.2.3.5. Bioactive Glasses

Bioactive glasses have been investigated for use as bone substitutes. Their dissolution leads to the deposition of an apatite layer on the glass surface that facilitates osteointegration [81]. Bioactive glasses can be prepared by the sol-gel method to contain an number of

components including silica, sodium, calcium, and phosphorus and other modifiers including magnesium, boron, aluminum, and silver [81]. Tsigkou et al investigated the response of osteoblasts to composites of PLLA and bioglass particles [82]. Osteoblast differentiation was stimulated by the presence of the bioglass particles. ALP activity and osteocalcin protein were significantly elevated on PLLA-bioglass composites, compared to PLLA alone.

1.3.2.3.6. Cements

Calcium phosphate cements consist of calcium phosphate powder and liquid or gel components that are prepared by dissolution and precipitate as calcium phosphate crystals. When injected, the cements are able to adapt to the shape of a bone defect, integrate into the bone structure, and be remodeled into new bone. However, they can have poor mechanical properties and degrade slowly *in vivo*. Julien et al created a composite calcium phosphate cement composed of HAP, β-TCP, α-TCP, monocalcium phosphate monohydrate, and ACP containing carbonate, magnesium, zinc, or fluoride (to achieve different rates of degradation, creating pores) [83]. The doping agent had an influence on crystal size of the hardened cement, as seen by SEM micrographs. Mg and Zn ACPs had smaller crystal sizes than ACP with fluoride. There was no difference in cell adhesion or ALP activity on the three CPCs with metal ions.

1.3.2.3.7. Calcium Phosphate Degradation and Dissolution

The dissolution of calcium phosphate bone substitutes is postulated to aid in the formation of mineralized matrix by osteoblasts, thereby facilitating osteointegration of the graft with host bone [70]. The ion products of dissolution have also been shown to have an effect on osteoblast function [80]. Dissolution kinetics are governed by physicochemical properties such as porosity, chemical composition, and crystal structure of the minerals. Therefore, the degradation, dissolution, and reprecipitation of various calcium phosphate minerals have been investigated. Klein et al investigated the degradation of various calcium phosphate minerals implanted in rabbit tibiae [69]. Hydroxyapatite (apatite crystal structure after sintering) and tricalcium phosphate (β-whitlockite structure after sintering) materials were fabricated with different porosity. Hydroxyapatite materials showed no detectable degradation, regardless of porosity. However, tricalcium phosphate materials with macropores, or with both micro- and macropores showed complete degradation after nine months. These results suggest that the

differences in biodegradation are related to crystal structure and Ca/P ratio. Klein et al [65] demonstrated the solubility of hydroxyapatite, tricalcium phosphate, and tetracalcium phosphate particles in vitro. Hydroxyapatite showed the lowest solubility, while tetracalcium phosphate was the most soluble. Gupta et al investigated the surface reactivity and dissolution kinetics of a novel porous silica-calcium phosphate nanocomposite and the effect on osteogenic gene expression [84]. The porous composites enhanced osteogenic differentiation when compared to HAP.

1.3.2.3.8. Osteointegration

Unlike synthetic materials, which usually have a hard time forming a strong bond with bone, calcium phosphates are commonly investigated for healing of bone defects because they are capable of bonding with native bone tissue. Ceramic bioactivity is characterized by surface-induced biomineralization of calcium phosphate nanocrystals [85]. This biomineralization is initiated by electrostatic interaction between surface functional groups and the calcium and phosphate ions in solution [85]. The dissolution of grafts containing bioactive ceramics is followed by the precipitation and rapid formation of a biological apatite layer at the graft-host interface [84]. The bone-like mineral, composed of HAP with ions of magnesium, chlorine, and carbonate, recruits osteoblasts to produce a mineralized extracellular matrix [85] that further supports osteointegration of the graft.

1.3.2.3.9. Doped Calcium Phosphates

Substitution with various ions can alter the properties of a calcium phosphate such as hydroxyapatite. Dopants have been added to calcium phosphates in order to further enhance properties pertinent to orthopedic and dental applications. Webster et al demonstrated increased osteoblast adhesion on HA doped with 2 mol% zinc when compared to undoped HA [86]. Webster et al continued these studies by testing the effect of HA doped with divalent (Mg^{2+} and Zn^{2+}) and trivalent (La^{3+}, Y^{3+}, In^{3+}, and Bi^{3+}) cations on osteoblast differentiation [87]. Results showed that doped HA enhanced ALP activity and deposition of calcified mineral when compared to undoped HA. Mineral deposition was enhanced greatest on HA doped with Zn^{2+}, In^{3+}, and Bi^{3+}. HA doped with zinc cations improved dissolution rate over other dopants and undoped HA. Santos et al developed a novel composite containing calcium phosphates and collagen, doped with zinc for orthopedic and dental applications [88]. The composites were

cytocompatible and stimulated ALP activity, as shown with other zinc-releasing calcium phosphates. Paul et al investigated the attachment and spreading of osteoblast-like cells on porous ceramic materials made from nanoparticles of zinc phosphate and calcium phosphate containing zinc and magnesium [67]. XRD spectra show that all substrates were crystalline. Cell adhesion and spreading was significant on HAP, calcium phosphates containing zinc, and calcium phosphates containing both zinc and magnesium.

Calcium phosphates have also been doped with metal ions and bisphosphonates to retard their conversion to hydroxyapatite [78, 79]. Stabilizing agents such as pyrophosphates and polyphosphates have been shown to regulate the autocatalytic crystallization of ACP [89]. Calcium phosphates have been stabilized with 1-hydroxyethylidene-1, 1-bisphosphonate (HEBP) (a clinically proven antimineralization agent) because it adsorbs on the surface of crystallites and hinders further crystal growth [78]. In one study, nickel had the greatest inhibitory effect on the rate of ACP transformation to HAP, comparable to HEBP [79]. Tin, copper, and zinc also had an inhibitory effect, but to a lesser extent. This was further investigated by determining the effect of 26 metal ions on the in vitro formation of calcium phosphate [78]. Nickel and HEBP had the greatest inhibitory effect. Nickel, tin, cobalt, manganese, copper, zinc, gallium, thallium, molybdenum, cadmium, magnesium, and mercury had a moderate inhibitory effect. Cesium, titanium, chromium, ferrous iron, iridium, palladium, platinum, silver, gold, aluminum, and lead had no effect on the transformation to HAP. Ferric iron and indium accelerated the transformation of ACP to HAP [78]. Skrtic et al demonstrated that ACPs hybridized with Zr and Si achieved enhanced stability and slowed the conversion of the hybrid ACPs to HAP [71]. It is proposed that stabilization is achieved when the hybridizing agents adsorb at active crystal growth sites.

1.3.2.3.10. Zinc-containing Calcium Phosphates

Zinc is an essential trace element in the development and maintenance of healthy bone and has been shown to increase osteoblast differentiation. Researchers have been incorporating zinc into bone substitutes to enhance osteoblast proliferation and differentiation. Storrie et al incorporated zinc into an organoapatite coating on titanium meshes that was released over a period of 12 days at concentrations of 10-20 μM [90]. These substrates resulted in elevated levels of ALP activity in MC3T3-E1 cells at days 4 and 8 and formed mineralized bone nodules within 12 days. Oki et al developed a bioglass material containing zinc that stimulated osteoblast

production of ALP [81]. Ito et al developed a zinc-doped β-tricalcium phosphate (β-TCP), hydroxyapatite composite to achieve a slow release of zinc and promote bone formation [91]. They showed that proliferation of MC3T3-E1 was increased on ZnTCP/HAP composites with zinc content from 0.6 to 1.2 wt%. However, zinc concentrations above 1.2% resulted in cytotoxicity. Santos et al developed a novel composite containing calcium phosphates and collagen, doped with zinc for orthopedic and dental applications [88]. This composite was cytocompatible, however, availability of the zinc ions was compromised by the presence of collagen molecules and therefore it did not stimulate ALP activity.

1.3.2.4. Composite Scaffolds

Natural bone is a composite material composed of an organic extracellular matrix reinforced with inorganic minerals. Thus, the design of calcium phosphate powder/PLGA composites can combine the advantages of the degradable polymer with osteoconductive calcium phosphate particles. A composite scaffold can be designed to mimic natural bone and optimize the physical and biological properties necessary for bone regeneration.

Composite scaffolds that contain multiple materials to maximize both osteoconduction and osteoinduction are a promising approach to biomaterial scaffolds. Calcium phosphate bone substitutes are relatively brittle and lack tensile strength desired for bone substitutes [2]. A composite scaffold of PLGA and ACP can take advantage of the biodegradable properties of PLGA and the osteoconductive properties of ACP. The incorporation of calcium phosphates has been shown to improve mechanical stiffness of PLGA foams [92]. Furthermore, the resorption products of calcium phosphate degradation may have the ability to buffer the acid byproducts of PLGA degradation [63].

Cushnie et al created composite scaffolds of sintered PLGA microspheres loaded with amorphous hydroxyapatite [93]. Composites of collagen and hydroxyapatite have also been developed to mimic the composition of natural bone [88, 94, 95]. Ogata et al developed a composite material of hydroxyapatite and soluble calcium phosphate to improve bioactivity, relative to inert HAP [55]. The composite exhibited a more rough surface morphology than HAP, which resulted in increased osteoblast adhesion. Cells cultured in the presence of the dissolution products of the substrate exhibited greater ALP activity, collagen production, and mineralization (alizarin red).

1.3.2.5. Scaffold Fabrication Techniques

Scaffolds for tissue engineering are fabricated by numerous processes to obtain a construct with the desired properties, such as porosity, strength, and degradability. Processes include phase inversion, electrospinning, solvent casting/particulate leaching, compression molding, and gas foaming [96].

Solvent casting/particulate leaching is a common method used to produce porous scaffolds [96]. The scaffold is produced by dispersing a mineral or organic particle in a polymer solution and then the dispersion is casted or freeze-dried to allow the solvent to evaporate. Finally, the particles are dissolved by an aqueous solvent to leave pores. The porosity of the scaffold can be controlled by the size and concentration of the porogen that is used. The method is relatively simple; however, it uses highly toxic processing chemicals that may be retained after scaffold synthesis.

Thermal phase inversion is a process in which the temperature of a polymer solution is decreased to induce the separation of two phases [92, 96]. One phase contains a high concentration of polymer which solidifies to form the scaffold. The other phase contains a high concentration of solvent which forms the pores of the scaffold upon removal. Pore architecture can be controlled by solvent choice or phase separation conditions. However, pores tend to be small and interconnectivity is difficult to achieve.

Gas foaming is a process which does not require organic solvents or high temperatures. The process involves exposing the polymer to high-pressure carbon dioxide to saturate the polymer with gas [96]. When the gas pressure is decreased, the dissolved carbon dioxide becomes unstable and phase separates from the polymer. This approach can achieve very high porosities, but pore interconnectivity is poor. Interconnectivity can be improved by addition of a porogen [97]. In addition, porosity can be increased by adding organic salts to the process.

Polymer microspheres can also be used to create biomaterial scaffolds. The fabrication process is either a single oil-in-water emulsion to make solid microspheres or double oil-in-water emulsion to create loaded microspheres [98]. Polymer is dissolved in an organic solvent and then added to an aqueous solution containing a dispersing agent. The emulsion is then stirred to allow for complete evaporation of the organic solvent and hardening of the polymer microspheres. In one scaffold fabrication technique, microspheres of a specific size range are thermally fused together to create a three-dimensional structure with an interconnected pore system [99-102]. Modulus and porosity of the scaffold can be adjusted by changing the size of the microspheres.

In contrast to the preceding methods that achieve high porosity (80-95%), sintering results in low porosity (30-40%), but may increase compressive modulus and strength. Nevertheless, when large particles are used (500-710 micron) good interconnectivity of pores is achieved [101].

1.3.3. Biochemical Factors

Biochemical factors provide the local cues that are responsible for differentiation of stem cells [103]. The incorporation of biomolecules within a defect site has been shown to influence bone formation [20]. Biomolecules can be added in the form of peptides, cytokines, growth factors, or DNA encoding a gene of interest [10]. For optimal bone regeneration, a combination of therapies or biomolecules may be most useful. Some of the growth factors that are being studied for bone regeneration and healing are bone morphogenetic proteins (BMPs), transforming growth factor beta (TGF-β), insulin-like growth factors (IGFs), platelet derived growth factors (PDGFs), and fibroblast growth factors (FGFs) [14, 20]. In addition, vascular endothelial growth factor (VEGF) is being used to induce vascularization of actively regenerating bone tissue [104].

1.3.3.1. Bone Morphogenetic Proteins

Bone morphogenetic proteins, part of the TGF-β superfamily, are the most commonly studied osteogenic cytokines [20]. The BMP family of osteoinductive cytokines currently consists of up to 40 genes which induce angiogenesis, chemotaxis, mitogenesis, proliferation and differentiation [14]. Of all the BMPs, bone morphogenetic proteins 2, 4, 6, and 7 are the most osteoinductive and play key roles in the differentiation of osteocytes and osteoblasts [14]. It has been suggested that BMPs interact to regulate each other [20]. The complex interactions between BMPs promote the proliferation and differentiation through a cascade of events that result in ossification.

Several studies in animal models, as well as clinical studies have been conducted to determine the effectiveness of BMPs in wound healing. Yasko et al used a rat segmental femoral defect model to test the osteoinductivity of recombinant human BMP-2 (rhBMP-2). Implants including both demineralized bone matrix and 11 μg rhBMP-2 resulted in significant bone formation when compared to demineralized matrix alone [105]. This study also showed that human BMP is effective for treatment in other species. Friedlaender et al [106] assessed the effectiveness of the OP-1 Device (Stryker Biotech, Hopkinton, MA) in healing tibial nonunions

compared with autografts. Nine months after surgery, radiographic assessments showed equivalent healing for both OP-1 and autografts. In a separate study, Govender et al [107] investigated the use of rhBMP-2 on an absorbable type-1 collagen sponge (INFUSE, Medtronic, Memphis, TN). Patients were divided into three groups: standard wound closure, standard closure plus 6 mg rhBMP-2, and standard closure plus 12 mg rhBMP-2. The group treated with the higher dose of rhBMP-2 required fewer interventions post-surgery and achieved improved wound healing.

1.3.3.2. Hepatocyte Growth Factor

HGF is a cytokine that is secreted by myeloma cells [108] and is found in high concentrations in the serum of multiple myeloma patients [109, 110]. Therefore, HGF has been the subject of a number of studies related to the formation of osteolytic bone lesions in multiple myeloma.

Recently, the effects of hepatocyte growth factor (HGF) on proliferation and osteogenic differentiation of different cell types have been investigated. One study found that HGF was a potent inhibitor of bone resorption by osteoclasts isolated from neonatal rat long bones [111]. However, when the same osteoclasts were cultured in the presence of osteosarcoma cells and HGF, resorption was stimulated. Inaba et al [112] demonstrated an increase in the proliferation and ALP activity of MC3T3-E1 cells in the presence of 150 ng/mL HGF. Ye and colleagues [113] investigated the effects of HGF on the proliferation and early stage differentiation of human DPSCs. Culture of DPSCs in the presence of 100 and 200 ng/mL HGF demonstrated an increase in proliferation and ALP activity, protein synthesis, and mRNA expression. *In vitro* studies of human mesenchymal stem cells in the presence of 100 ng/mL HGF and 300 ng/mL BMP-2 demonstrated the inhibition of BMP-induced osteoblast differentiation and thus enhancing bone resorption [114].

Studies of the effects of HGF on osteoblast differentiation are limited, showing only the effects of the cytokine on proliferation and ALP activity. Very few studies have been conducted to investigate the effect of HGF on late markers of osteoblast differentiation. Furthermore, the limited studies that have been conducted are contradictory between cell lines. However, it is possible that different cell types react differently to HGF.

1.3.3.3. Ions and Minerals

Extracellular matrix mineralization by osteoblasts is achieved through a rich source of calcium and phosphate ions. Release of calcium ions from glass ceramics have been shown to stimulate osteogenic differentiation in osteoblast-like cells [115]. Organic phosphate has long been used in cell culture to induce osteoblast differentiation [116, 117]. Organic phosphate is hydrolyzed by ALP to make inorganic phosphate available for mineralization [118]. Recently, several studies have shown that calcium and phosphate supplementation of osteoblast cultures enhances bone mineralization. Chang and colleagues [119] investigated the effect of calcium and phosphate supplementation on in vitro osteoblast mineralization. Rat calvarial osteoblast-like cultures supplemented with 1.8 mM Ca^{2+} and 5 mM β-glycerophosphate for 12 days showed increased alizarin red staining and bone nodule formation when compared to non-supplemented cultures. In another study, proliferation of mouse primary osteoblasts was maximized at supplemental calcium concentrations of 2-6 mM, while differentiation and matrix mineralization were maximized at 6-10 mM Ca^{2+} [120]. It is thought that calcium and phosphate ions are modulators of osteoblast differentiation and mineralization in vitro [119-122]. Therefore, a calcium phosphate ceramic that can release calcium and phosphate ions during ceramic degradation offers great potential to stimulate osteogenesis.

1.4. Objective

Tissue engineering is a multidisciplinary effort combining the principles of engineering, materials science, biology, and medicine to create materials, devices, or therapies to facilitate healing or regeneration of damaged tissue or organs. Current strategies for tissue regeneration may include: (1) a scaffold for osteoconduction, (2) bioactive molecules for osteoinduction, (3) and osteoprogenitor cells to actively repair the wound site.

The overall objective of this research was to develop a bioactive, composite scaffold by incorporating ion-eluting calcium phosphate minerals into a PLGA microsphere matrix to facilitate healing of bone defects. To accomplish this goal, rat bone marrow stromal cell (BMSC) cultures were supplemented with zinc to determine the effects of zinc release from zinc-stabilized ACP. Next, HAP, zirconium- and zinc- stabilized ACPs were synthesized, characterized to determine ion release and crystallinity over 96 hours, and then incorporated into a porous sintered PLGA microsphere matrix. Scaffolds were fabricated using non-aqueous process to retain the amorphous structure of the calcium phosphates before cell culture. The microsphere scaffolds [99-102] were created by relying on the driving force of sintering the microspheres above the glass transition temperature of the polymer. Particles of ACP were adhered to the PLGA microspheres to allow for dissolution and release of ions to surrounding osteoprogenitor cells. To determine the effectiveness of the scaffold as an implantable construct, properties such as compressive modulus and mineral precipitation on the scaffolds were evaluated. Finally, MC3T3-E1 cells were cultured in the scaffolds to evaluate the effect of the three calcium phosphates on osteoblast proliferation and differentiation.

1.5. Experimental Plan

1.5.1. Aim 1: Determine the effect of zinc on osteoprogenitor cell differentiation

Amorphous calcium phosphates (ACPs) are attractive fillers for osseous defects and are stabilized through the incorporation of transition metals such as zirconium and zinc. As ACP is converted in solution to hydroxyapatite (HAP), the transient release of calcium and phosphate ions is capable of stimulating osteoblastic differentiation. Zinc is known to retard ACP conversion to HAP, and – when incorporated into ceramic biomaterials – has been shown to stimulate osteoblastic differentiation. Because zinc deficiency *in vivo* is marked by skeletal defects, we postulated that zinc ions released from ACP and other minerals could stimulate proliferation and osteoblastic differentiation of progenitor cells. To test this hypothesis, rat bone marrow stromal cells (BMSCs) were cultured in osteogenic medium containing 3×10^{-6} to 4×10^{-5} M Zn^{2+} for up to 3 weeks.

1.5.2. Aim 2: Fabricate and characterize PLGA/ACP composite scaffold

Calcium phosphates such as hydroxyapatite and tricalcium phosphate are commonly used in bone substitutes because of their similarities to natural bone. Amorphous calcium phosphate (ACP) is a soluble mineral that releases Ca^{2+} and PO_4^{3-} ions during conversion to hydroxyapatite (HAP). It is postulated that these ions can stimulate osteogenic differentiation [119, 123] and facilitate mineralization at the graft-host interface [85]. Therefore, I propose that the immobilization of ACP particles in a scaffold will provide sustained release of Ca^{2+} and PO_4^{3-} to stimulate new bone formation and graft integration.

For this study, a non-aqueous scaffold fabrication process was used to retain the amorphous ACP structure prior to contact with cells. Therefore, a sintered microsphere scaffold [99-102] was created, relying on the driving force of particle fusion above the glass transition temperature of the polymer. This fabrication procedure allowed for ACP adherence to the surface of the PLGA particles to be available for later dissolution and release of ions to surrounding osteoprogenitor cells.

This study characterized the dissolution and conversion of zirconium- and zinc-stabilized ACPs. The incorporation of HAP and the stabilized ACPs into a sintered PLGA microsphere matrix was evaluated by SEM and mechanical properties were measured.

1.5.3. Aim 3: Determine the effect of PLGA/ACP composite scaffolds on osteoprogenitor proliferation and differentiation.

Calcium phosphates such as hydroxyapatite and tricalcium phosphate are commonly used in bone substitutes because of their similarities to natural bone. Amorphous calcium phosphate (ACP) is a mineral that solubilizes under aqueous conditions, releasing Ca^{2+} and PO_4^{3-} ions during conversion to hydroxyapatite (HAP). It is postulated that these ions can stimulate osteogenic differentiation [119, 123]. However, our previous research has shown that direct contact of unrestrained ACP particles with BMSCs has a negative effect on cell proliferation and differentiation. Therefore, we propose restraining the ACP particles within a PLGA microsphere matrix. Our hypothesis is that the incorporation of ACP within a composite scaffold, addressed in Aim 2, will enhance osteogenic differentiation of osteoprogenitor cells. Furthermore, results will provide insight into the effectiveness of the construct in facilitating bone healing in vivo.

This study examined the effect of composite PLGA scaffolds containing three different calcium phosphate powders (HAP, ZrACP, and ZnACP) on the osteogenic differentiation of MC3T3-E1 osteoprogenitor cells. Cell number, ALP activity, PGE_2 accumulation in the culture medium, and expression of growth and transcription factors and bone matrix proteins were measured.

Reprinted from Popp, J.R. et al. *Journal of Biomedical Materials Research, Part A* 81A(3): 766-9 (2007), with permission from John Wiley and Sons publishers.

Chapter 2: Effect of Soluble Zinc on Differentiation of Osteoprogenitor Cells

Jenni R. Popp[1], Brian J. Love[1,2], and Aaron S. Goldstein[1,3]

[1]Virginia Tech-Wake Forest School of Biomedical Engineering
[2]Department of Materials Science and Engineering
[3]Department of Chemical Engineering
Virginia Polytechnic Institute and State University
Blacksburg, VA 24061

2.1. Abstract

Amorphous calcium phosphates (ACPs) are attractive fillers for osseous defects and are stabilized through the incorporation of transition metals such as zirconium and zinc. As ACP converts in solution to hydroxyapatite (HAP) in a manner marked by a transient release of calcium and phosphate ions, it is capable of stimulating osteoblastic differentiation. Zinc is known to retard ACP conversion to HAP, and – when incorporated into ceramic biomaterials – has been shown to stimulate osteoblastic differentiation. Because zinc deficiency in vivo is marked by skeletal defects, we postulated that zinc ions released from ACP and other minerals could stimulate proliferation and osteoblastic differentiation of progenitor cells. To test this hypothesis, rat bone marrow stromal cells (BMSCs) were cultured in osteogenic medium containing 3×10^{-6} to 4×10^{-5} M Zn^{2+} for up to 3 weeks. No significant effects of zinc concentration on cell number, alkaline phosphatase (ALP) activity, total protein content, collagen synthesis, or matrix mineralization were found.

2.2. Introduction

Calcium phosphate minerals such as hydroxyapatite (HAP) and β-tricalcium phosphate (β-TCP) have been studied extensively as fillers for bone defects and scaffolds for engineered bone tissue [66]. The advantage of these insoluble calcium phosphate ceramics in osseous reconstruction and regeneration is their biocompatibility and osteoconductivity [68]. However, amorphous calcium phosphates (ACPs) – which are soluble under aqueous conditions – may be attractive alternatives given that they can transiently stimulate osteoblastic differentiation as they release calcium and phosphate ions and raise the local pH [80]. Although a limitation of ACPs has been their rapid dissolution, divalent cations such as Zn^{2+} and Cu^{2+} – which are essential for normal cell function –retard the rate of ACP conversion [78]. Interestingly, the process of ACP conversion may serve as means for delivering osteogenic divalent cations.

Zinc is a trace element necessary for mammalian growth [124], and zinc deficiency leads to skeletal defects and retardation in bone growth [125]. In vitro, zinc-containing biomaterials have been shown to enhance phenotypic markers of osteoblastic differentiation of osteoprogenitor cells. In particular, incorporating zinc into β-TCP stimulated alkaline phosphatase (ALP) activity of bone marrow stromal cells (BMSCs) [126], while zinc-organoapatite films accelerated ALP activity and bone nodule formation by MC3T3-E1 cells [90]. What is not clear from these studies is whether the reported osteoinductive effect is related to alteration of the mineral structure with incorporation of zinc, or a consequence of the release of zinc ions into the cell microenvironment. To test the latter mechanism, we examined the effect of soluble Zn^{2+} on proliferation and differentiation of rat BMSCs. Cells were cultured for up to 3 weeks in osteogenic medium containing Zn^{2+} at concentrations of 3×10^{-6} to 4×10^{-5} M. The effect of zinc concentration on cell number, ALP activity, total protein content, collagen synthesis, and matrix mineralization was determined.

2.3. Materials and Methods

2.3.1. Materials

Chemicals were obtained from Sigma-Aldrich (St. Louis, MO) and materials were obtained from Fisher Scientific (Pittsburgh, PA) unless otherwise specified. Primary medium for cell culture was Minimum Essential Medium Alpha Modification (αMEM, Invitrogen,

Gaithersburg, MD) with 10% fetal bovine serum (Gemini Biosciences, Calabasas, CA) and 1% antibiotic/antimycotic (Invitrogen). Osteogenic medium was primary medium supplemented with 2 mM β-glycerophosphate, 0.13 mM L-ascorbic acid 2-phosphate, and 0.01 μM dexamethasone [127]. The concentration of Zn^{2+} in osteogenic medium was systematically varied by adding $ZnCl_2$ to the osteogenic medium and the resultant zinc concentrations – as determined by atomic absorption spectroscopy (Perkin-Elmer 5100-PC, Wellesley, MA) – were 3×10^{-6}, 1×10^{-5}, and 4×10^{-5} M.

2.3.2. Cell Culture

Studies were performed using rat bone marrow stromal cells (BMSCs) obtained from 125 to 150 g male Sprague-Dawley rats (Harlan, Dublin, VA) in accordance with the Animal Care Committee at Virginia Tech [127]. Cells were expanded under subconfluent conditions and used at passages 2-4. Cells were seeded into 12-well plates at 10^5 cells per well and allowed to attach overnight in primary medium. The following day, denoted as day 0, culture medium was replaced with osteogenic medium containing different concentrations of zinc. Cells were analyzed for cell number and ALP activity at days 7 and 14, for collagen synthesis at day 14, for total protein synthesis at days 14, and for mineralization at day 21.

2.3.3. Cell Number and ALP Activity

Cell number was determined by fluorometric analysis of total DNA content using Hoechst 33258 dye. ALP activity was determined colorimetrically by the hydrolysis of *p*-nitrophenyl phosphate, and then normalized by cell number. These assays are described in detail elsewhere [128].

2.3.4. Total Protein

To quantify total protein, cell layers were washed twice with phosphate buffered saline (PBS) and mechanically scraped in the presence of 0.1 mL 1X Laemmli Buffer with protease inhibitors (950 μL Laemmli stock solution (Biorad, Hercules, CA), 50 μL β-mercaptoethanol (Fisher Scientific), 10 μL 100× protease inhibitors (0.2 mg/mL aprotinin, 0.2 mg/mL leupeptin, 0.1 mg/mL pepstatin (Calbiochem, La Jolla, CA)) and 1 mL PBS). Total protein per well was

determined by colorimetric assay (RC DC Protein Assay, Bio-Rad) according to the manufacturer's instructions and normalized by cell number.

2.3.5. Collagen Synthesis

Collagen synthesis was determined by incubating cell layers with 3 μCi/mL of ^{3}H-proline (ICN, Irvine, CA) for 48 h. Cell layers were collected, separated into collagenase digestible and non-collagenase digestible fractions, and collagen content was determined by scintillation counting and reported as a percentage of total, as previously described [80].

2.3.6. Mineralization

Mineralization of cells layers was assessed by Alizarin Red S staining of calcium deposits as described elsewhere [129]. Briefly, cell layers were stained with 1 mL of 40 mM Alizarin Red S, pH 4.1 for 20 min. The dye was extracted with 0.8 mL 10 % (v/v) acetic acid and absorbance of the extract was measured at 405 nm. Cell layers in primary medium containing 3×10^{-6} M zinc were used as a negative control.

2.3.7. Statistics

Values are presented as means ± standard deviation. Statistical analyses were performed using Origin 6.1 (OriginLab Corporation, Northampton, MA). A one-way analysis of variance (ANOVA) procedure with a significance level of $p=0.05$ was used to determine significance between groups.

2.4. Results

To test the effects of zinc concentration on cell proliferation, cells were seeded at 10^5 cells per well, cultured in osteogenic medium containing zinc for 7 and 14 days and assayed for cell number. Measurements of cell number are consistent with a 4 to 5-fold increase in cell number (Figure 1) and the achievement of monolayer coverage. However, no stimulatory effect of Zn^{2+} on cell proliferation was noted. Concurrent analysis of ALP activity indicated the development of the osteoblastic phenotype, but did not indicate a stimulatory effect of Zn^{2+} (Figure 2).

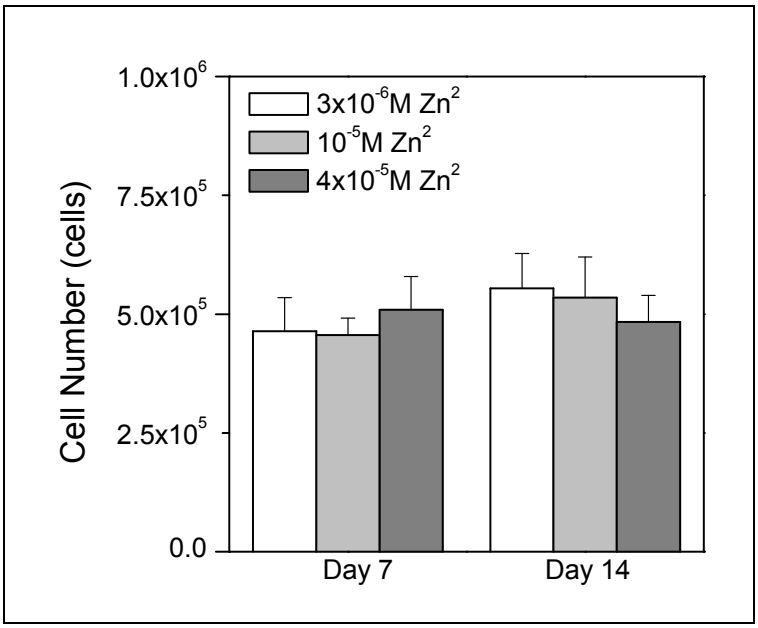

Figure 2.1. Cell number as a function of Zn^{2+} concentration and time in culture. Bars correspond to the mean ± standard deviation for n=8 samples. An asterisk denotes significant difference relative to the control.

Zinc ions have been shown to increase protein synthesis in osteoblasts [130]. To test for the effects of zinc concentration on total protein content, cells were cultured with osteogenic medium containing zinc 3×10^{-6}, 1×10^{-5}, and 4×10^{-5} M Zn^{2+} for a period of 14 days. At the end of this period, protein content was found to be the same for all treatment groups, indicating that zinc supplementation does not affect the protein content of osteoblasts in vitro (Figure 3a). Concurrently, collagen synthesis was determined by ^{3}H-proline addition to culture on day 12 followed by a 48 h incubation to allow for incorporation of the radioactive proline into newly formed protein. Measurements of collagen synthesis, reported as percent collagenous protein per cell layer, were similar for all treatment groups (Figure 3b).

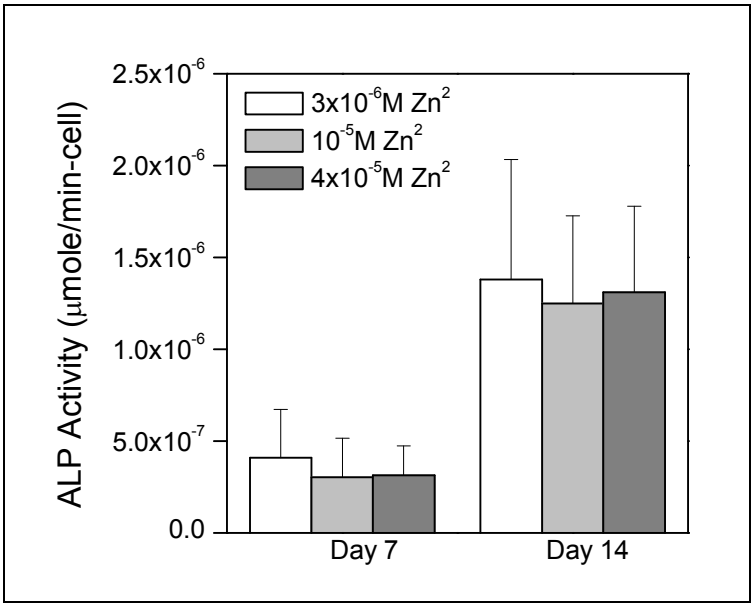

Figure 2.2. Alkaline phosphatase activity as a function of Zn^{2+} concentration and time in culture. Activity data is normalized by cell number. Bars correspond to the mean ± standard deviation for n=8 samples.

The effect of Zn^{2+} on deposition of a mineralized extracellular matrix was determined by Alizarin red staining of calcium depositions at day 21, followed by acid extraction and colorimetric analysis. Phase contrast micrographs revealed little mineralization for all treatment groups (data not shown), and analysis of the extracted dye indicated only slight differences in mineralization between groups (Figure 4).

2.5. Discussion

Zinc is a trace mineral, essential for the function of normal mammalian cell processes such as DNA [131, 132] and protein synthesis [130, 133, 134]. Previous studies using serum-free medium without zinc supplementation demonstrated diminished ALP activity [135, 136] and synthesis of collagen [136, 137] and bone sialoprotein [138]. In contrast, this study found that addition of $ZnCl_2$ had no measurable effect on ALP activity, protein synthesis, or collagen content. A likely explanation for this difference is the use of 10% serum in this study, which provided the trace amounts of zinc (3×10^{-6} M) necessary to maintain normal cell function.

One mechanism by which zinc may regulate protein synthesis is through Class I aminoacyl-tRNA synthetase activity. Aminoacyl-tRNA synthetases are the family of enzymes responsible for covalently attaching amino acids to tRNAs, and zinc has been shown to be essential for the aminoacylation step [139]. In particular, supplementation of serum-free medium with zinc sulfate resulted in a significant increase in aminoacyl-tRNA synthetase activity in MC3T3-E1 cells [130].

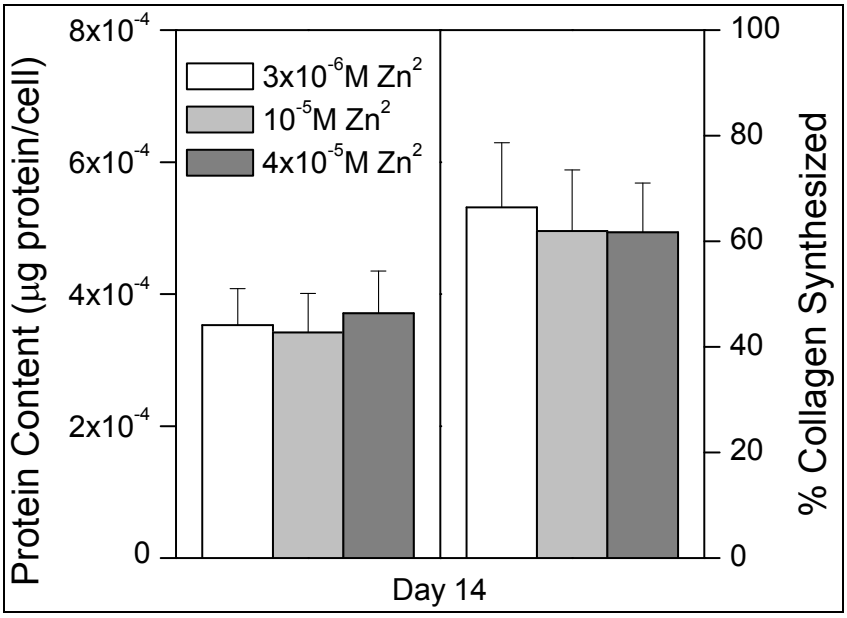

Figure 2.3. Protein and collagen synthesis as a function of Zn^{2+} concentration on Day 14. a) Total protein in cell layers normalized by cell number. b) Collagen as a percent of total protein. Bars correspond to the mean ± standard deviation for n=8 and n=4 samples for (a) and (b), respectively.

Zinc also has been shown to affect cell proliferation. Studies have shown that addition of zinc to serum-free medium results in restoration of DNA synthesis in MC3T3-E1 osteoprogenitor cells and rat femoral tissue [132, 140]. This stimulatory effect is likely regulated by new protein synthesis because pre-treatment of cultures with cycloheximide – an inhibitor of protein synthesis – abolished the stimulatory effect of zinc on DNA synthesis [132]. Further, one protein likely involved in the stimulatory effect of zinc on cell protein is insulin-like growth factor-I [140, 141], which is also known to stimulate osteoblastic cell proliferation.

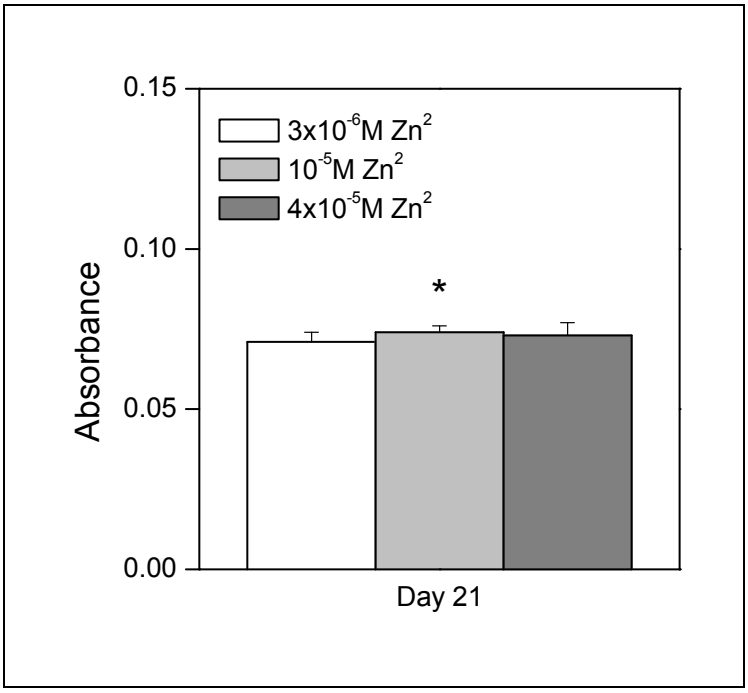

Figure 2.4. Mineral deposition as a function of Zn^{2+} concentration on Day 21. Control group was cultured in primary medium containing 3×10^{-6} M zinc without osteogenic factors. Mineral deposition was quantified as the absorbance (at 405 nm) of Alizarin red extracted from cell layers. Bars correspond to the mean ± standard deviation for n=6 samples. An asterisk denotes statistical significance compared to the control.

In this study supplementation of culture medium with soluble zinc did not affect proliferation and osteoblastic differentiation of model osteoprogenitor cells. Although the range tested is narrow it was constrained by level of zinc in 10% serum (3×10^{-6} M) and published data suggesting that 9×10^{-5} M inhibits normal osteoblast function [142]. These results of this study indicate that sufficient zinc is provided in normal serum, and that zinc supplementation through controlled release from ceramic biomaterials is not anticipated to alter development of a bone-like tissue *in vitro*, or the healing of a bone defect *in vivo*.

Acknowledgements

The authors are grateful to Elizabeth Smiley (Virginia Tech Department of Civil and Environmental Engineering, Blacksburg, VA) for measuring Zn^{2+} concentrations. This research was funded by the NIH (R03-DE015229).

Chapter 3: Fabrication and Characterization of poly(Lactic-co-Glycolic Acid)-Calcium Phosphate Composite Scaffolds

Jenni R. Popp[1], Kate E. Laflin[2], Brian J. Love[1,3], and Aaron S. Goldstein[1,2]

[1]Virginia Tech-Wake Forest School of Biomedical Engineering
Departments of [2]Chemical Engineering and [3]Materials Science and Engineering
Virginia Polytechnic Institute and State University
Blacksburg, VA 24061

3.1. Abstract

The design of polymer-calcium phosphate powder composites is a promising approach to create bioactive scaffolds for bone regeneration that combines the advantages of biodegradable polymers with osteoconductive calcium phosphate particles. Hydroxyapatite and β-tricalcium phosphate have been used to increase the osteoconductivity of polymer scaffolds, however these materials lack osteoinductive factors to induce osteoblast differentiation. Conversely, amorphous calcium phosphates (ACPs) hybridized with divalent cations exhibit controlled dissolution, releasing calcium, phosphate, and zinc ions. When combined with a biodegradable polymer matrix, ACPs could improve osteoinductivity by delivering ions to surrounding osteoprogenitor cells. In this study, a zinc-hybridized ACP (ZnACP) was synthesized that achieved sustained release of zinc, calcium, and phosphorus ions. Composite scaffolds were then fabricated by incorporating hydroxyapatite, zinc-hybridized ACP, or zirconia-hybridized ACP into a porous, sintered PLGA microsphere matrix.

Calcium, phosphorus, and zinc concentrations released from the minerals were measured. Elevated concentrations suggested sustained ion release over the course of 96 hours and enhanced solubility of ZrACP and ZnACP. X-ray diffraction analysis showed a conversion of ZrACP to a semi-crystalline material after 96 hours, but ZnACP showed no conversion after 96 hours. Scanning electron microscopy revealed a porous microsphere matrix with calcium phosphate powders distributed on the surface of the microspheres. Measurements of mechanical properties indicated that incorporation of 0.5 wt% calcium phosphates resulted in a 30% decrease in compressive modulus, while still remaining greater than 50 MPa. These results demonstrate

that ion-releasing, PLGA-calcium phosphate composites may serve as promising scaffolds for bone tissue regeneration.

3.2. Introduction

Biomaterial scaffolds are promising alternatives to autografts and allografts as bone tissue replacements. Biodegradable scaffolds facilitate tissue regeneration by providing a temporary framework for new tissue growth. Synthetic polymers such as poly(DL-lactic-co-glycolic acid) (PLGA) have been used alone and in conjunction with other materials as scaffolds for bone regeneration [143]. PLGA is a biocompatible, biodegradable co-polymer whose mechanical properties and degradation rate can be tailored by altering the ratio of the co-polymers - lactic and glycolic acid [100, 144]. PLGA scaffolds have been processed through a number of techniques including solvent casting, phase inversion, and microsphere sintering to create porous 3D architectures to facilitate osteogenic differentiation and bone healing [5, 101]. However, PLGA scaffolds lack osteoconductivity to promote osteoblast attachment, proliferation, and differentiation.

Calcium phosphate ceramics are commonly incorporated into biomaterial scaffolds to improve osteoblast adhesion and differentiation. Synthetic hydroxyapatite (HAP) has been studied extensively as a filler for bone defects and scaffold for engineered bone tissue [2]. Synthetic HAP is an osteoconductive mineral that supports osteoblast attachment. However HAP lacks osteoinductive properties and is resistant to biodegradation; which hinders new tissue in-growth and integration with native bone [55, 73]. In contrast, amorphous calcium phosphate (ACP) is a soluble, bioactive ceramic that dissolves and reprecipitates as semi-crystalline HAP under aqueous conditions [72]. ACPs may be an attractive alternative to conventional ceramics, as they have been shown to transiently stimulate osteoblastic differentiation as they release calcium and phosphate ions and raise the local pH when immersed in aqueous solution [80]. However, ACPs have seen limited use as bone grafts because of their rapid dissolution, leading to diminished mechanical properties before sufficient in-growth of new tissue can occur. Divalent cations such as Zn^{2+} and Cu^{2+} have been integrated into the ACP to retard conversion to HAP [78, 79]. Interestingly, the process of ACP conversion may serve as mechanism for delivery of osteogenic divalent cations. Moreover, availability of calcium and phosphate ions may also facilitate osteointegration through mineralization of a thin layer of calcium phosphate at the graft-host interface [85]. Therefore, a calcium phosphate ceramic that releases calcium

and phosphate ions during ceramic degradation may enhance bone regeneration and graft integration over non-degradable ceramics.

The objective of this study was to fabricate and characterize scaffolds composed of soluble and insoluble calcium phosphate minerals, embedded within a PLGA microsphere scaffold to create a bioactive, composite scaffold to stimulate bone healing. Hybridized ACPs were synthesized using zinc (ZnACP) and zirconium (ZrACP) salts with the cations acting as stabilizers to maintain the amorphous structure and solubility. Ion release from the calcium phosphates, changes in pH, and changes in crystallinity under aqueous conditions were measured when immersed in solution. ZrACP, ZnACP, and HAP powders were incorporated into the PLGA microsphere matrix at a concentration of 0.5% (w/v). Scaffold architecture was examined using SEM and mechanical properties were measured.

3.3. Materials and Methods

3.3.1. Materials

Chemicals were obtained from Sigma-Aldrich (St. Louis, MO) and materials were obtained from Fisher Scientific (Pittsburgh, PA) unless otherwise specified.

3.3.2. Calcium Phosphate Synthesis

Zr-ACP was synthesized according to Skrtic et al [71]. Briefly, a precipitate instantly formed upon simultaneous addition of 85 mL 880 mM $Ca(NO_3)$-$4H_2O$ and 40 mL 250mM $ZrOCl_2$ (GFS Chemicals, Columbus, OH) to a 125 mL solution of 536 mM Na_2HPO_4 and 11 mM $Na_4P_2O_7$-10 H_2O. Stirring was maintained at room temperature, between pH 8.5 and 9.0 for 5 min or until pH stabilized. The suspension was then vacuum filtered, rinsed twice with ammoniated water, once with cold acetone (Fisher) and then lyophilized (VirTis Bench Top, SP Industries, Warminster, PA) overnight at -70°C and 5 mTorr. Zn-ACP was synthesized using the same protocol substituting $ZnCl_2$ for $ZrOCl_2$. HAP was synthesized using the protocol for Zr-ACP and adjusting the reaction pH to 6.5 to accelerate conversion of the ACP to HAP [71]. Mineral particles were separated using commercially available sieves into the following size ranges: <106 μm; 106-300 μm; 300-500 μm; 500-710 μm; and >710 μm. Powders were placed in a desiccator until scaffold fabrication.

3.3.3. Evaluation of Calcium Phosphate Composition and Dissolution

The dissolution and conversion of calcium phosphate minerals was assessed by measuring changes in pH, Ca^{2+}, PO_4^{3-}, and Zn^{2+} concentrations, and mineral crystallinity after incubation in cell culture medium (αMEM, 10% FBS, 1% antibiotic/antimycotic). Primary medium was incubated at 37°C, 5% CO_2, and 95% relative humidity for 24 h to equilibrate pH. Minerals were then added at a concentration of 5 mg/mL. Samples were collected at predetermined time points and centrifuged to sediment minerals. The supernatant was removed to measure pH. Ion concentrations in the medium were then measured using an Agilent 7500ce inductively coupled plasma mass spectrometer (ICP-MS, Agilent Technologies, Santa Clara, CA). Sedimented minerals were then washed with acetone to remove water, frozen at -70 °C, and lyophilized. Relative crystallinity of freeze-dried minerals was determined by X-ray diffraction.

3.3.4. X-Ray Diffraction

The crystallinity of the dried minerals was analyzed by powder X-ray diffraction (XRD). The XRD profiles were recorded from 5º to 70º 2θ with CuKα radiation (λ=1.54 Å), operating at 40 kV and 40 mA. The sample was step scanned in intervals of 0.020º 2θ at a scanning speed of 2.000 deg/min.

3.3.5. Microsphere Synthesis

Microspheres were fabricated using an oil-in-water emulsion technique [145]. Poly(lactic-co-glycolic acid) (PLGA) [75:25] (M_w = 97,100, inherent viscosity[η] = 0.55-0.75 dL/g, Lactel Biodegradable Polymers, Birmingham, AL) was dissolved in methylene chloride to give a 1:5 (w/v) solution. This was injected into a stirred solution of 1% poly(vinyl alcohol) (PVA; M_w = 25,000, 88% mole hydrolyzed) using a syringe and 18-gauge needle. The resulting solution, a 1:30 oil:water (v/v) solution, was stirred at 200 rpm for 24 h to allow for complete evaporation of the methylene chloride. The microspheres were isolated from the aqueous PVA solution by vacuum filtration, washed with deionized water, and then vacuum-dried for an additional 24 h. Microspheres were then separated using commercially available sieves into the

following size ranges: <106 μm; 106-300 μm; 300-500 μm; 500-710 μm; and >710 μm. Microspheres were placed in a desiccator until scaffold fabrication.

3.3.6. Composite Scaffold Fabrication

PLGA microspheres with diameters ranging from 300 to 500 μm were poured into a 24-well plate and heated at 70°C for 24 h. For scaffolds containing 0.5% calcium phosphate (in the form of HAP, ZrACP, or ZnACP), mineral particles with diameters < 106 μm were mixed with PLGA microspheres, added to the 24-well plate and heated at 70°C for 24 h. After heating, the scaffolds were cooled at room temperature and then placed in a desiccator. Resulting scaffolds were approximately 2 mm in height and 15 mm in diameter.

3.3.7. Scanning Electron Microscopy

Scanning electron microscopy (SEM) was used to evaluate scaffold morphology after fabrication and precipitation of mineral after incubating the scaffolds in growth medium for 14 days. To induce mineral precipitation, scaffolds were incubated at 37°C, 5% CO_2, and 95% relative humidity in growth medium for 14 days. Media were changed twice per week. After 14 days, medium was removed, scaffolds were rinsed with PBS and oven-dried overnight. Scaffolds before and after incubation were mounted onto studs and sputtered with a 40 nm layer of palladium (Model 208HR, Cressington Scientific Instruments, Cranberry Township, PA). Images were acquired at 10kV using a LEO 1550 Field Emission SEM (Carl Zeiss SMT, Thornwood, NY) equipped with INCA Energy E2H X-ray Energy Dispersive Spectrometer (EDS) (Oxford Instruments, Concord, MA). Elemental EDS maps of the scaffold surfaces were performed to probe for calcium and phosphorus deposits.

3.3.8. Mechanical Testing

Compression tests were performed to determine compressive modulus and yield strength of the scaffolds. Cylindrical scaffolds (12.5 mm diameter, 22 mm height) were tested under uniaxial compression. Scaffolds were soaked in PBS for 15 hours prior to testing at 37°C in PBS. Compression tests were conducted at a crosshead speed of 0.5 mm/min. Modulus was

calculated from the slope of the stress-strain curve in the linear region. Compressive yield strength was defined as the stress at which mechanical failure occurred.

3.3.9. Statistical Analysis

Values are presented as means ± standard deviation. Statistical analyses were performed using Origin 7.5 (OriginLab Corporation, Northampton, MA). A one-way analysis of variance (ANOVA) procedure and Tukey post hoc means comparisons with a significance level of $p<0.05$ was used to determine significant differences between groups.

3.4. Results

3.4.1. Calcium Phosphate Composition

Calcium phosphate powders were synthesized according to Skrtic et al [71]. The resultant materials were white powders with a broad particle distribution with particulate diameters ranging from 1 μm to > 80 μm [80]. The composition of the calcium phosphate powders were dissolved in a sulfuric acid solution and analyzed by inductively coupled plasma mass spectrometry (ICP-MS). Table 3.1 shows the weight percentage of ions in zirconia hybridized amorphous calcium phosphate (ZrACP), zinc hybridized ACP (ZnACP), and hydroxyapatite (HAP). Oxygen and zirconium could not be detected by ICP-MS.

Table 3.1: Calcium phosphate powder compositions as determined by ICP-MS. Values are presented as weight percent.

Metal	ZrACP	Zn ACP	HAP
Al	0.01%	0.02%	0.05%
As	0.00%	0.00%	0.00%
Ca	24.88%	21.93%	22.56%
Cd	0.00%	0.00%	0.00%
Cl	7.59%	1.01%	5.08%
Co	0.00%	0.00%	0.00%
Cr	0.01%	0.01%	0.01%
Cu	0.01%	0.00%	0.08%
Fe	0.08%	0.08%	0.08%
K	0.10%	0.14%	0.30%
Mg	0.01%	0.01%	0.05%
Mn	0.00%	0.00%	0.00%
Mo	0.00%	0.00%	0.00%
Na	3.92%	2.36%	9.17%
Ni	0.00%	0.00%	0.00%
P	13.93%	16.32%	11.78%
Pb	0.00%	0.00%	0.08%
S	6.54%	6.54%	7.18%
Si	0.00%	0.00%	0.00%
Sn	0.01%	0.01%	0.00%
V	0.00%	0.00%	0.00%
Zn	0.04%	13.18%	0.16%
Ca/P (molar)	1.38	1.04	1.48

Powders were composed mainly of calcium and phosphorus with impurities of sodium, chloride, and sulfur. Calcium content of the three calcium phosphates was between 21.9% and 24.9% by weight and phosphorus content was between 11.8% and 16.3% for the three powders. Resultant molar calcium to phosphorus ratios were calculated to be 1.38, 1.04, and 1.48 for ZrACP, ZnACP, and HAP respectively. ZnACP contained 13.18 wt% zinc.

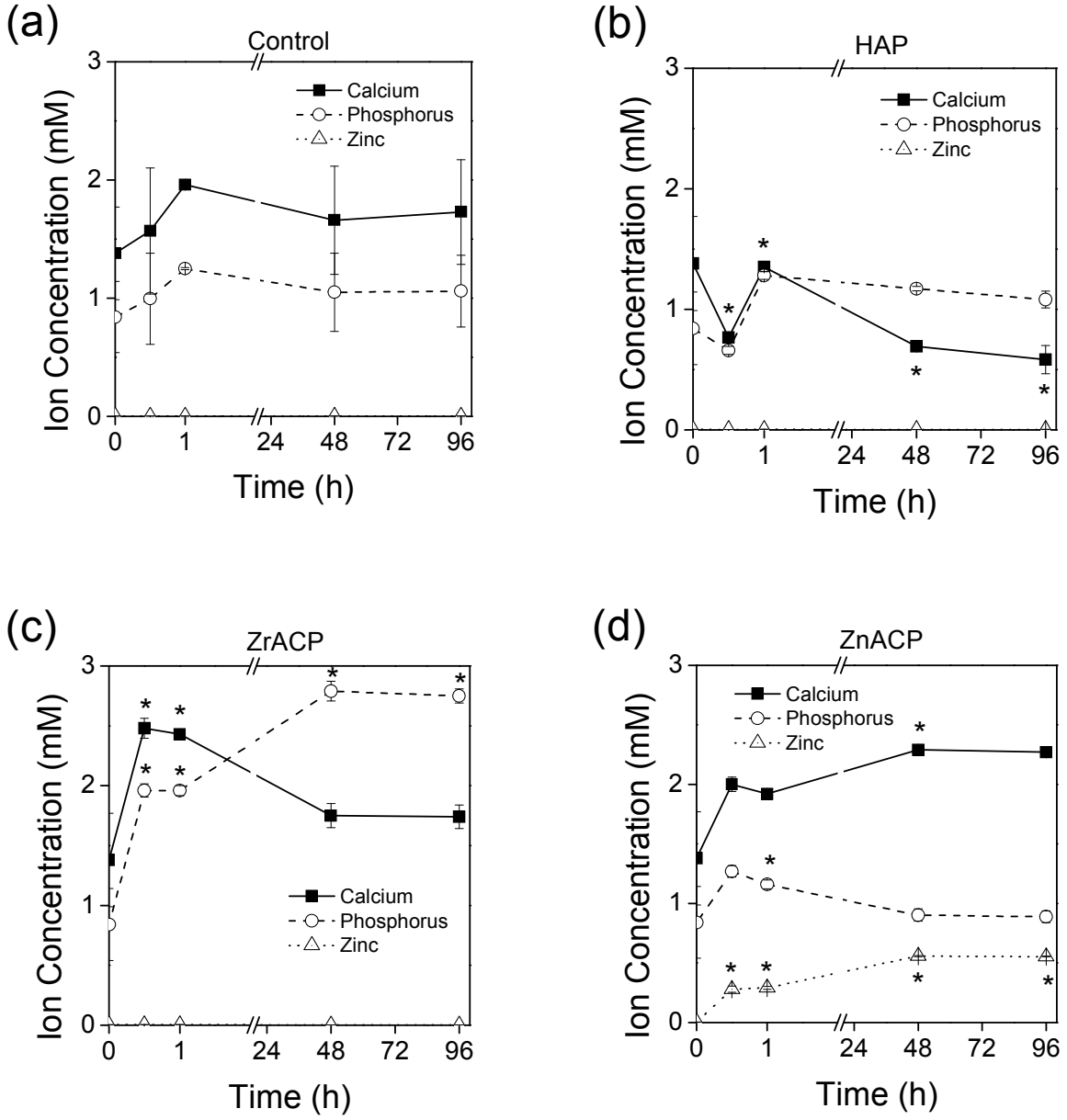

Figure 3.1. Kinetic release of calcium, phosphorus, and zinc from calcium phosphates. Ion concentrations were measured in medium containing (a) no mineral; or 5 mg/mL (b) HAP, (c) ZrACP, (d) ZnACP. Mean ion concentrations ± standard deviation for n=3. * significantly different from control containing no mineral, $p < 0.05$.

3.4.2. Acellular Dissolution of Calcium Phosphates

To investigate the dissolution of calcium phosphate minerals under aqueous conditions, 5 mg/mL of each mineral was incubated in growth medium for up to four days. ICP-MS analysis tracked ion release from calcium phosphates and demonstrates the increased solubility of ZrACP (Fig. 3.1c) and ZnACP (Fig. 3.1d) relative to HAP (Fig. 3.1b). Medium containing HAP showed

an initial decrease in calcium and phosphorus concentration at 30 min, followed by a slight increase at 1 hour (Fig. 3.1b). The concentration of calcium then decreased, while the concentration of phosphorus remained at levels not significantly different from the initial concentration, suggesting precipitation of the minerals in the cell culture medium.

Medium containing ZrACP showed a significant increase in both calcium and phosphorus after 30 min. After 48 hours, calcium concentration decreased significantly, while phosphorus concentration increased significantly (Fig. 3.1c). Similarly, ZnACP showed a slight increase in calcium and phosphorus concentrations at 30 min (Fig. 3.1d). Calcium and zinc concentrations continued to increase over 96 hours while phosphorus concentration decreased to the initial concentration.

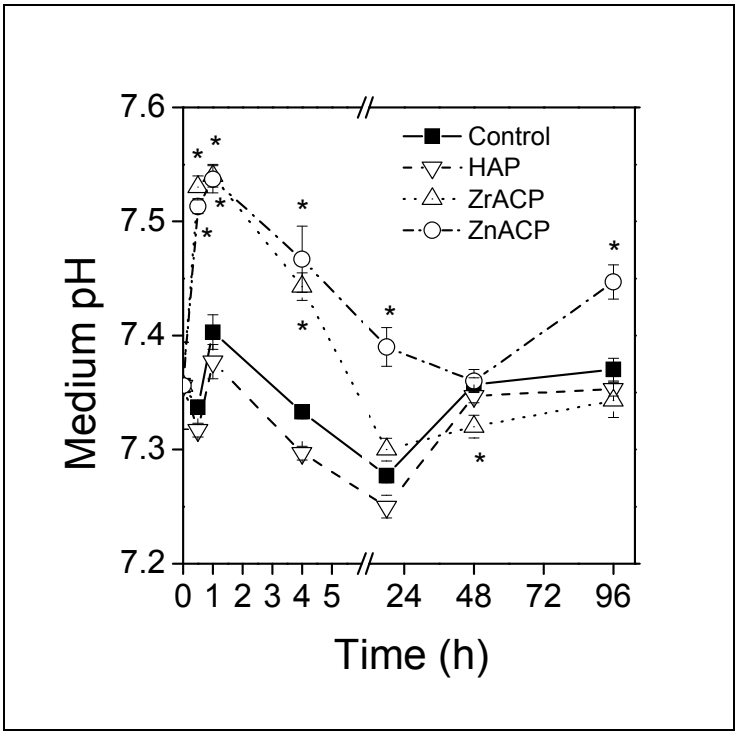

Figure 3.2. Dynamic change in pH of primary medium incubated with 5 mg/mL calcium phosphate powders. Mean +/- standard deviation for n=3 samples. * significantly different from control containing no mineral.

Figure 3.2 shows the dynamic change in pH for calcium phosphate powders in primary medium (αMEM, 10% FBS, 1% antibiotic/antimycotic). The control contained no mineral. Over the course of 96 hours, the pH of medium containing HAP was not significantly different from medium devoid of mineral. This is consistent with Figure 3.1, which shows no ion release from HAP. In contrast, ZrACP and ZnACP significantly elevated the pH of the medium at 0.5 and 1 hour. The pH remained elevated until 24 hours for ZrACP and 48 hours for ZnACP. It is important to note that minerals were incubated in medium containing sodium bicarbonate a 5% CO_2 incubator. These conditions help maintain a constant pH during cell culture. However, despite these conditions, ACP dissolution elevated medium pH.

The crystallinity of each mineral after having been incubated in growth medium for up to 96 hours was examined by x-ray diffraction. Figure 3.3a depicts the dynamic x-ray diffraction (XRD) pattern of HAP after incubation in growth medium. The patterns show distinct peaks near 12, 26 and 32 degrees, which are diffraction lines characteristic of the (100), (002), and (211) planes reported for the hexagonal HAP crystal [146, 147]. In contrast, ZnACP retained the characteristic amorphous diffraction halo and exhibited no long range ordering after 96 hours in culture medium (Fig. 3.3c). The broad peaks suggest the presence of an amorphous structure. ZrACP, however, showed signs of conversion to HAP after 48 hours, supported by the appearance of diffraction lines near 12, 26, and 32 degrees (Figure 3.3b).

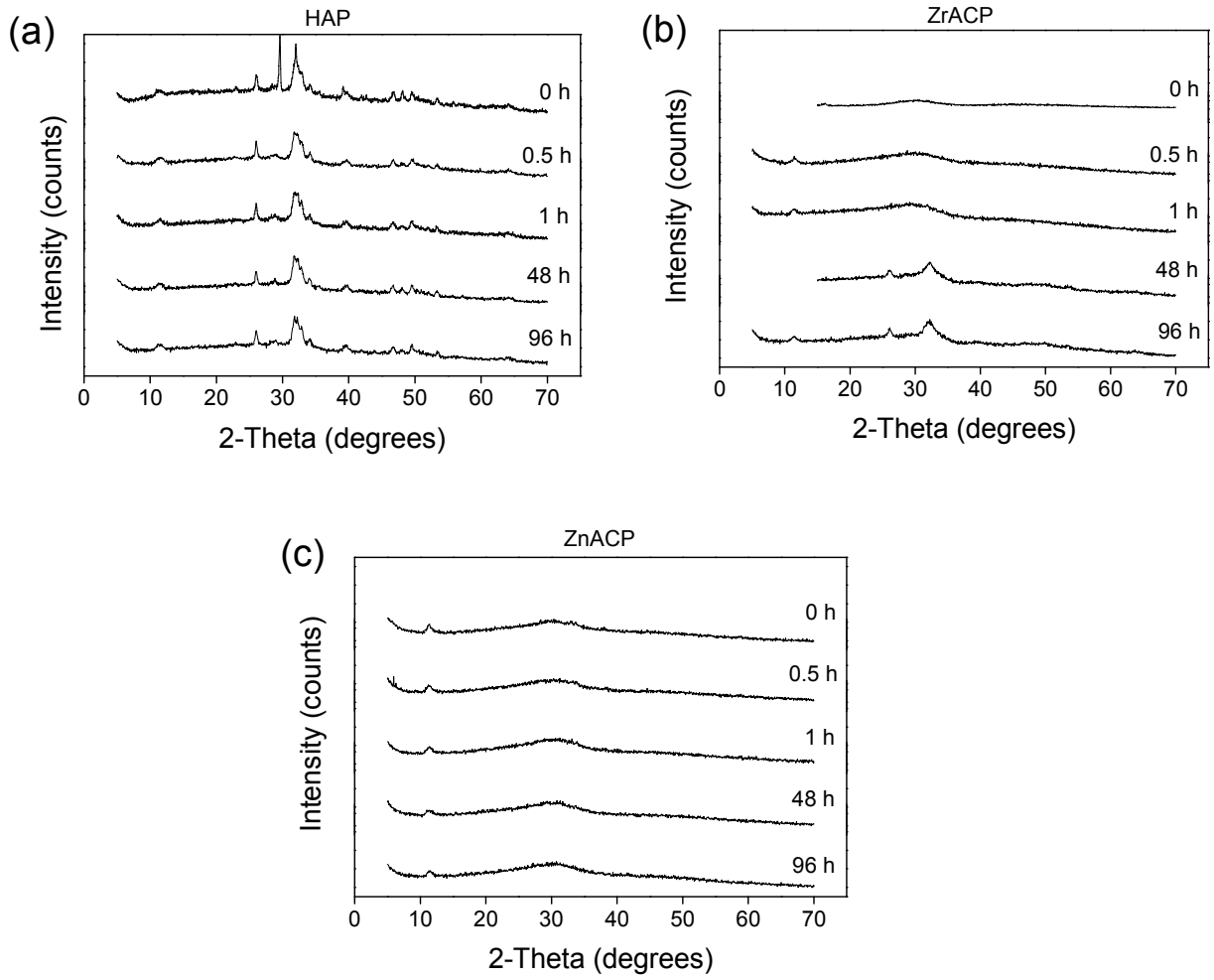

Figure 3.3. X-ray diffraction profiles of (a) HAP, (b) ZrACP, and (c) ZnACP powders after incubation in growth medium (5 mg/mL) for up to 96 hours.

3.4.3. Scaffold Characterization

Scaffold architecture was determined by SEM analysis. SEM micrographs depict the fusion of PLGA microspheres to create a porous matrix (Fig. 3.4). ZrACP and ZnACP particles were evenly distributed over the surface of the microspheres with particle sizes less than 100 μm (Fig. 3.6, 3.7, respectively). However, scaffolds containing HAP showed fewer, larger mineral deposits relative to ACPs for similar weight fractions of mineral (Fig. 3.5). Electrostatic interactions between the HAP particles may have caused large agglomerates of mineral, not seen with the ACPs.

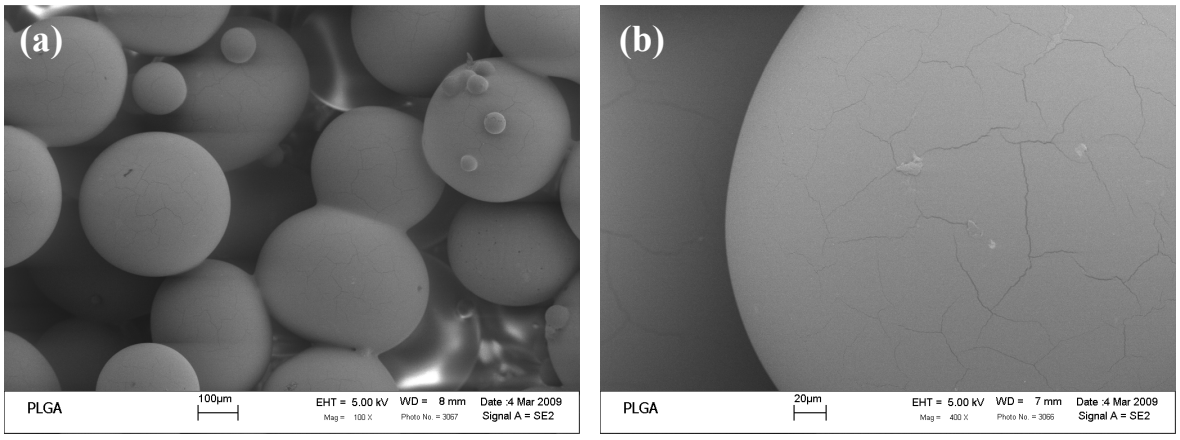

Figure 3.4. SEM micrographs of PLGA microsphere scaffolds; 100X magnification (a) showing microsphere fusion and pores; 400X magnification (b) showing smooth microsphere surface.

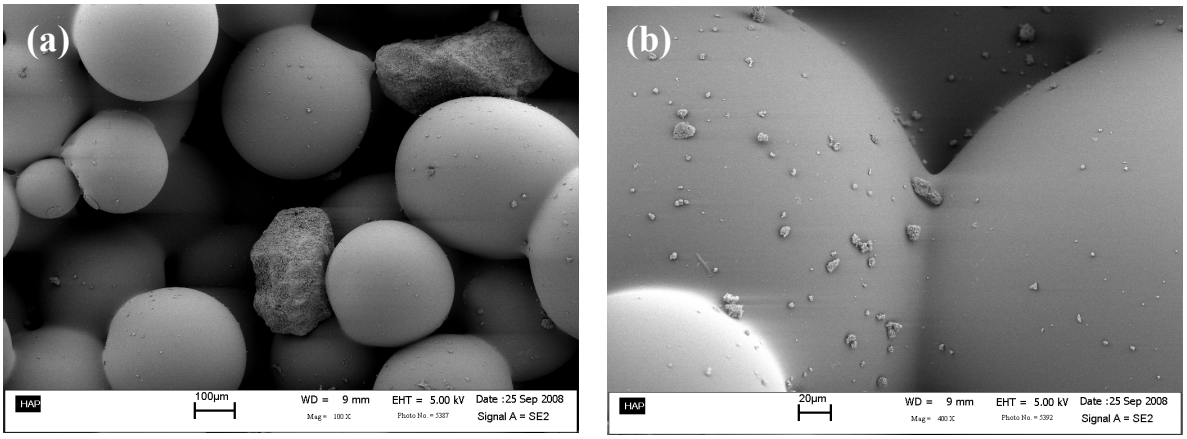

Figure 3.5. SEM micrographs of HAP scaffolds; 100X magnification (a) showing large HAP agglomerates; 400X magnification (b) showing HAP particles smaller than 20 µm.

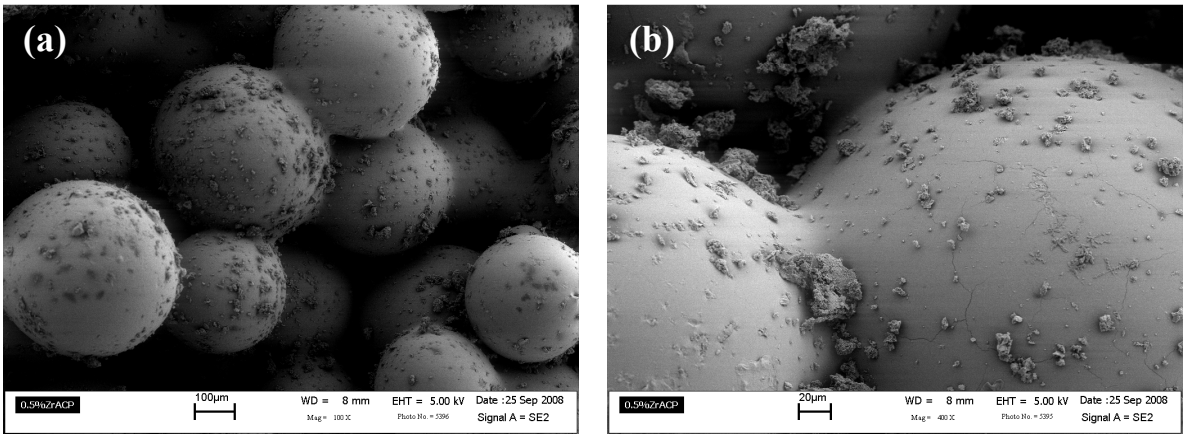

Figure 3.6. SEM Micrographs of ZrACP scaffolds; 100X magnification (a) showing an even mineral distribution; 400X magnification (b) showing ZrACP particles less than 100 µm.

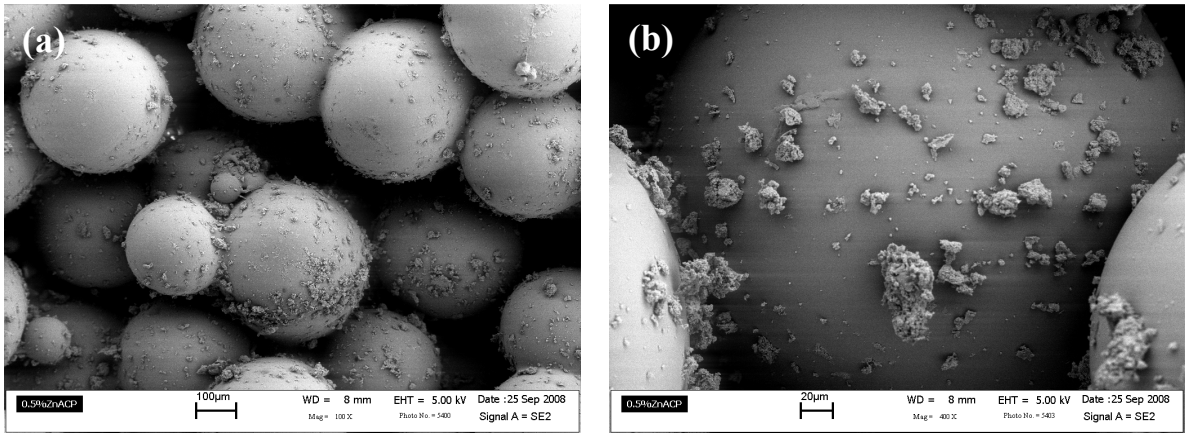

Figure 3.7. SEM Micrographs of ZnACP scaffolds; 100X magnification (a) showing an even mineral distribution; 400X magnification (b) showing ZnACP particles less than 100 µm.

EDS was used to confirm the presence of calcium and phosphate on the surface of the scaffolds. The EDS elemental map depicts calcium (red) and phosphorus (green) distributed over the surface of HAP and ZrACP scaffolds (Fig. 3.8, 3.9, respectively). Co-located deposits containing both elements are shown in yellow. Figure 3.8 demonstrates the large HAP deposits, containing both calcium and phosphate, sparsely located in the scaffolds. Few minerals are shaded yellow on ZrACP scaffolds (Fig. 3.9); however, this was a limitation of software pixel resolution. Nevertheless, spectral analysis of selected areas of mineral confirms both calcium and phosphate in mineral particles.

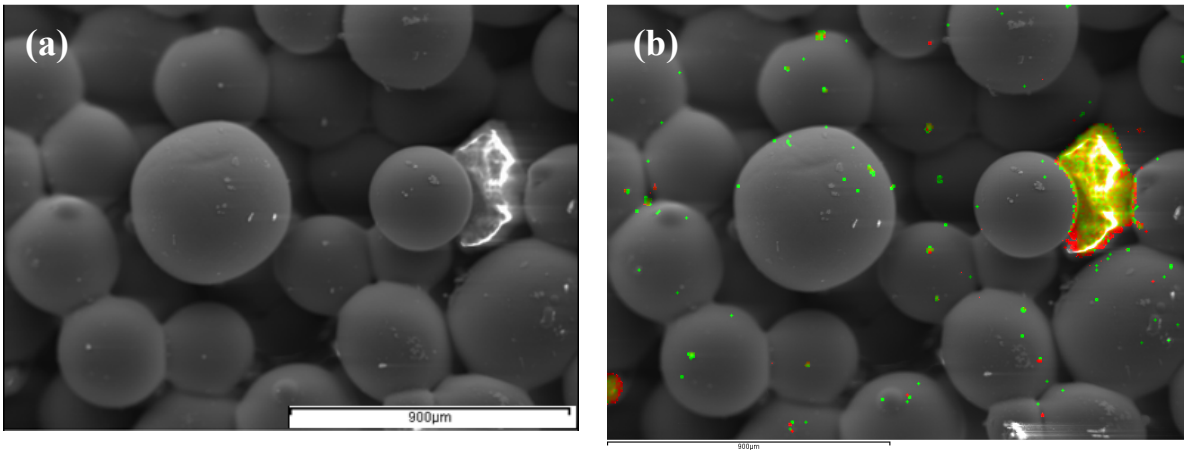

Figure 3.8. EDS of HAP scaffolds with corresponding SEM (Ca – Red, P – Green). SEM image (a) and EDS elemental map (b) of PLGA microsphere scaffold containing 0.5% HAP.

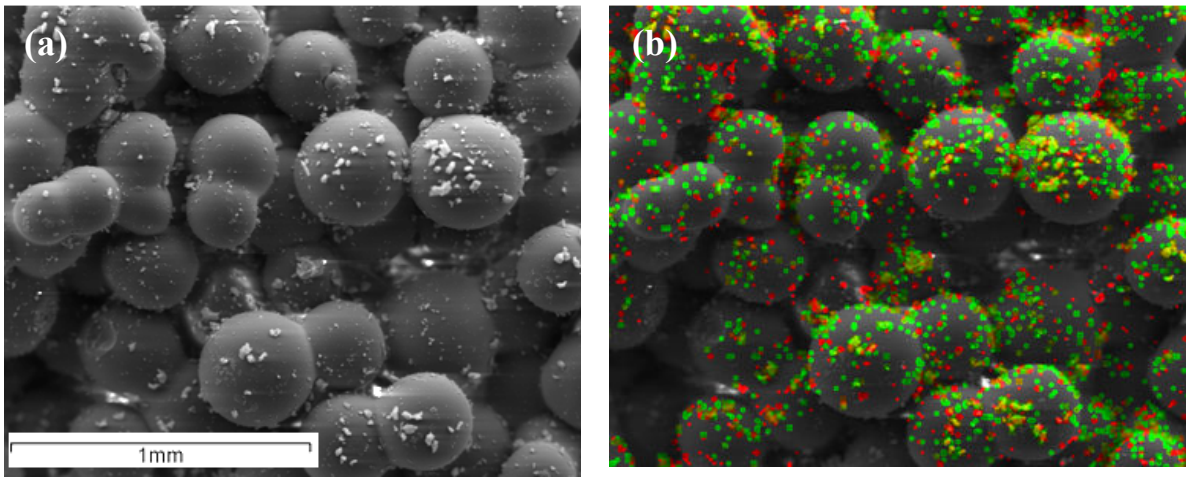

Figure 3.9. EDS with corresponding SEM (Ca – Red, P – Green). SEM image (a) and EDS elemental map (b) of PLGA microsphere scaffold containing 0.5% ZrACP.

Mechanical properties were measured to determine the effect of the addition of calcium phosphates to the PLGA microsphere matrix on scaffold integrity. Figure 3.10 is a representative stress-strain curve of the scaffolds. The toe region of the curve is the region in which the material begins to resist the load. The linear region of the curve is the elastic region and the slope is the modulus of elasticity. Scaffold yield strength was calculated as the maximum stress before plastic deformation.

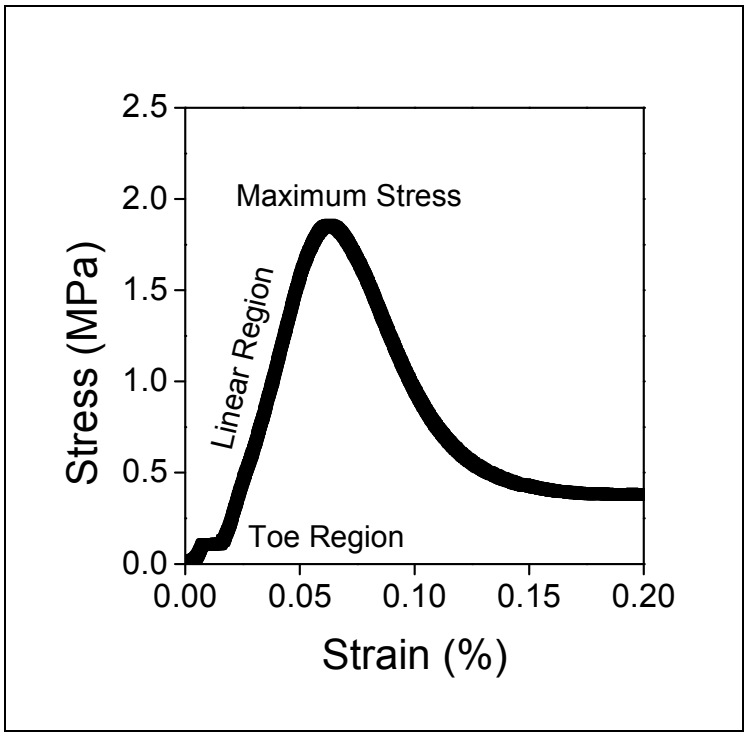

Figure 3.10. Stress-strain curve of PLGA microsphere scaffold.

The compressive modulus of composite scaffolds was approximately 30% lower than PLGA scaffolds with no mineral (Fig. 3.11). However, there was no significant difference in compressive modulus. Scaffolds containing no calcium phosphate mineral had a modulus of 127.7 ± 88.3 MPa. Scaffolds containing 0.5 wt% HAP, ZrACP, and ZnACP had moduli of 79.6 ± 39.4, 89.4 ± 49.1, and 74.2 ± 29.0 MPa, respectively. A similar result was seen with scaffold yield strength (Fig. 3.11). The compressive yield strength of composite scaffolds was lower than PLGA scaffolds, but was not significantly different.

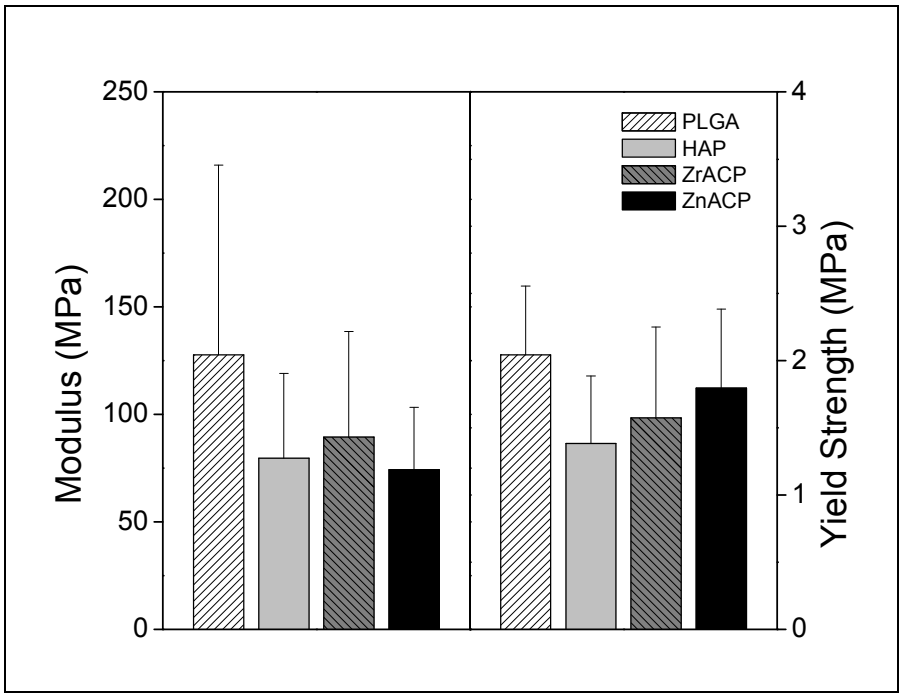

Figure 3.11. Compressive modulus and compressive yield strength of PLGA microsphere scaffolds and scaffolds containing 0.5 wt% calcium phosphates. Mean +/- standard deviation for n=4 samples.

3.4.4. Mineral Reprecipitation

Reprecipitation of minerals on the scaffolds was evaluated by SEM analysis. Scaffolds were incubated in growth medium for 14 days and medium was changed twice per week. SEM micrographs demonstrate mineral deposition at microsphere fusion zones and on the surface incorporated particles. PLGA scaffolds had deposits of salts or minerals that precipitated from the growth medium (Figure 3.12a). Composite scaffolds show evidence of significant mineral precipitation. HAP and ZnACP scaffolds appear to have mineral precipitation on to native mineral particles (Fig. 3.12b,d, respectively). When compared to HAP and ZnACP scaffolds before incubation (Fig. 3.5, 3.7 respectively), minerals on day 14 scaffolds appear smoother and have a more globular than particulate shape. ZrACP scaffolds displayed evidence of more significant mineral precipitation at microsphere fusion regions (Fig.3.12c). A smooth accumulation of mineral precipitation is shown aligned along the microsphere fusion zone.

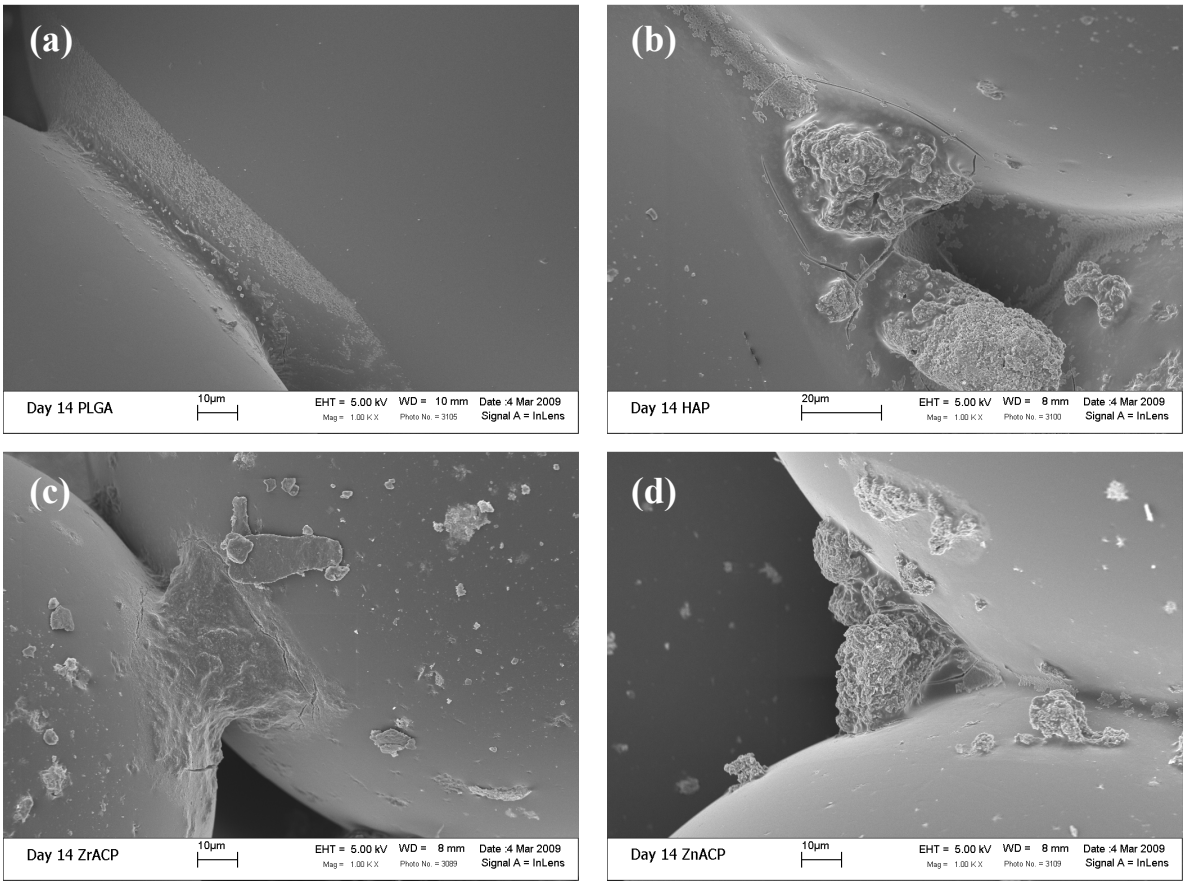

Figure 3.12. SEM micrographs of scaffolds incubated in growth medium for 14 days. Images depict mineral precipitation at microsphere fusion regions of (a) PLGA, (b) HAP, (c) ZrACP, (d) ZnACP scaffolds.

3.5. Discussion

In this study, porous, biodegradable, bioactive scaffolds were created by combining the osteoconductive properties of calcium phosphate powders with a sintered PLGA microsphere matrix. Zirconium-stabilized and zinc-stabilized ACP were synthesized to achieve sustained release of calcium, phosphorus, and zinc. The composition and dissolution kinetics of each calcium phosphate powder was investigated before adding it to the PLGA microsphere matrix. Elevated concentrations of calcium, phosphorus, and zinc suggested sustained ion release over the course of 96 hours and enhanced solubility of ZrACP and ZnACP. X-ray diffraction analysis showed a conversion of ZrACP to a semi-crystalline material after 96 hours, but ZnACP showed no conversion after 96 hours. Scaffold architecture, mechanical properties, and mineral precipitation were observed after calcium phosphate incorporation. Scanning electron

microscopy revealed a porous microsphere matrix with calcium phosphate powders distributed on the surface of the microspheres. Measurements of mechanical properties indicated that incorporation of 0.5 wt% calcium phosphates resulted in a 30% decrease in compressive modulus, but values remained about 50 MPa. These results demonstrate that ion-releasing, PLGA-calcium phosphate composites may serve as promising scaffolds for bone tissue regeneration.

Analysis of calcium phosphate composition revealed powders composed mainly of calcium and phosphorus, with impurities of sodium, chloride, and sulfur. The precipitation of sodium chloride during the calcium phosphate synthesis is likely due to saline saturation by the solution reactants (Na_2HPO_4, $Na_4P_2O_7$-10 H_2O, $ZnCl_2$, or $ZrOCl_2$). The presence of sulfur may be an artifact of the ICP-MS analysis process, in which the minerals were dissolved in sulfuric acid. Calcium phosphate ratios were 1.38, 1.04, and 1.48 for ZrACP, ZnACP, and HAP respectively. These ratios were lower than the expected 1.45 for ACPs [72] and 1.60 for HAP [65]. The presence of impurities such as sodium phosphate or zinc phosphate that co-precipitated during the calcium phosphate synthesis likely raised the phosphate concentration but decreased the calcium to phosphate ratio. Small amounts of HPO_4^{2-} can also lower the Ca/P ratio of ACPs [72].

Medium containing HAP showed no significant increase in ion concentrations relative to control medium devoid of mineral. However, calcium concentration decreased significantly after 48 hours, suggesting mineral precipitation. It is possible that while HAP did not release calcium or phosphorus into the culture medium, but the mineral provided a surface to initiate crystallization of a form of calcium phosphate.

Medium containing ZrACP and ZnACP showed significant increases in both ionic calcium and phosphorus concentrations after 30 min. After 48 hours, calcium concentration decreased significantly, as phosphorus concentration increased significantly in medium containing ZrACP. This is explained by the continued release of calcium and phosphorus from ZrACP and a simultaneous reprecipitation of calcium phosphate. In medium containing ZnACP, calcium and zinc continued to increase over 96 hours while phosphorus decreased to the initial concentration. As with ZrACP, this is explained by the release of the ions from ZnACP and reprecipitation of minerals such as calcium phosphate ($Ca_3(PO_4)_2$) and zinc phosphate ($Zn_3(PO_4)_2$). Zinc and calcium compete as divalent cations to bind with phosphate and form

precipitates. While all three ions continue to be released from the dissolving ZnACP, phosphorus would be expected to reprecipitate at a higher rate than calcium and zinc.

The pH of the medium containing ZrACP paralleled the concentration of calcium, showing a significant increase early and then decreasing to initial levels as calcium concentration decreased. The pH of the medium containing ZnACP also increased significantly after one hour, coinciding with the initial ion release. Such a localized increase in pH is commonly seen with soluble calcium phosphates, due to mineral dissolution [80].

The crystallinity of each mineral incubated in growth medium for up to 96 hours was examined by x-ray diffraction. The XRD pattern of hexagonal HAP shows distinct peaks near 27 and 32 degrees. ZrACP, however, showed signs of conversion to a poorly crystalline apatite structure, with appearance of peaks at 27 and 32 degrees after 48 hours. ACP likely dissolves and then reprecipitates as a thin crystalline layer on the initial surface [65]. The mineral precipitate is a poorly crystalline HAP mineral, probably with contaminants such as carbonates and other salts contained in the culture medium [70]. In contrast, ZnACP had the characteristic amorphous halo and exhibited no long range ordering after 96 hours in culture medium. Hybridizing ACP with zinc maintained an amorphous structure longer than hybridizing the mineral with zirconium.

The sustained ion release from hybridized ACPs is consistent the work of others who have shown increased dissolution and slowed conversion of doped ACPs [80, 83]. Certain metal ions such as magnesium and zinc stabilize the amorphous structure and impede the formation of a more crystalline apatite structure [79]. It is thought that the metal ions adsorb to the growing crystallites and inhibit further growth by affecting the exchange of calcium and phosphate ions between the solid and the solution [71, 78]. The XRD profile of ZnACP (Fig. 3.3c) is consistent with an inhibition of crystallization.

Slower conversion of hybridized ACPs to HAP and sustained ion release is desired for composites designed to stimulate bone healing. HAP is not sufficiently soluble to be effective as a bioactive, mineralizing material. These stabilized ACPs can actively promote osteoblast mineralization by providing a richer, sustained source of calcium and phosphate [80]. Therefore, the calcium phosphate powders capable of ionic release were incorporated into a sintered PLGA microsphere matrix.

SEM images depict the fusion of PLGA microspheres to create a porous matrix. ZrACP and ZnACP were uniformly spread over the surface of the microspheres with particle sizes less

than 100 μm, but HAP particles were sparse and greater than 100 μm. Before addition to the PLGA microsphere matrix, minerals were sieved to select particles less than 106 μm. However, greater electrostatic interactions between the HAP particles relative to ACP particles may explain larger mineral agglomerates on HAP scaffolds. Skrtic et al showed that ACPs hybridized with Si and Zr had a higher specific surface area than unhybridized ACPs suggesting that the hybridizers may have decreased ACP particle size or degree of agglomeration [71].

Mechanical testing of scaffolds resulted in a decrease in compressive modulus and compressive yield strength for scaffolds with calcium phosphates. This is consistent with similar scaffolds made with calcium phosphate-loaded microsphere scaffolds [93]. Addition of the calcium phosphate powders likely interfered slightly with the polymer fusion process, causing weaker connections between particles and slightly lower mechanical integrity.

The results of this investigation demonstrate the enhanced solubility of ACPs, relative to HAP, by stabilizing them with Zr or Zn. Furthermore, differences in ion release profiles and mineral conversion between ZrACP and ZnACP have the potential to elicit different cell responses. Combining these ACPs with PLGA microspheres to create a composite scaffold could enhance osteoconductivity and mineralization in a bone defect.

Chapter 4: In Vitro Evaluation of poly(Lactic-co-Glycolic Acid)-Calcium Phosphate Composite Scaffolds

Jenni R. Popp[1], Kate E. Laflin[2], Brian J. Love[1,3], and Aaron S. Goldstein[1,2]

[1]Virginia Tech-Wake Forest School of Biomedical Engineering
Departments of [2]Chemical Engineering and [3]Materials Science and Engineering
Virginia Polytechnic Institute and State University
Blacksburg, VA 24061

4.1. Abstract

Polymer-calcium phosphate powder composites are promising scaffolds for bone tissue engineering that combine the advantages of biodegradable polymers with osteoconductive calcium phosphate particles to stimulate osteoblast adhesion and differentiation. Amorphous calcium phosphates (ACPs) have been hybridized with divalent cations to achieve sustained dissolution and release of calcium and phosphate ions. Supplementation of culture medium with calcium and phosphate ions has been shown to stimulate osteoblast differentiation. When combined with a biodegradable polymer matrix, ACPs could improve osteoinductivity by delivering osteogenic ions to surrounding osteoprogenitor cells. To investigate the effect of calcium phosphate release from composite PLGA-calcium phosphate scaffolds, hydroxyapatite (HAP), zinc-hybridized ACP (ZnACP), or zirconia-hybridized ACP (ZrACP) were incorporated into a porous, sintered PLGA microsphere matrix. MC3T3-E1 cells were cultured in sintered PLGA microsphere scaffolds with or without 0.5 wt% HAP, ZrACP, or ZnACP for 14 days. Cell number, alkaline phosphatase activity, and gene expression were measured to evaluate the effect of the three calcium phosphates on osteoblast proliferation and differentiation. Cell number on the composite scaffolds was greater than on PLGA controls and a significant increase in cell number was measured on ZrACP and ZnACP scaffolds from day 7 to day 10. Alkaline phosphatase activity was significantly elevated on ZnACP scaffolds compared to all other scaffolds on day 7. Prostaglandin E_2 accumulation in culture media was highest on composite

scaffolds on day 4 and 7, and significantly greater only on ZnACP scaffolds on day 10. Gene expression of osteopontin (OPN) was enhanced on all composite scaffolds and osteocalcin (OCN), bone sialoprotein (BSP), osterix (OSX), and vascular endothelial growth factor A (VEGF-A) were elevated on HAP scaffolds only. These results indicate the addition of calcium phosphate minerals to PLGA scaffolds supported cell growth and stimulated osteogenic differentiation, making the scaffolds a promising alternative for bone tissue regeneration.

4.2. Introduction

Biodegradable scaffolds facilitate tissue regeneration by providing a temporary framework for new tissue growth. Synthetic polymers such as poly(DL-lactic-co-glycolic acid) (PLGA) have been used alone and in conjunction with other materials as scaffolds for bone regeneration [143]. PLGA is a biocompatible, biodegradable co-polymer whose mechanical properties and degradation rate can be tailored by altering the ratio of the co-polymers - lactic and glycolic acid [100, 144]. PLGA scaffolds have been processed through a number of techniques including solvent casting, phase inversion, and microsphere sintering to create porous 3D architectures to facilitate osteogenic differentiation and bone healing [5, 101]. However, PLGA scaffolds lack osteoconductivity to promote osteoblast attachment, proliferation, and differentiation.

Calcium phosphate ceramics are commonly incorporated into biomaterial scaffolds to improve osteoblast adhesion and differentiation. Synthetic HAP has been studied extensively as a filler for bone defects and scaffold for engineered bone tissue [2]. However it lacks osteoinductive properties and is resistant to biodegradation [55, 73]. In contrast, amorphous calcium phosphate (ACP) is a soluble, bioactive ceramic that dissolves and reprecipitates as semi-crystalline HAP under aqueous conditions [72]. However, ACPs have seen limited use as bone grafts because of their rapid dissolution, leading to diminished mechanical integrity. Divalent cations such as Zn^{2+} and Cu^{2+} have been shown to stabilize ACP to retard conversion to HAP and achieve sustained ion release [78, 79]. Further, stabilized ACPs have been shown to transiently stimulate osteoblastic differentiation as they release calcium and phosphate ions and raise the local pH *in vitro* [80]. Calcium and phosphate ions are thought to be modulators of osteoblast differentiation and mineralization *in vitro* [119-122] and may also facilitate osteointegration through mineralization of a thin layer of calcium phosphate at the graft-host interface [85]. We hypothesize that incorporation of soluble calcium phosphate minerals into a biodegradable polymer matrix can improve graft osteoinductivity to stimulate osteoblast differentiation, enhance graft integration and facilitate bone healing.

Osteoblast differentiation *in vitro* is characterized by three stages of development and differentiation: proliferation, matrix synthesis and maturation, and matrix mineralization [50]. The proliferation phase is marked by a rapid increase in cell number. The matrix maturation phase is characterized by high levels of ALP activity and synthesis of COLI. The final, matrix mineralization phase is characterized by expression of extracellular matrix proteins such as OPN,

OCN, and BSP [103]. Other molecules involved in the differentiation of osteoblasts include bone morphogenetic proteins, prostaglandins, and the transcription factor, osterix. Bone morphogenetic proteins (BMPs) are members of the transforming growth factor beta (TGF-β) family of proteins [20]. BMP-2, -4, and -7 are secreted by osteoblasts and bind cell receptors to initiate a signaling cascade that stimulates bone formation [20]. Prostaglandins are thought to mediate the effects of mechanical stress [148] and surface roughness on osteoblasts [149]. Osterix is a transcription factor that is responsible for the induction of osteocalcin and is required for osteoblast differentiation [150]. Furthermore, overexpression of OSX results in increased expression of markers of osteoblast differentiation [151].

The objective of this study was to determine how soluble and insoluble calcium phosphate minerals, embedded within PLGA microsphere scaffolds, affected the osteogenic differentiation of MC3T3-E1 osteoprogenitor cells. MC3T3-E1 cells are a mouse clonal cell line that express markers of the osteoblast phenotype, including alkaline phosphatase (ALP) activity, type I collagen (COLI), osteopontin (OPN), and osteocalcin (OCN) and are used as a model to study the effects of materials on osteoblast differentiation [152]. Three different types of calcium phosphate powders were incorporated at a concentration of 0.5 wt%. Scaffold architecture was observed using SEM. Cell number, alkaline phosphatase activity, and PGE_2 concentration were measured at 7 and 10 days of culture. Gene expression of markers of osteoblast differentiation was measured 14 days post-seeding.

4.3. Materials and Methods

4.3.1. Materials

Chemicals were obtained from Sigma-Aldrich (St. Louis, MO) and materials were obtained from Fisher Scientific (Pittsburgh, PA) unless otherwise specified.

4.3.2. Calcium Phosphate Synthesis

Zr-ACP was synthesized according to Skrtic et al [71]. Briefly, a precipitate instantly formed upon simultaneous addition of 85 mL 880 mM $Ca(NO_3)$-$4H_2O$ and 40 mL 250mM $ZrOCl_2$ (GFS Chemicals, Columbus, OH) to a 125 mL solution of 536 mM Na_2HPO_4 and 11 mM $Na_4P_2O_7$-10 H_2O. Stirring was maintained at room temperature, between pH 8.5 and 9.0 for 5

min or until pH stabilized. The suspension was then vacuum filtered, rinsed twice with ammoniated water, once with cold acetone (Fisher) and then lyophilized (VirTis Bench Top, SP Industries, Warminster, PA) overnight at -70°C and 5 mTorr. Zn-ACP was synthesized using the same protocol substituting $ZnCl_2$ for $ZrOCl_2$ at the same concentration. HAP was synthesized using the protocol for ZrACP and adjusting the reaction pH to 6.5 to accelerate conversion of the ACP to HAP. Mineral particles were separated using commercially available sieves into the following size ranges: <106 μm; 106-300 μm; 300-500 μm; 500-710 μm; and >710 μm. Powders were placed in a desiccator until scaffold fabrication.

4.3.3. Microsphere Synthesis

Microspheres were fabricated using an oil-in-water emulsion technique [145]. Poly(lactic-co-glycolic acid) (PLGA) [75:25] (M_w = 97,100, inherent viscosity [η] = 0.55-0.75 dL/g, Lactel Biodegradable Polymers, Birmingham, AL) was dissolved in methylene chloride to give a 1:5 (w/v) solution. This was injected into a solution of 1% poly(vinyl alcohol) (PVA; M_w = 25,000, 88% mole hydrolyzed) stirring at 200 rpm using a syringe and 18-gauge needle. The resulting solution, a 1:30 oil:water (v/v) solution, was stirred at 200 rpm for 24 h to allow for complete evaporation of the solvent. The microspheres were isolated from the aqueous PVA solution by vacuum filtration, washed with deionized water, and then vacuum-dried for an additional 24 h. Microspheres were then separated using commercially available sieves into the following size ranges: <106 μm; 106-300 μm; 300-500 μm; 500-710 μm; and >710 μm. Microspheres were placed in a desiccator until scaffold fabrication.

4.3.4. Composite Scaffold Fabrication

Substrates for studies were three-dimensional scaffolds consisting of PLGA microspheres and calcium phosphate particles. PLGA microspheres with diameters ranging from 300 to 500 μm were poured into a 24-well plate and heated at 70°C for 24 h. For scaffolds containing 0.5% calcium phosphate (in the form of HAP, ZrACP, or ZnACP), mineral particles with a size less than 106 μm were mixed with PLGA microspheres, added to the 24-well plate and heated at 70 °C for 24 h. After heating, the scaffolds were cooled at room temperature and then placed in a desiccator. Resulting scaffolds were approximately 2 mm in height and 15 mm in diameter. The scaffolds were sterilized under UV light for 24 hours prior to cell culture studies.

4.3.5. Scanning Electron Microscopy

Scaffold architecture was determined by scanning electron microscopy (SEM) [153]. Briefly, scaffolds were mounted onto studs and sputtered with 20 nm of gold-palladium (Model 208HR, Cressington Scientific Instruments, Cranberry Township, PA). Images were acquired using a LEO 1550 Field Emission SEM (Carl Zeiss SMT, Thornwood, NY) operating at 5-10 kV with an 8 mm working distance.

4.3.6. Cell Culture

The capacity of the various calcium phosphates to stimulate cell proliferation and osteoblastic differentiation was determined by culturing MC3T3-E1 pre-osteoblasts (ATCC, Manassas, VA) on the scaffolds. MC3T3-E1 cells, passage 20 and below, were seeded onto constructs at a density of 7.5×10^4 cells per substrate and allowed to attach overnight in primary medium (minimum essential medium alpha modification (αMEM, Invitrogen, Gaithersburg, MD)), 10% fetal bovine serum (FBS, Gemini Bioproducts, Calabasas, CA), and 1% antibiotic/antimycotic (penicillin, streptomycin, neomycin, fungizone; Invitrogen). The following day, denoted as day 0, culture medium was replaced with differentiation medium (primary medium supplemented with 0.13 mM L-ascorbic acid 2-phosphate). β-glycerophosphate, a substrate commonly used in osteogenic medium [116], was excluded to more rigorously test cell response to ACP dissolution. Cells were grown in a 5% CO_2, 95% relative humidity incubator at 37ºC, and culture medium was changed every 3 to 4 days. Samples were collected at days 7 and 10 to measure cell number and ALP activity and at day 14 to measure gene expression of bone extracellular matrix proteins: OCN, OPN, BSP, and COLI; the transcription factor OSX, and growth factors: BMP2, BMP4, and VEGF-A. Samples of conditioned medium were collected on days 4, 7, and 10 to measure PGE_2. Cells cultured on tissue culture polystyrene (TCPS) and PLGA scaffolds, containing no calcium phosphate, were used as controls.

4.3.7. Cell Number

Cell number was quantified by fluorometric analysis of total DNA content using Hoechst 33258 dye (Sigma Aldrich) [80]. Briefly, scaffolds were cut up to facilitate detachment of cells within the scaffold and transferred into 1 mL of 10 mM ethylenediaminetetraacetic acid (EDTA),

pH 12.3, and stored at -70 °C until analysis. For analysis, samples were thawed, hand-sonicated and briefly centrifuged to sediment microspheres and calcium phosphate particles. DNA standards of 0, 1, 2, 4, 6, 8 μg were prepared in 1 mL of 10mM EDTA (pH 12.3). Here, a 50 μg/mL DNA solution gives an absorbance of 1.00 at 260 nm. A volume of 0.2 mL of 1M KH_2PO_4 was added to neutralize pH of samples and standards. Volumes of 0.4 mL of samples or DNA standards and 1.6 mL of dye solution (5 μL of 1 mg/mL Hoechst 33258 dye in 50 mL of 10 mM Trizma hydrochloride, 100 mM NaCl, pH 7.0) were combined, and fluorescence was measured immediately using a DyNAQuant 200 (Hoefer Scientific Instruments, San Francisco, CA). A linear standard curve of fluorescence with respect to concentration of the DNA standards was used to determine DNA concentrations of the unknown samples, and a conversion factor of 9.1 pg DNA per cell was used to calculate cell number. All measurements were performed in duplicate.

4.3.8. Alkaline Phosphatase Activity

ALP activity was determined colorimetrically by the hydrolysis of *p*-nitrophenyl phosphate to produce *p*-nitrophenol and inorganic phosphate [154]. Scaffolds were rinsed with PBS, cut and collected into 990 μL of TGT solution (50 mM Trizma hydrochloride, 100 mM glycine, 0.1% Triton X100) and 10 μL of protease inhibitors (0.2 mg/mL aprotinin, 0.2 mg/mL leupeptin, and 0.1 mg/mL pepstatin A (Calbiochem, La Jolla, CA)) and stored at -70°C until analysis. For analysis, samples were thawed, hand-sonicated, and briefly centrifuged. The ALP reagent was prepared according to the manufacturer's instructions (Biotron Diagnostics, Hemet, CA). ALP activity was measured by adding 500 μL of ALP reagent at 37°C to 200 μL of sample. After incubating for 15 min, 500 μL of 0.3 M NaOH was added to quench the reaction. The absorbance of each sample was then measured at 405 nm using a Multiskan RC plate reader (Labsystems, Helsinki, Finland). Enzyme activity was calculated from the slope of absorbance versus time and then normalized by cell number and reported in units of μmoles of *p*-nitrophenol per minute, per cell.

4.3.9. Gene Expression (Quantitative RT-PCR)

The gene expression of target genes was determined quantitatively by real-time RT-PCR [155]. Total RNA was isolated from cell layers using the RNeasy mini kit with on-column

DNase digestion (Qiagen, Valencia, CA) according to the manufacturer's instructions. Total RNA concentration was quantified using RiboGreen RNA reagent kit (Invitrogen, Carlsbad, CA) according to manufacturer's instructions. Next, 1 μg of RNA was reverse transcribed to cDNA using the Superscript FirstStrand cDNA Synthesis kit (Invitrogen) with random hexamers as primers. Real-time PCR amplification of target cDNA was performed using an ABI 7300 sequence detection system (Applied Biosciences, Foster City, CA), SYBR green master mix (Applied Biosystems) and specific primers for β-actin, OPN, OCN, BSP, BMP-2, BMP-4, OSX, and VEGF-A (Integrated DNA Technologies, Coralville, IA). Primer sequences are shown in Table 4.1. Quantification of target gene expression was performed using the $2^{-\Delta\Delta Ct}$ method, with β-actin as the internal control [156].

Table 4.1. Mouse primer sequences for quantitative RT-PCR

PROTEIN	FORWARD PRIMER	REVERSE PRIMER	PRODUCT SIZE (bps)	ACCESSION NUMBER
β-actin	TGCTCCCCGGGCTGTATT	ACATAGGAGTCCTTCTGACCCATT	87	NM_007393
BMP-2	CGCAGCTTCCATCACGAA	GTTCCCGGAAGATCTGGAGTTC	136	NM_007553
BMP-4	TGTGAGGAGTTTCCATCACGAA	TGAGGTTGAAGAGGAAACGAAAA	86	NM_007554
Osterix	AGCAAATTTGGCGGCTCTAG	GAAAGGTCAGCGTATGGCTTCT	83	NM_130458
VEGF-A	GCAGGCTGCTGTAACGATGA	CATCTCTCCTATGTGCTGGCTTT	111	NM_009505
Osteopontin	GATTTGCTTTTGCCTGTTTGG	TGAGCTGCCAGAATCAGTCACT	67	NM_009263
Osteocalcin	CCCTGGCTGCGCTCTGT	GACATGAAGGCTTTGTCAGACTCA	76	NM_007541
Bone Sialoprotein	CATGCCTACTTTTATCCTCCTCTGA	CGGAACTATCGCAGTCTCCATT	87	NM_008318

4.3.10. Prostaglandin E_2 Accumulation

Prostaglandin E_2 concentration in conditioned medium was determined using enzyme linked immunoassay (Assay Designs, Ann Arbor, MI) according to the manufacturer's

instructions [157]. Samples of conditioned medium were collected into 1.5 mL microcentrifuge tubes on days 4, 7, and 10. The assay was performed according to the manufacturer's instructions. Absorption was measured on a plate reader Multiskan RC plate reader (Labsystems, Helsinki, Finland) and converted to concentration using standards provided by the manufacturer.

4.3.11. Statistical Analysis

Values are presented as means ± standard deviation. Data was analyzed using a one-way ANOVA followed by Tukey post hoc means comparisons. An asterisk denotes a statistically significant difference ($p<0.05$) relative to the TCPS control. A pound symbol denotes a statistically significant difference ($p<0.05$) relative to PLGA scaffolds prepared without calcium phosphates. Studies were performed in duplicate with n=4 samples and combined to n=8 samples for graphical presentation and statistical analysis.

4.4. Results

4.4.1. Scaffold Architecture

PLGA microspheres were combined with three different calcium phosphate powders and sintered to create a porous, composite scaffold. Scaffold architecture was determined by SEM analysis. SEM micrographs depict the fusion of PLGA microspheres to create a porous matrix (Fig. 4.1a). ZrACP and ZnACP particles were evenly distributed over the surface of the microspheres with particle sizes less than 100 μm (Fig. 4.1c, d, respectively). However, scaffolds containing HAP showed fewer, larger mineral deposits relative to ACPs for similar weight fractions of mineral (Fig. 4.1b).

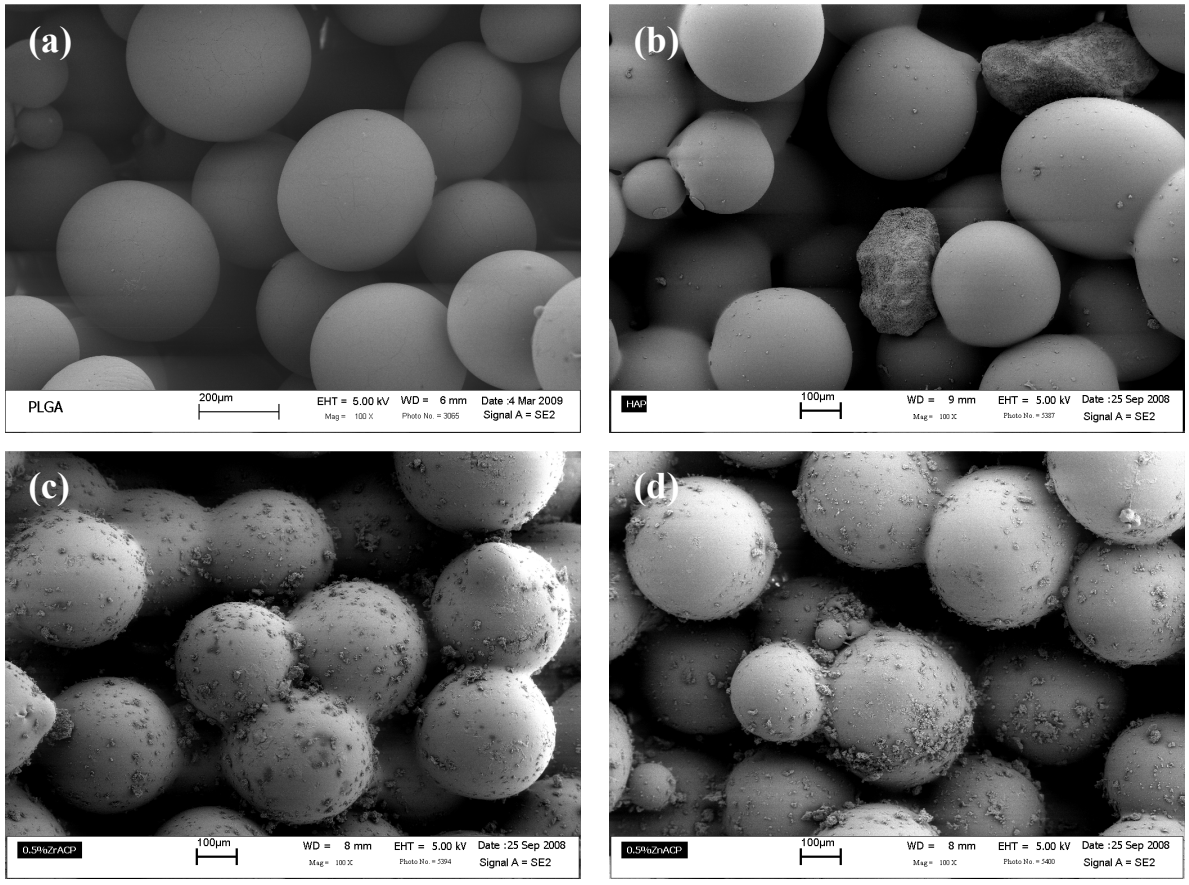

Figure 4.1. Scanning electron micrographs of scaffolds (a) PLGA (b) HAP, (c) ZrACP, (d) ZnACP.

4.4.2. Cell Number

The capacity of the three calcium phosphates to support cell proliferation and stimulate osteoblast differentiation was determined by culturing MC3T3-E1 pre-osteoblasts on the composite scaffolds. Cell number on all scaffolds was significantly diminished relative to TCPS controls at both time points (Fig. 4.2), indicative of decreased cell adhesion on the scaffolds. However, cell number on all composite scaffolds was significantly greater than on PLGA controls, suggesting the calcium phosphates enhance initial osteoblast attachment. Furthermore, a significant increase in cell number was observed on TCPS, ZrACP, and ZnACP scaffolds between time points.

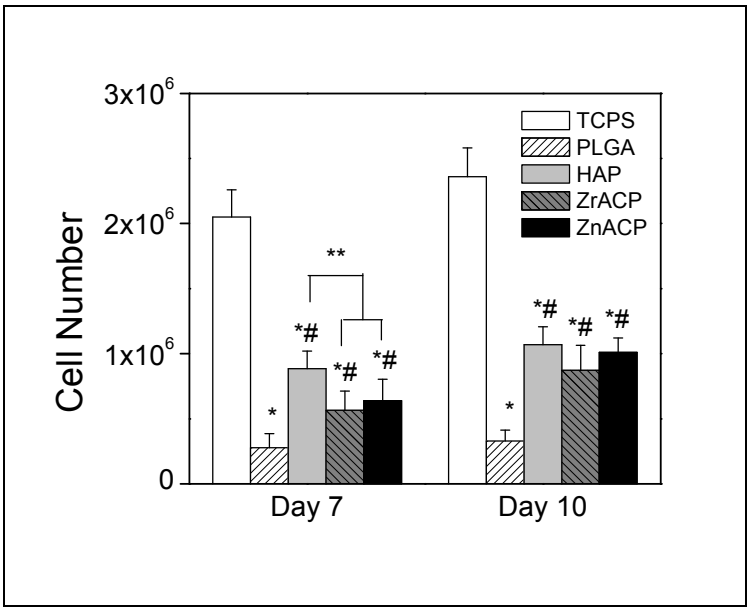

Figure 4.2. Cell number of MC3T3-E1 cells on composite scaffolds at 7 and 10 days. Tissue culture polystyrene (TCPS) and PLGA scaffolds without minerals were used as controls. Data are mean ± standard deviation for n=8 samples. * corresponds to statistical difference from TCPS. # corresponds to statistical difference from PLGA scaffold. ** corresponds to statistical difference from HAP scaffold.

4.4.3. Osteoblast Differentiation

Alkaline phosphatase activity, an early marker of osteogenic differentiation, was measured on all surfaces at day 7 and day 10 (Fig. 4.3). ALP activity per cell for PLGA scaffolds and scaffolds containing both ZrACP and ZnACP were significantly elevated compared to cell layers on TCPS at both time points. Further, ALP activity on ZnACP scaffolds was significantly elevated relative to PLGA, and HAP scaffolds at day 7. Additionally, ALP activity on HAP scaffolds was significantly lower than both TCPS and PLGA controls at day 10.

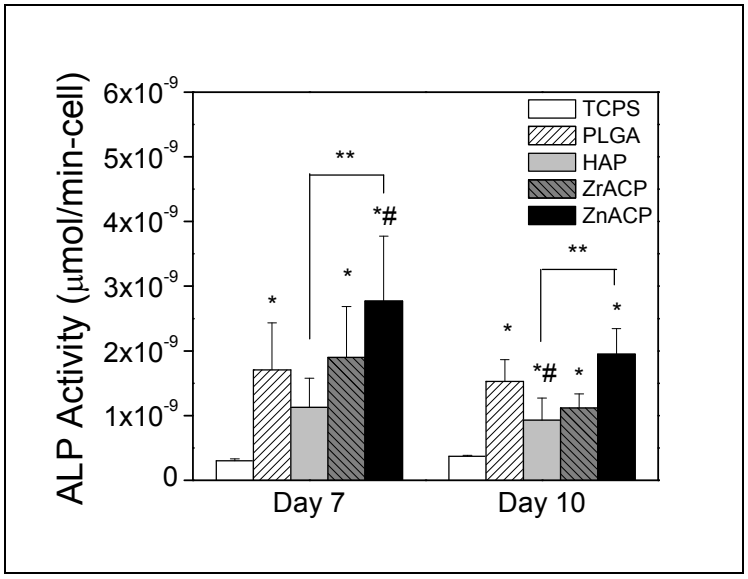

Figure 4.3. Alkaline phosphatase activity of MC3T3-E1 cells on composite scaffolds at 7 and 10 days. TCPS and PLGA scaffolds without mineral were used as controls. Data are mean ± standard deviation for n=8 samples. Activity per cell was determined by normalizing activity per cell layer by cell number. * corresponds to statistical difference from TCPS. # corresponds to statistical difference from PLGA scaffold. ** corresponds to statistical difference from HAP scaffold.

Prostaglandin E_2 accumulation in culture medium was measured for all scaffolds at days 4, 7, and 10 post-seeding (Fig. 4.4). PGE_2 was significantly elevated on all composite scaffolds relative to TCPS and PLGA controls on day 4 and day 7. However, on day 10, only scaffolds containing ZnACP had significantly elevated levels of PGE_2.

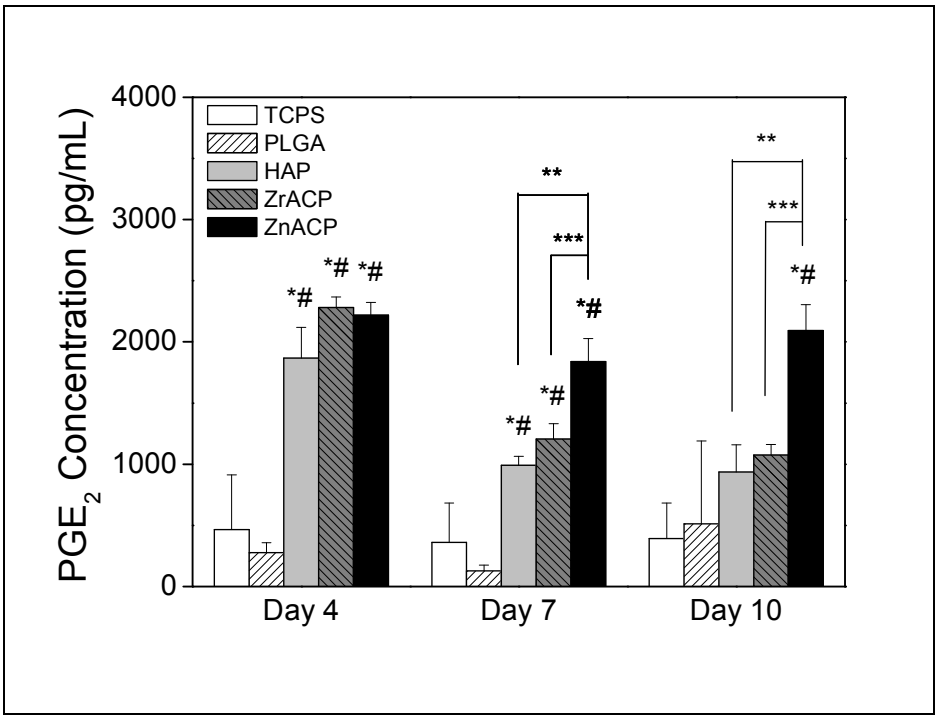

Figure 4.4. PGE_2 accumulation in culture medium at day 4, 7, and 10 of MC3T3-E1 cells on composite scaffolds. TCPS and PLGA scaffolds without mineral were used as controls. Means ± standard deviation, n=4. Data are mean ± standard deviation for n=8 samples. * corresponds to statistical difference from TCPS. # corresponds to statistical difference from PLGA scaffold.

Cells were cultured on scaffolds to determine the effects of the different mineral chemistries on osteogenic gene expression. Analysis of markers of osteoblast differentiation at 14 days post-seeding revealed different effects of the three minerals. Cells cultured on HAP scaffolds had elevated gene expression of the extracellular matrix proteins osteopontin (OPN), bone sialoprotein (BSP), and osteocalcin (OCN) (Fig. 4.5), suggesting enhanced osteoblast differentiation and matrix development. In contrast, scaffolds containing ZrACP or ZnACP had elevated levels of OPN only and diminished expression of OCN and collagen I (COLI).

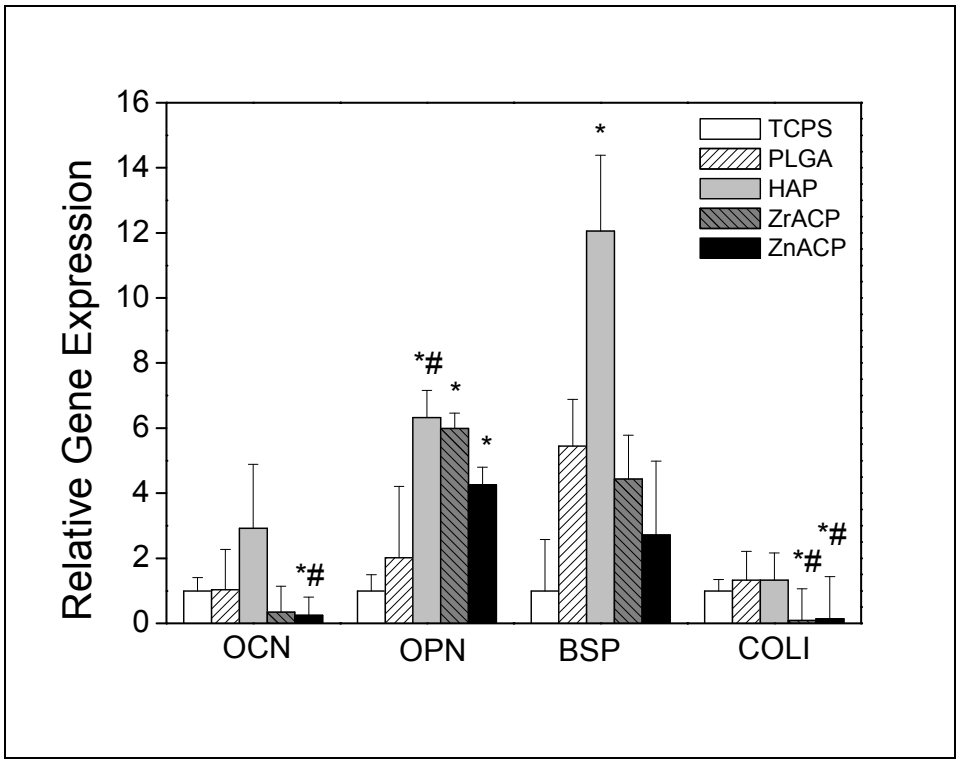

Figure 4.5. mRNA expression of osteoblast extracellular matrix proteins at day 14, relative to β-actin, the internal control. MC3T3-E1 cells were cultured on composite scaffolds. TCPS and PLGA scaffolds without mineral were used as controls. Data are mean ± standard deviation for n=8 samples. * corresponds to statistical difference from TCPS. # corresponds to statistical difference from PLGA scaffold.

Gene expression of growth factors and the transcription factor, osterix, was measured at day 14. Osterix, a transcription factor that is essential for osteoblast differentiation, was elevated on scaffolds containing HAP, but not on ACP scaffolds. Further, vascular endothelial growth factor A (VEGF-A), a growth factor involved in angiogenesis, was significantly elevated on HAP scaffolds, but only slightly elevated on ACP scaffolds. The expression of BMP-2, BMP-4 was not significantly elevated on any of the scaffolds.

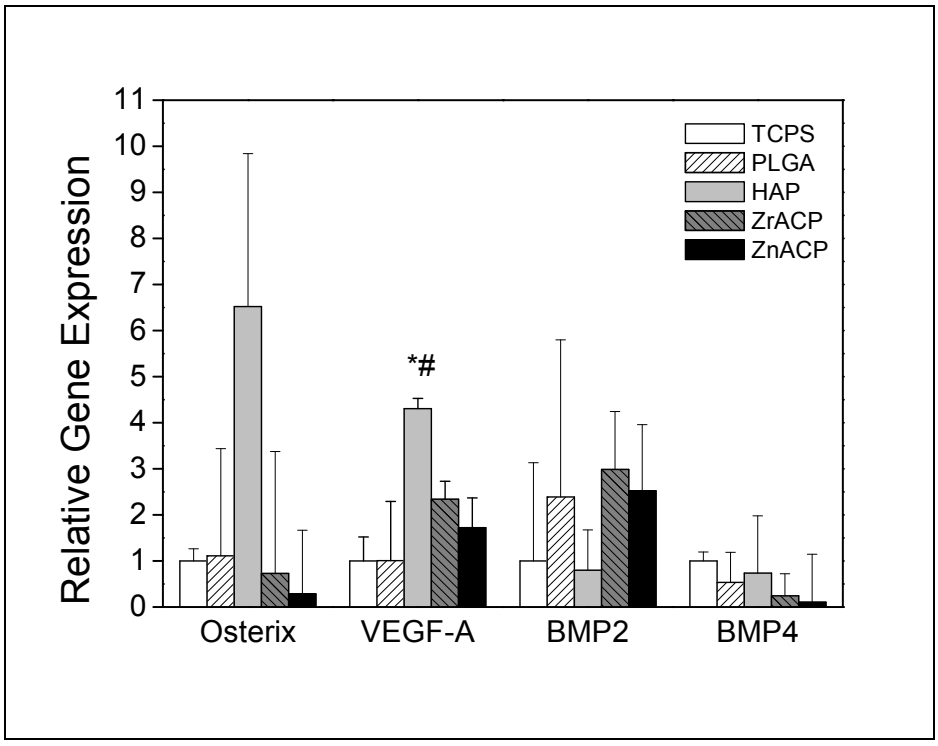

Figure 4.6. mRNA expression of growth factors VEGF-A, BMP-2, and BMP-4, and transcription factor osterix at day 14 relative to β-actin, the internal control. MC3T3-E1 cells were cultured on composite scaffolds. TCPS and PLGA scaffolds without mineral were used as controls. Data are mean ± standard deviation for n=8 samples. * corresponds to statistical difference from TCPS. # corresponds to statistical difference from PLGA scaffold.

4.5. Discussion

The goal of this study was to determine the effect of incorporating calcium phosphate ceramic particles on the proliferation and differentiation of MC3T3-E1 osteoblast like cells. Cell number, ALP activity, PGE accumulation, and gene expression of growth and transcriptions factors and bone matrix proteins were measured. Cell number on the composite scaffolds was greater than on PLGA controls and a significant increase in cell number was measured on ZrACP and ZnACP scaffolds from day 7 to day 10. Alkaline phosphatase activity was significantly elevated on ZnACP scaffolds compared to all other scaffolds on day 7. Prostaglandin E_2 accumulation in culture media was highest on composite scaffolds on day 4 and

7, and significantly greater only on ZnACP scaffolds on day 10. Gene expression of OPN was enhanced on all composite scaffolds and expression of OCN, BSP, OSX, and VEGF-A was elevated on HAP scaffolds only.

Cell number was significantly lower on all scaffolds compared to TCPS controls, suggesting decreased cell adhesion on the scaffolds. Fibronectin is commonly used to increase cell adhesion on polymer substrates [155]. However, in this study, it was omitted prior to cell seeding to avoid initiating conversion of ACP to HAP. This could partially explain the significantly lower cell numbers on the scaffolds. However, elevated cell numbers on scaffolds containing calcium phosphates relative to PLGA scaffolds suggests that calcium phosphate minerals enhance osteoblast attachment.

Alkaline phosphatase is an enzyme that hydrolyzes organic phosphates to make inorganic phosphate available for mineralization by osteoblasts [118]. It is highly active during the matrix synthesis phase of osteoblast differentiation, after extensive proliferation [51]. Our results show that ALP activity on PLGA, ZrACP, and ZnACP scaffolds was significantly greater than on TCPS at both time points and activity on HAP scaffolds was significantly greater on day 10. These results suggest the three dimensional scaffolds have a stimulatory effect on ALP activity. Further, ALP activity on ZnACP scaffolds was significantly greater than on all other scaffolds on day 7. This is consistent with other studies demonstrating increased ALP activity on Zn-releasing calcium phosphate scaffolds [90, 126]. Studies have also demonstrated that ALP activity is sensitive to extracellular pH, showing an increase in activity as pH increases [158, 159]. In this study, the local increase in pH due to ACP dissolution (Chapter 3, Fig. 3.2) could be partially responsible for the increase in ALP activity on ACP scaffolds.

Prostaglandins are thought to be stimulated by mechanical stress [148] and surface roughness [149]. Sun et al showed that PGE_2 concentration and ALP activity were elevated when osteoblasts were cultured in the presence of HAP and β-TCP particles [160]. In this study, elevated PGE_2 concentrations also corresponded to the increase in ALP activity. In a similar study, Lohmann et al [161] examined the response of osteoblast-like cells to aluminum oxide (Al_2O_3), zirconium oxide (ZrO_2), and polymethylmethacrylate (PMMA) particles. The effect of the particles on the cells was dependent on particle composition and concentration. Cells cultured with ZrO_2 and PMMA particles exhibited higher cell number, ALP activity, and PGE_2 concentration compared to the control with no particles. These results are consistent with our

findings that scaffolds containing ceramic particles have higher cell number, ALP activity, and PGE_2 concentration than controls without calcium phosphate particles.

The surface morphology of materials can have a great effect on the function of osteoblasts. Webster et al investigated the functions of osteoblasts on nanophase (grain sizes less than 100 nm) alumina, titania, and HAP [56]. Osteoblast proliferation, ALP activity, and calcium deposition were significantly greater on nanophase ceramics than conventional ceramic surfaces. Liu et al investigated the function of osteoblasts on nanophase titania/PLGA composites with nanometer level surface roughness [58]. Sonication controlled the dispersion of titania in the PLGA and the composite surface roughness. Composites with nanometer roughness had greater cell density, collagen content, ALP activity, and calcium deposition than smoother surfaces [58].

In this study, ACP scaffolds exhibited a rough topography with mineral particles less than 100 μm distributed over the entire scaffold. In contrast, HAP scaffolds exhibited mixed topography with sparse deposits of mineral particles greater than 100 μm and a low concentration of particles less than 20 μm distributed over the microsphere surfaces. Electrostatic interactions between the HAP particles may have caused large agglomerates of mineral, not seen with the ACPs. These differences in scaffold topography likely elicited differences in gene expression. Expression of OCN, BSP, OSX, and VEGF-A was elevated on HAP scaffolds, but not ZrACP and ZnACP scaffolds. OCN and COLI expression were diminished on ACP scaffolds. Further studies will be conducted to better understand the effects of particle size and distribution on the microsphere surface.

In Chapter 3, three different types of calcium phosphate scaffolds – HAP, ZrACP, and ZnACP – were investigated to characterize mineral dissolution and crystallinity. HAP minerals exhibited no ion release or change in medium pH and scaffolds contained sparse deposits of mineral greater than 100 μm. ZrACP minerals had a sustained release of calcium and phosphate ions over 96 hours, with an initial elevation in pH. ZnACP minerals also had a sustained release of calcium and phosphate ions, as well zinc, with a similar increase in pH. In addition, ZnACP particles had a higher pH at 96 hours, significantly lower phosphorus concentration than ZrACP, and no signs of conversion to HAP after 96 hours in culture medium. Scaffolds containing ZrACP and ZnACP had a generous, even distribution of mineral particles less than 100 μm in size. The results of these cell cultures studies reflect these differences in calcium phosphate ion release from the three minerals.

ZnACP scaffolds resulted in elevated levels of ALP activity and PGE_2 in the culture medium, likely the result of elevated pH and cellular interaction with particles less than 100 μm in size. In contrast, scaffolds containing large deposits of crystalline HAP resulted in the highest expression of bone extracellular matrix proteins OPN, OCN, BSP. Therefore, it can be implied that late stage osteoblast differentiation was enhanced on HAP scaffolds, relative to ACP scaffolds.

Differences in cell response to HAP, ZrACP, and ZnACP containing scaffolds reflect differences in pH and ion concentrations in the cell microenvironment, and mineral distribution on the scaffold surface. In future studies, we will attempt to decouple these effects to resolve osteoblast response to these composite scaffolds.

Chapter 5: Conclusions and Future Work

5.1. Conclusions

The goals of this research were to develop a bioactive, composite scaffold by incorporating ion-eluting calcium phosphate minerals into a PLGA microsphere matrix and determine the osteogenic potential of the composite scaffolds. To accomplish these goals, rat bone marrow stromal cell (BMSC) cultures were supplemented with zinc to determine the effects of zinc release from zinc-stabilized ACP. Next, HAP, zirconium- and zinc- stabilized ACPs were synthesized, characterized to determine ion release and crystallinity over 96 hours, and then incorporated into a porous sintered PLGA microsphere matrix. Finally, MC3T3-E1 cells were cultured in the scaffolds to determine the effect of the three calcium phosphates on proliferation and differentiation.

In the first study, rat BMSCs were cultured in the presence of soluble zinc to determine the implications of stabilizing ACP with zinc. Supplementation of culture medium with soluble zinc did not affect proliferation and osteoblastic differentiation of model osteoprogenitor cells. Although the range tested was narrow it was constrained by level of zinc in 10% serum (3×10^{-6} M) and published data suggesting that concentrations higher than 9×10^{-5} M inhibit normal osteoblast function [142]. The results of this study indicate that sufficient zinc is provided in normal serum, and that zinc supplementation through controlled release from ceramic biomaterials is not anticipated to alter development of a bone-like tissue *in vitro*, or the healing of a bone defect *in vivo*.

In the second study, HAP and zirconium- and zinc-stabilized ACPs were synthesized, characterized, and incorporated into a sintered PLGA microsphere matrix. Zinc and zirconia co-precipitated and stabilized ACPs exhibited a sustained release of calcium, phosphorus, and zinc ions over the course of 96 hours, while HAP showed no ion release. Some decreases in calcium and phosphorus concentrations were seen, suggesting reprecipitation of mineral. This was also seen in XRD spectra of the minerals in culture medium for 96 hours. Over time, ZrACP converted into a poorly crystalline material, resembling HAP. After 96 hours, ZnACP had not converted to a crystalline material. Minerals were then incorporated into a fused PLGA microsphere matrix to produce composite mineral scaffolds. Scaffolds containing ACPs had an even distribution of mineral over the surface of the microspheres, while scaffolds containing HAP and large, sparse deposits of mineral between the microspheres with some nanoparticles

scattered on the microspheres surfaces. Incorporation of calcium phosphates resulted in a decrease in the mechanical properties of the scaffolds, but compressive moduli remained above 50 MPa. These results demonstrate that PLGA-calcium phosphate composites may serve as promising scaffolds for delivery of calcium, phosphorus, and zinc ions to stimulate bone tissue regeneration.

In the third study, MC3T3-E1 osteoblast-like cells were cultured in the composite scaffolds. Cells were cultured in scaffolds with or without HAP, ZrACP, or ZnACP for 14 days and cell number, alkaline phosphatase activity, and gene expression were measured. Cell number on the composite scaffolds was greater than on PLGA controls and significant proliferation was seen on ZrACP and ZnACP scaffolds from day 7 to day 10. Alkaline phosphatase activity was significantly elevated on ZnACP scaffolds compared to all other scaffolds on day 7. Prostaglandin E_2 accumulation in culture media was highest on composite scaffolds on day 4 and 7, and significantly greater only on ZnACP scaffolds on day 10. Gene expression of OPN was enhanced on all composite scaffolds and OCN, BSP, OSX, and VEGF-A was elevated on HAP scaffolds only. These results indicate that adding ACP minerals to PLGA scaffolds supported cell growth and stimulated early osteogenic differentiation; while the addition of HAP stimulated late markers of osteogenic differentiation; making the scaffolds a promising alternative for bone tissue regeneration. Further investigation is required to determine mineral concentrations and combinations of ACP and HAP to stimulate both early and late stage osteogenic differentiation and mineralization.

5.2. Future Work

The results of this work demonstrate different cell responses with respect to the three calcium phosphates. Early osteoblast differentiation was stimulated by ZnACP, while late stage differentiation was stimulated by HAP. However, it is unclear if these results are due to differences in mineral solubility or scaffold topography. Therefore, we envision future experiments regarding this work will include efforts to decouple the effects of scaffold topography and calcium phosphate solubility on osteoblast differentiation. Further studies will investigate the effect of calcium phosphate concentration and the combination of ACP and HAP on osteoblast differentiation.

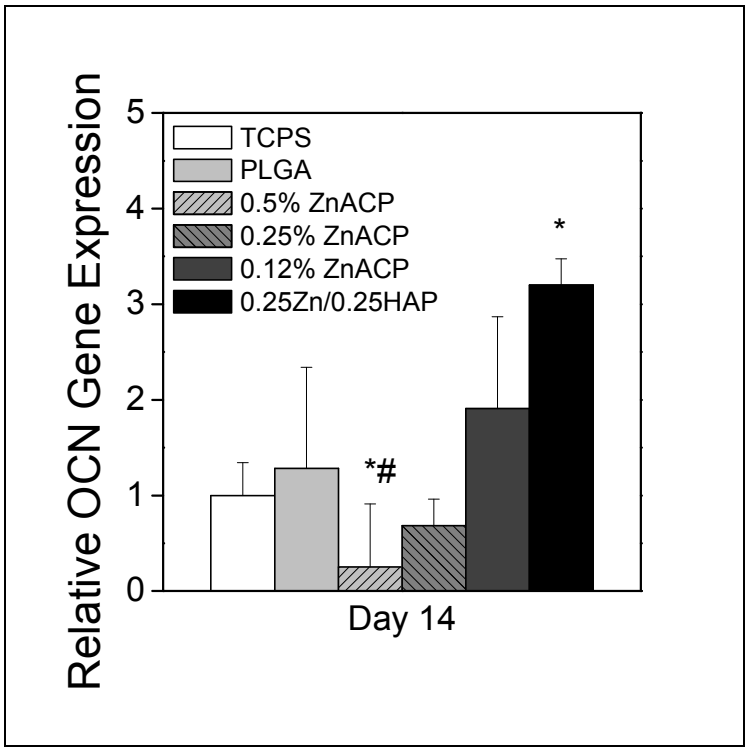

Figure 5.1. Osteocalcin gene expression of MC3T3-E1 cells cultured on composite scaffolds for 14 days, relative to internal control, β-actin.

5.2.1. Calcium Phosphate Particle Size

The differentiation of osteoblasts is greatly influenced by surface chemistry and topography. In this work, differences in calcium phosphate particle sizes resulted in vastly different scaffold surface topographies, which elicited different cell responses. To determine the

effects of composite scaffold surface chemistry and topography on osteoblast differentiation, scaffolds will be fabricated with a distinct range of particle sizes for each HAP, ZrACP, and ZnACP. Scaffolds will be imaged using SEM to measure and verify particle sizes for each calcium phosphate and cells will be cultured in the scaffolds to determine the effect on osteogenic differentiation. From these studies, we expect to learn 1) how osteoblasts respond to differences in particle size for each calcium phosphate and 2) how the differences in chemistry of calcium phosphate particles of the same size affect osteoblast differentiation.

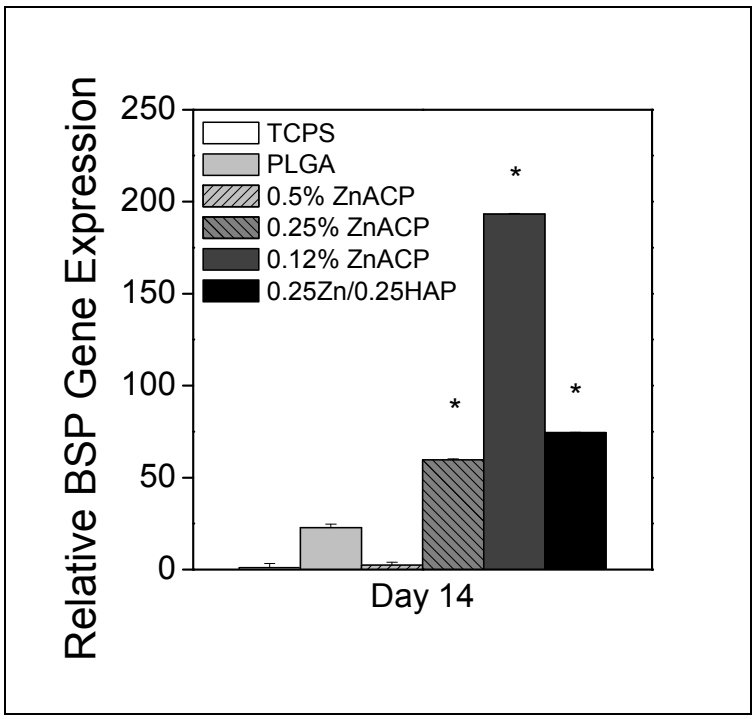

Figure 5.2. Bone sialoprotein gene expression of MC3T3-E1 cells cultured on composite scaffolds for 14 days, relative to internal control, β-actin.

5.2.2. Amorphous Calcium Phosphate Concentration

The concentration of ACP in the scaffolds could have an effect on the attachment, survival, and differentiation of osteoblasts by altering scaffold surface topography and ion release from the scaffolds. To determine the effect of ACP concentration on osteoblast differentiation, scaffolds will be fabricated with a range of ZnACP. Preliminary experiments were conducted and scaffolds were made with 0.12, 0.25, and 0.50 wt% ZnACP, seeded with MC3T3-E1 cells, and gene expression was measured at day 14. Gene expression of OCN (Fig.

5.1), BSP (Fig. 5.2), and OPN (Fig. 5.3) was greatest on scaffolds with 0.12% ZnACP. The increase in gene expression could be related to a change in scaffold surface topography or a change in ion release kinetics. These results are promising, but further characterization of the scaffolds and subsequent *in vitro* cell culture experiments could clarify cell response.

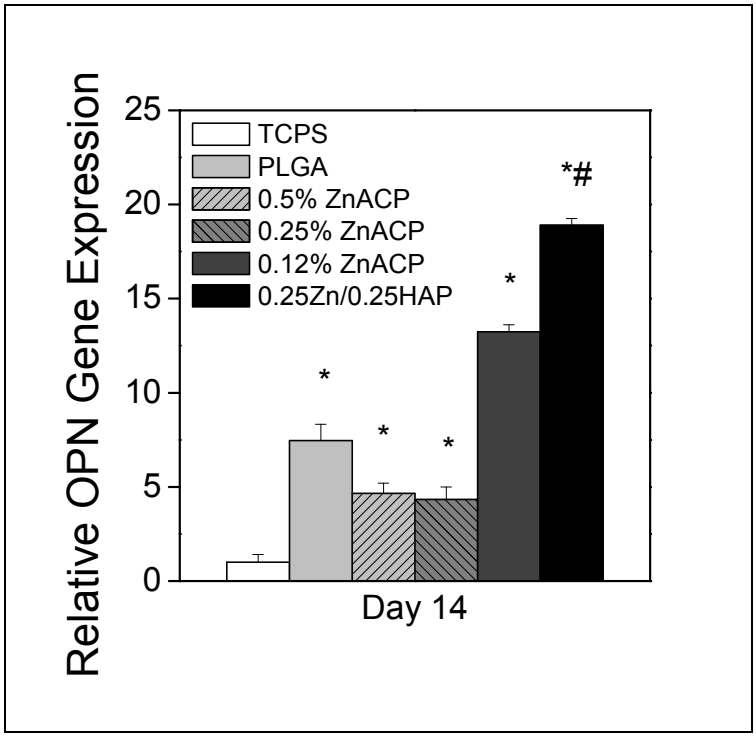

Figure 5.3. Osteopontin gene expression of MC3T3-E1 cells cultured on composite scaffolds for 14 days, relative to internal control, β-actin.

5.2.3. Hydroxyapatite/Zinc Amorphous Calcium Phosphate Composite Scaffold

In the current work, ACPs stimulated early osteogenic differentiation, but HAP stimulated late markers of osteoblast differentiation. Therefore, we postulate that a composite of both soluble and insoluble calcium phosphates may stimulate osteogenic differentiation more than either component alone [55]. Preliminary experiments were conducted to determine the osteogenic potential of scaffolds containing a combination of soluble ACP and osteoconductive HAP. Scaffolds were made with a combination of 0.25 wt% ZnACP and 0.25 wt% HAP, seeded

with MC3T3-E1 cells, and gene expression was measured at day 14. Gene expression of BSP and OCN on scaffolds containing both HAP and ZnACP was significantly elevated compared to TCPS. Expression of OPN on HAP/ZnACP scaffolds was significantly greater than PLGA scaffolds. These results suggest that combining two types of calcium phosphates with different solubility, crystallinity, and particle size may have a larger and more effective stimulatory effect on osteoblast differentiation. Further studies would include scaffold characterization and additional measurements of osteoblast differentiation.

References

[1] P. V. Giannoudis, H. Dinopoulos, and E. Tsiridis, "Bone substitutes: an update," *Injury,* vol. 36 Suppl 3, pp. S20-7, Nov 2005.

[2] W. G. De Long, Jr., T. A. Einhorn, K. Koval, M. McKee, W. Smith, R. Sanders, and T. Watson, "Bone grafts and bone graft substitutes in orthopaedic trauma surgery. A critical analysis," *J Bone Joint Surg Am,* vol. 89, pp. 649-58, Mar 2007.

[3] C. Laurencin, Y. Khan, and S. F. El-Amin, "Bone graft substitutes," *Expert Rev Med Devices,* vol. 3, pp. 49-57, Jan 2006.

[4] M. K. Sen and T. Miclau, "Autologous iliac crest bone graft: should it still be the gold standard for treating nonunions?," *Injury,* vol. 38 Suppl 1, pp. S75-80, Mar 2007.

[5] A. J. Salgado, O. P. Coutinho, and R. L. Reis, "Bone tissue engineering: state of the art and future trends," *Macromol Biosci,* vol. 4, pp. 743-65, Aug 9 2004.

[6] G. J. Tortora and S. R. Grabowski, *Principles of anatomy and physiology*, 10th ed. New York: Wiley, 2003.

[7] A. C. Guyton and J. E. Hall, *Textbook of medical physiology*, 11th ed. Philadelphia: Elsevier Saunders, 2006.

[8] A. R. Boccaccini and J. E. Gough, *Tissue engineering using ceramics and polymers*. Boca Raton, Cambridge, England: CRC Press ; Woodhead Publishing, 2007.

[9] K. A. Athanasiou, C. Zhu, D. R. Lanctot, C. M. Agrawal, and X. Wang, "Fundamentals of biomechanics in tissue engineering of bone," *Tissue Eng,* vol. 6, pp. 361-81, Aug 2000.

[10] U. Meyer and H. P. Wiesmann, *Bone and cartilage engineering*. Berlin ; New York: Springer, 2006.

[11] S. A. Goldstein, "The mechanical properties of trabecular bone: dependence on anatomic location and function," *J Biomech,* vol. 20, pp. 1055-61, 1987.

[12] S. C. Cowin and S. B. Doty, *Tissue mechanics*. New York, NY: Springer, 2007.

[13] T. M. Keaveny and W. C. Hayes, "A 20-year perspective on the mechanical properties of trabecular bone," *J Biomech Eng,* vol. 115, pp. 534-42, Nov 1993.

[14] A. M. Phillips, "Overview of the fracture healing cascade," *Injury,* vol. 36 Suppl 3, pp. S5-7, Nov 2005.

[15] V. Kumar, A. K. Abbas, N. Fausto, S. L. Robbins, and R. S. Cotran, *Robbins and Cotran pathologic basis of disease*, 7th ed. Philadelphia: Elsevier Saunders, 2005.

[16] N. Giuliani, V. Rizzoli, and G. D. Roodman, "Multiple myeloma bone disease: Pathophysiology of osteoblast inhibition," *Blood,* vol. 108, pp. 3992-6, Dec 15 2006.

[17] R. Bataille, D. Chappard, C. Marcelli, P. Dessauw, J. Sany, P. Baldet, and C. Alexandre, "Mechanisms of bone destruction in multiple myeloma: the importance of an unbalanced process in determining the severity of lytic bone disease," *J Clin Oncol,* vol. 7, pp. 1909-14, Dec 1989.

[18] T. Vejlgaard, N. Abildgaard, H. Jans, J. L. Nielsen, and L. Heickendorff, "Abnormal bone turnover in monoclonal gammopathy of undetermined significance: analyses of type I collagen telopeptide, osteocalcin, bone-specific alkaline phosphatase and propeptides of type I and type III procollagens," *Eur J Haematol,* vol. 58, pp. 104-8, Feb 1997.

[19] C. T. Laurencin, Y. Khan, M. Kofron, S. El-Amin, E. Botchwey, X. Yu, and J. A. Cooper, Jr., "The ABJS Nicolas Andry Award: Tissue engineering of bone and ligament: a 15-year perspective," *Clin Orthop Relat Res,* vol. 447, pp. 221-36, Jun 2006.

[20] S. T. Yoon and S. D. Boden, "Osteoinductive molecules in orthopaedics: basic science and preclinical studies," *Clin Orthop Relat Res,* pp. 33-43, Feb 2002.
[21] A. I. Caplan and S. P. Bruder, "Mesenchymal stem cells: building blocks for molecular medicine in the 21st century," *Trends Mol Med,* vol. 7, pp. 259-64, Jun 2001.
[22] A. I. Caplan, "Mesenchymal stem cells," *J Orthop Res,* vol. 9, pp. 641-50, Sep 1991.
[23] P. Bianco and P. G. Robey, "Stem cells in tissue engineering," *Nature,* vol. 414, pp. 118-21, Nov 1 2001.
[24] C. Jorgensen, J. Gordeladze, and D. Noel, "Tissue engineering through autologous mesenchymal stem cells," *Curr Opin Biotechnol,* vol. 15, pp. 406-10, Oct 2004.
[25] H. K. Vaananen, "Mesenchymal stem cells," *Ann Med,* vol. 37, pp. 469-79, 2005.
[26] F. P. Barry and J. M. Murphy, "Mesenchymal stem cells: clinical applications and biological characterization," *Int J Biochem Cell Biol,* vol. 36, pp. 568-84, Apr 2004.
[27] M. F. Pittenger, A. M. Mackay, S. C. Beck, R. K. Jaiswal, R. Douglas, J. D. Mosca, M. A. Moorman, D. W. Simonetti, S. Craig, and D. R. Marshak, "Multilineage potential of adult human mesenchymal stem cells," *Science,* vol. 284, pp. 143-7, Apr 2 1999.
[28] C. Maniatopoulos, J. Sodek, and A. H. Melcher, "Bone formation in vitro by stromal cells obtained from bone marrow of young adult rats," *Cell Tissue Res,* vol. 254, pp. 317-30, Nov 1988.
[29] A. Schaffler and C. Buchler, "Concise review: adipose tissue-derived stromal cells--basic and clinical implications for novel cell-based therapies," *Stem Cells,* vol. 25, pp. 818-27, Apr 2007.
[30] F. H. Shen, Q. Zeng, Q. Lv, L. Choi, G. Balian, X. Li, and C. T. Laurencin, "Osteogenic differentiation of adipose-derived stromal cells treated with GDF-5 cultured on a novel three-dimensional sintered microsphere matrix," *Spine J,* vol. 6, pp. 615-23, Nov-Dec 2006.
[31] A. J. Katz, A. Tholpady, S. S. Tholpady, H. Shang, and R. C. Ogle, "Cell surface and transcriptional characterization of human adipose-derived adherent stromal (hADAS) cells," *Stem Cells,* vol. 23, pp. 412-23, Mar 2005.
[32] A. R. Prusa and M. Hengstschlager, "Amniotic fluid cells and human stem cell research: a new connection," *Med Sci Monit,* vol. 8, pp. RA253-7, Nov 2002.
[33] M. S. Tsai, J. L. Lee, Y. J. Chang, and S. M. Hwang, "Isolation of human multipotent mesenchymal stem cells from second-trimester amniotic fluid using a novel two-stage culture protocol," *Hum Reprod,* vol. 19, pp. 1450-6, Jun 2004.
[34] P. De Coppi, G. Bartsch, Jr., M. M. Siddiqui, T. Xu, C. C. Santos, L. Perin, G. Mostoslavsky, A. C. Serre, E. Y. Snyder, J. J. Yoo, M. E. Furth, S. Soker, and A. Atala, "Isolation of amniotic stem cell lines with potential for therapy," *Nat Biotechnol,* vol. 25, pp. 100-6, Jan 2007.
[35] S. Gronthos, M. Mankani, J. Brahim, P. G. Robey, and S. Shi, "Postnatal human dental pulp stem cells (DPSCs) in vitro and in vivo," *Proc Natl Acad Sci U S A,* vol. 97, pp. 13625-30, Dec 5 2000.
[36] S. Gronthos, J. Brahim, W. Li, L. W. Fisher, N. Cherman, A. Boyde, P. DenBesten, P. G. Robey, and S. Shi, "Stem cell properties of human dental pulp stem cells," *J Dent Res,* vol. 81, pp. 531-5, Aug 2002.
[37] G. Laino, A. Graziano, R. d'Aquino, G. Pirozzi, V. Lanza, S. Valiante, A. De Rosa, F. Naro, E. Vivarelli, and G. Papaccio, "An approachable human adult stem cell source for hard-tissue engineering," *J Cell Physiol,* vol. 206, pp. 693-701, Mar 2006.
[38] G. Laino, F. Carinci, A. Graziano, R. d'Aquino, V. Lanza, A. De Rosa, F. Gombos, F. Caruso, L. Guida, R. Rullo, D. Menditti, and G. Papaccio, "In vitro bone production

using stem cells derived from human dental pulp," *J Craniofac Surg,* vol. 17, pp. 511-5, May 2006.
[39] W. Zhang, X. F. Walboomers, S. Shi, M. Fan, and J. A. Jansen, "Multilineage Differentiation Potential of Stem Cells Derived from Human Dental Pulp after Cryopreservation," *Tissue Eng,* Sep 1 2006.
[40] G. Papaccio, A. Graziano, R. d'Aquino, M. F. Graziano, G. Pirozzi, D. Menditti, A. De Rosa, F. Carinci, and G. Laino, "Long-term cryopreservation of dental pulp stem cells (SBP-DPSCs) and their differentiated osteoblasts: a cell source for tissue repair," *J Cell Physiol,* vol. 208, pp. 319-25, Aug 2006.
[41] X. Wei, J. Ling, L. Wu, L. Liu, and Y. Xiao, "Expression of mineralization markers in dental pulp cells," *J Endod,* vol. 33, pp. 703-8, Jun 2007.
[42] S. Shi, P. G. Robey, and S. Gronthos, "Comparison of human dental pulp and bone marrow stromal stem cells by cDNA microarray analysis," *Bone,* vol. 29, pp. 532-9, Dec 2001.
[43] G. Laino, R. d'Aquino, A. Graziano, V. Lanza, F. Carinci, F. Naro, G. Pirozzi, and G. Papaccio, "A new population of human adult dental pulp stem cells: a useful source of living autologous fibrous bone tissue (LAB)," *J Bone Miner Res,* vol. 20, pp. 1394-402, Aug 2005.
[44] G. T. Huang, W. Sonoyama, J. Chen, and S. H. Park, "In vitro characterization of human dental pulp cells: various isolation methods and culturing environments," *Cell Tissue Res,* vol. 324, pp. 225-36, May 2006.
[45] S. Otaki, S. Ueshima, K. Shiraishi, K. Sugiyama, S. Hamada, M. Yorimoto, and O. Matsuo, "Mesenchymal progenitor cells in adult human dental pulp and their ability to form bone when transplanted into immunocompromised mice," *Cell Biol Int,* vol. 31, pp. 1191-7, Oct 2007.
[46] W. Zhang, X. F. Walboomers, J. G. Wolke, Z. Bian, M. W. Fan, and J. A. Jansen, "Differentiation ability of rat postnatal dental pulp cells in vitro," *Tissue Eng,* vol. 11, pp. 357-68, Mar-Apr 2005.
[47] W. Zhang, X. Frank Walboomers, T. H. van Kuppevelt, W. F. Daamen, Z. Bian, and J. A. Jansen, "The performance of human dental pulp stem cells on different three-dimensional scaffold materials," *Biomaterials,* vol. 27, pp. 5658-68, Nov 2006.
[48] J. E. Aubin, F. Liu, L. Malaval, and A. K. Gupta, "Osteoblast and chondroblast differentiation," *Bone,* vol. 17, pp. 77S-83S, Aug 1995.
[49] J. R. Nefussi, G. Brami, D. Modrowski, M. Oboeuf, and N. Forest, "Sequential expression of bone matrix proteins during rat calvaria osteoblast differentiation and bone nodule formation in vitro," *J Histochem Cytochem,* vol. 45, pp. 493-503, Apr 1997.
[50] L. D. Quarles, D. A. Yohay, L. W. Lever, R. Caton, and R. J. Wenstrup, "Distinct proliferative and differentiated stages of murine MC3T3-E1 cells in culture: an in vitro model of osteoblast development," *J Bone Miner Res,* vol. 7, pp. 683-92, Jun 1992.
[51] T. A. Owen, M. Aronow, V. Shalhoub, L. M. Barone, L. Wilming, M. S. Tassinari, M. B. Kennedy, S. Pockwinse, J. B. Lian, and G. S. Stein, "Progressive development of the rat osteoblast phenotype in vitro: reciprocal relationships in expression of genes associated with osteoblast proliferation and differentiation during formation of the bone extracellular matrix," *J Cell Physiol,* vol. 143, pp. 420-30, Jun 1990.
[52] S. I. Deliloglu-Gurhan, H. S. Vatansever, F. Ozdal-Kurt, and I. Tuglu, "Characterization of osteoblasts derived from bone marrow stromal cells in a modified cell culture system," *Acta Histochem,* vol. 108, pp. 49-57, 2006.

[53] J. H. Kuhne, R. Bartl, B. Frisch, C. Hammer, V. Jansson, and M. Zimmer, "Bone formation in coralline hydroxyapatite. Effects of pore size studied in rabbits," *Acta Orthop Scand,* vol. 65, pp. 246-52, Jun 1994.
[54] A. J. Engler, S. Sen, H. L. Sweeney, and D. E. Discher, "Matrix elasticity directs stem cell lineage specification," *Cell,* vol. 126, pp. 677-89, Aug 25 2006.
[55] K. Ogata, S. Imazato, A. Ehara, S. Ebisu, Y. Kinomoto, T. Nakano, and Y. Umakoshi, "Comparison of osteoblast responses to hydroxyapatite and hydroxyapatite/soluble calcium phosphate composites," *J Biomed Mater Res A,* vol. 72, pp. 127-35, Feb 1 2005.
[56] T. J. Webster, C. Ergun, R. H. Doremus, R. W. Siegel, and R. Bizios, "Enhanced functions of osteoblasts on nanophase ceramics," *Biomaterials,* vol. 21, pp. 1803-10, Sep 2000.
[57] T. J. Webster, C. Ergun, R. H. Doremus, R. W. Siegel, and R. Bizios, "Specific proteins mediate enhanced osteoblast adhesion on nanophase ceramics," *J Biomed Mater Res,* vol. 51, pp. 475-83, Sep 5 2000.
[58] H. Liu, E. B. Slamovich, and T. J. Webster, "Increased osteoblast functions among nanophase titania/poly(lactide-co-glycolide) composites of the highest nanometer surface roughness," *J Biomed Mater Res A,* vol. 78, pp. 798-807, Sep 15 2006.
[59] C. J. Koh and A. Atala, "Tissue engineering, stem cells, and cloning: opportunities for regenerative medicine," *J Am Soc Nephrol,* vol. 15, pp. 1113-25, May 2004.
[60] J. Baier Leach, K. A. Bivens, C. W. Patrick, Jr., and C. E. Schmidt, "Photocrosslinked hyaluronic acid hydrogels: natural, biodegradable tissue engineering scaffolds," *Biotechnol Bioeng,* vol. 82, pp. 578-89, Jun 5 2003.
[61] Y. Ikada, *Tissue engineering : fundamentals and applications*. Amsterdam ; Boston: Elsevier, 2006.
[62] W. W. Thein-Han and Y. Kitiyanant, "Chitosan scaffolds for in vitro buffalo embryonic stem-like cell culture: an approach to tissue engineering," *J Biomed Mater Res B Appl Biomater,* vol. 80, pp. 92-101, Jan 2007.
[63] D. W. Hutmacher, "Scaffolds in tissue engineering bone and cartilage," *Biomaterials,* vol. 21, pp. 2529-43, Dec 2000.
[64] S. F. El-Amin, H. H. Lu, Y. Khan, J. Burems, J. Mitchell, R. S. Tuan, and C. T. Laurencin, "Extracellular matrix production by human osteoblasts cultured on biodegradable polymers applicable for tissue engineering," *Biomaterials,* vol. 24, pp. 1213-21, Mar 2003.
[65] C. P. Klein, J. M. de Blieck-Hogervorst, J. G. Wolke, and K. de Groot, "Studies of the solubility of different calcium phosphate ceramic particles in vitro," *Biomaterials,* vol. 11, pp. 509-12, Sep 1990.
[66] M. Bohner, "Calcium orthophosphates in medicine: from ceramics to calcium phosphate cements," *Injury,* vol. 31 Suppl 4, pp. 37-47, Dec 2000.
[67] W. Paul and C. P. Sharma, "Effect of calcium, zinc and magnesium on the attachment and spreading of osteoblast like cells onto ceramic matrices," *J Mater Sci Mater Med,* vol. 18, pp. 699-703, May 2007.
[68] A. Boyde, A. Corsi, R. Quarto, R. Cancedda, and P. Bianco, "Osteoconduction in large macroporous hydroxyapatite ceramic implants: evidence for a complementary integration and disintegration mechanism," *Bone,* vol. 24, pp. 579-89, Jun 1999.
[69] C. P. Klein, A. A. Driessen, K. de Groot, and A. van den Hooff, "Biodegradation behavior of various calcium phosphate materials in bone tissue," *J Biomed Mater Res,* vol. 17, pp. 769-84, Sep 1983.

[70] F. Barrere, C. A. van Blitterswijk, and K. de Groot, "Bone regeneration: molecular and cellular interactions with calcium phosphate ceramics," *Int J Nanomedicine,* vol. 1, pp. 317-32, 2006.
[71] D. Skrtic, J. M. Antonucci, E. D. Eanes, and R. T. Brunworth, "Silica- and zirconia-hybridized amorphous calcium phosphate: effect on transformation to hydroxyapatite," *J Biomed Mater Res,* vol. 59, pp. 597-604, Mar 15 2002.
[72] E. D. Eanes, "Amorphous calcium phosphate," *Monogr Oral Sci,* vol. 18, pp. 130-47, 2001.
[73] J. F. Osborn and H. Newesely, "The material science of calcium phosphate ceramics," *Biomaterials,* vol. 1, pp. 108-11, Apr 1980.
[74] J. B. Park, *Bioceramics : properties, characterizations, and applications*. New York: Springer, 2008.
[75] K. Yamaguchi, T. Hirano, G. Yoshida, and K. Iwasaki, "Degradation-resistant character of synthetic hydroxyapatite blocks filled in bone defects," *Biomaterials,* vol. 16, pp. 983-5, Sep 1995.
[76] J. Dong, T. Uemura, Y. Shirasaki, and T. Tateishi, "Promotion of bone formation using highly pure porous beta-TCP combined with bone marrow-derived osteoprogenitor cells," *Biomaterials,* vol. 23, pp. 4493-502, Dec 2002.
[77] R. W. Bucholz, "Nonallograft osteoconductive bone graft substitutes," *Clin Orthop Relat Res,* pp. 44-52, Feb 2002.
[78] Y. Okamoto and S. Hidaka, "Studies on calcium phosphate precipitation: effects of metal ions used in dental materials," *J Biomed Mater Res,* vol. 28, pp. 1403-10, Dec 1994.
[79] S. Hidaka, Y. Okamoto, and K. Abe, "Elutions of metal ions from dental casting alloys and their effect on calcium phosphate precipitation and transformation," *J Biomed Mater Res,* vol. 28, pp. 175-80, Feb 1994.
[80] B. M. Whited, D. Skrtic, B. J. Love, and A. S. Goldstein, "Osteoblast response to zirconia-hybridized pyrophosphate-stabilized amorphous calcium phosphate," *J Biomed Mater Res A,* Nov 8 2005.
[81] A. Oki, B. Parveen, S. Hossain, S. Adeniji, and H. Donahue, "Preparation and in vitro bioactivity of zinc containing sol-gel-derived bioglass materials," *J Biomed Mater Res A,* vol. 69, pp. 216-21, May 1 2004.
[82] O. Tsigkou, L. L. Hench, A. R. Boccaccini, J. M. Polak, and M. M. Stevens, "Enhanced differentiation and mineralization of human fetal osteoblasts on PDLLA containing Bioglass composite films in the absence of osteogenic supplements," *J Biomed Mater Res A,* vol. 80, pp. 837-51, Mar 15 2007.
[83] M. Julien, I. Khairoun, R. Z. LeGeros, S. Delplace, P. Pilet, P. Weiss, G. Daculsi, J. M. Bouler, and J. Guicheux, "Physico-chemical-mechanical and in vitro biological properties of calcium phosphate cements with doped amorphous calcium phosphates," *Biomaterials,* vol. 28, pp. 956-65, Feb 2007.
[84] G. Gupta, S. Kirakodu, and A. El-Ghannam, "Dissolution kinetics of a Si-rich nanocomposite and its effect on osteoblast gene expression," *J Biomed Mater Res A,* vol. 80, pp. 486-96, Feb 2007.
[85] K. Y. Lee, M. Park, H. M. Kim, Y. J. Lim, H. J. Chun, H. Kim, and S. H. Moon, "Ceramic bioactivity: progresses, challenges and perspectives," *Biomed Mater,* vol. 1, pp. R31-7, Jun 2006.
[86] T. J. Webster, C. Ergun, R. H. Doremus, and R. Bizios, "Hydroxylapatite with substituted magnesium, zinc, cadmium, and yttrium. II. Mechanisms of osteoblast adhesion," *J Biomed Mater Res,* vol. 59, pp. 312-7, Feb 2002.

[87] T. J. Webster, E. A. Massa-Schlueter, J. L. Smith, and E. B. Slamovich, "Osteoblast response to hydroxyapatite doped with divalent and trivalent cations," *Biomaterials,* vol. 25, pp. 2111-21, May 2004.
[88] M. H. Santos, P. Valerio, A. M. Goes, M. F. Leite, L. G. Heneine, and H. S. Mansur, "Biocompatibility evaluation of hydroxyapatite/collagen nanocomposites doped with Zn+2," *Biomed Mater,* vol. 2, pp. 135-41, Jun 2007.
[89] E. D. Eanes, I. H. Gillessen, and A. S. Posner, "Intermediate states in the precipitation of hydroxyapatite," *Nature,* vol. 208, pp. 365-7, Oct 23 1965.
[90] H. Storrie and S. I. Stupp, "Cellular response to zinc-containing organoapatite: an in vitro study of proliferation, alkaline phosphatase activity and biomineralization," *Biomaterials,* vol. 26, pp. 5492-9, Sep 2005.
[91] A. Ito, K. Ojima, H. Naito, N. Ichinose, and T. Tateishi, "Preparation, solubility, and cytocompatibility of zinc-releasing calcium phosphate ceramics," *J Biomed Mater Res,* vol. 50, pp. 178-83, May 2000.
[92] B. M. Whited, A. S. Goldstein, D. Skrtic, and B. J. Love, "Fabrication and characterization of poly(DL-lactic-co-glycolic acid)/zirconia-hybridized amorphous calcium phosphate composites," *J Biomater Sci Polym Ed,* vol. 17, pp. 403-18, 2006.
[93] E. K. Cushnie, Y. M. Khan, and C. T. Laurencin, "Amorphous hydroxyapatite-sintered polymeric scaffolds for bone tissue regeneration: physical characterization studies," *J Biomed Mater Res A,* vol. 84, pp. 54-62, Jan 2008.
[94] X. Niu, Q. Feng, M. Wang, X. Guo, and Q. Zheng, "Porous nano-HA/collagen/PLLA scaffold containing chitosan microspheres for controlled delivery of synthetic peptide derived from BMP-2," *J Control Release,* Dec 3 2008.
[95] S. S. Liao, F. Z. Cui, W. Zhang, and Q. L. Feng, "Hierarchically biomimetic bone scaffold materials: nano-HA/collagen/PLA composite," *J Biomed Mater Res B Appl Biomater,* vol. 69, pp. 158-65, May 15 2004.
[96] P. X. Ma and J. H. Elisseeff, *Scaffolding in tissue engineering*. Boca Raton: Taylor&Francis, 2005.
[97] L. D. Shea, D. Wang, R. T. Franceschi, and D. J. Mooney, "Engineered bone development from a pre-osteoblast cell line on three-dimensional scaffolds," *Tissue Eng,* vol. 6, pp. 605-17, Dec 2000.
[98] I. D. Rosca, F. Watari, and M. Uo, "Microparticle formation and its mechanism in single and double emulsion solvent evaporation," *J Control Release,* vol. 99, pp. 271-80, Sep 30 2004.
[99] M. Borden, S. F. El-Amin, M. Attawia, and C. T. Laurencin, "Structural and human cellular assessment of a novel microsphere-based tissue engineered scaffold for bone repair," *Biomaterials,* vol. 24, pp. 597-609, Feb 2003.
[100] M. Borden, M. Attawia, and C. T. Laurencin, "The sintered microsphere matrix for bone tissue engineering: in vitro osteoconductivity studies," *J Biomed Mater Res,* vol. 61, pp. 421-9, Sep 5 2002.
[101] M. Borden, M. Attawia, Y. Khan, and C. T. Laurencin, "Tissue engineered microsphere-based matrices for bone repair: design and evaluation," *Biomaterials,* vol. 23, pp. 551-9, Jan 2002.
[102] M. Borden, M. Attawia, Y. Khan, S. F. El-Amin, and C. T. Laurencin, "Tissue-engineered bone formation in vivo using a novel sintered polymeric microsphere matrix," *J Bone Joint Surg Br,* vol. 86, pp. 1200-8, Nov 2004.
[103] J. P. Bilezikian, L. G. Raisz, and G. A. Rodan, *Principles of bone biology*, 2nd ed. San Diego: Academic Press, 2002.

[104] Y. C. Huang, D. Kaigler, K. G. Rice, P. H. Krebsbach, and D. J. Mooney, "Combined angiogenic and osteogenic factor delivery enhances bone marrow stromal cell-driven bone regeneration," *J Bone Miner Res,* vol. 20, pp. 848-57, May 2005.
[105] A. W. Yasko, J. M. Lane, E. J. Fellinger, V. Rosen, J. M. Wozney, and E. A. Wang, "The healing of segmental bone defects, induced by recombinant human bone morphogenetic protein (rhBMP-2). A radiographic, histological, and biomechanical study in rats," *J Bone Joint Surg Am,* vol. 74, pp. 659-70, Jun 1992.
[106] G. E. Friedlaender, C. R. Perry, J. D. Cole, S. D. Cook, G. Cierny, G. F. Muschler, G. A. Zych, J. H. Calhoun, A. J. LaForte, and S. Yin, "Osteogenic protein-1 (bone morphogenetic protein-7) in the treatment of tibial nonunions," *J Bone Joint Surg Am,* vol. 83-A Suppl 1, pp. S151-8, 2001.
[107] S. Govender, C. Csimma, H. K. Genant, A. Valentin-Opran, Y. Amit, R. Arbel, H. Aro, D. Atar, M. Bishay, M. G. Borner, P. Chiron, P. Choong, J. Cinats, B. Courtenay, R. Feibel, B. Geulette, C. Gravel, N. Haas, M. Raschke, E. Hammacher, D. van der Velde, P. Hardy, M. Holt, C. Josten, R. L. Ketterl, B. Lindeque, G. Lob, H. Mathevon, G. McCoy, D. Marsh, R. Miller, E. Munting, S. Oevre, L. Nordsletten, A. Patel, A. Pohl, W. Rennie, P. Reynders, P. M. Rommens, J. Rondia, W. C. Rossouw, P. J. Daneel, S. Ruff, A. Ruter, S. Santavirta, T. A. Schildhauer, C. Gekle, R. Schnettler, D. Segal, H. Seiler, R. B. Snowdowne, J. Stapert, G. Taglang, R. Verdonk, L. Vogels, A. Weckbach, A. Wentzensen, and T. Wisniewski, "Recombinant human bone morphogenetic protein-2 for treatment of open tibial fractures: a prospective, controlled, randomized study of four hundred and fifty patients," *J Bone Joint Surg Am,* vol. 84-A, pp. 2123-34, Dec 2002.
[108] M. Borset, H. Hjorth-Hansen, C. Seidel, A. Sundan, and A. Waage, "Hepatocyte growth factor and its receptor c-met in multiple myeloma," *Blood,* vol. 88, pp. 3998-4004, Nov 15 1996.
[109] C. Seidel, M. Borset, I. Turesson, N. Abildgaard, A. Sundan, and A. Waage, "Elevated serum concentrations of hepatocyte growth factor in patients with multiple myeloma. The Nordic Myeloma Study Group," *Blood,* vol. 91, pp. 806-12, Feb 1 1998.
[110] C. Seidel, M. Borset, O. Hjertner, D. Cao, N. Abildgaard, H. Hjorth-Hansen, R. D. Sanderson, A. Waage, and A. Sundan, "High levels of soluble syndecan-1 in myeloma-derived bone marrow: modulation of hepatocyte growth factor activity," *Blood,* vol. 96, pp. 3139-46, Nov 1 2000.
[111] K. Fuller, J. Owens, and T. J. Chambers, "The effect of hepatocyte growth factor on the behaviour of osteoclasts," *Biochem Biophys Res Commun,* vol. 212, pp. 334-40, Jul 17 1995.
[112] M. Inaba, H. Koyama, M. Hino, S. Okuno, M. Terada, Y. Nishizawa, T. Nishino, and H. Morii, "Regulation of release of hepatocyte growth factor from human promyelocytic leukemia cells, HL-60, by 1,25-dihydroxyvitamin D3, 12-O-tetradecanoylphorbol 13-acetate, and dibutyryl cyclic adenosine monophosphate," *Blood,* vol. 82, pp. 53-9, Jul 1 1993.
[113] L. Ye, L. Peng, H. Tan, and X. Zhou, "HGF enhanced proliferation and differentiation of dental pulp cells," *J Endod,* vol. 32, pp. 736-41, Aug 2006.
[114] T. Standal, N. Abildgaard, U. M. Fagerli, B. Stordal, O. Hjertner, M. Borset, and A. Sundan, "HGF inhibits BMP-induced osteoblastogenesis: possible implications for the bone disease of multiple myeloma," *Blood,* vol. 109, pp. 3024-30, Apr 1 2007.
[115] H. Matsuoka, H. Akiyama, Y. Okada, H. Ito, C. Shigeno, J. Konishi, T. Kokubo, and T. Nakamura, "In vitro analysis of the stimulation of bone formation by highly bioactive apatite- and wollastonite-containing glass-ceramic: released calcium ions promote

osteogenic differentiation in osteoblastic ROS17/2.8 cells," *J Biomed Mater Res,* vol. 47, pp. 176-88, Nov 1999.
[116] H. C. Tenenbaum, "Role of organic phosphate in mineralization of bone in vitro," *J Dent Res,* vol. 60 Spec No C, pp. 1586-9, Aug 1981.
[117] R. Robison and K. M. Soames, "The Possible Significance of Hexosephosphoric Esters in Ossification: Part II. The Phosphoric Esterase of Ossifying Cartilage," *Biochem J,* vol. 18, pp. 740-54, 1924.
[118] R. Fortuna, H. C. Anderson, R. P. Carty, and S. W. Sajdera, "Enzymatic characterization of the matrix vesicle alkaline phosphatase isolated from bovine fetal epiphyseal cartilage," *Calcif Tissue Int,* vol. 30, pp. 217-25, 1980.
[119] Y. L. Chang, C. M. Stanford, and J. C. Keller, "Calcium and phosphate supplementation promotes bone cell mineralization: implications for hydroxyapatite (HA)-enhanced bone formation," *J Biomed Mater Res,* vol. 52, pp. 270-8, Nov 2000.
[120] S. Maeno, Y. Niki, H. Matsumoto, H. Morioka, T. Yatabe, A. Funayama, Y. Toyama, T. Taguchi, and J. Tanaka, "The effect of calcium ion concentration on osteoblast viability, proliferation and differentiation in monolayer and 3D culture," *Biomaterials,* vol. 26, pp. 4847-55, Aug 2005.
[121] H. C. Tenenbaum and J. N. Heersche, "Differentiation of osteoblasts and formation of mineralized bone in vitro," *Calcif Tissue Int,* vol. 34, pp. 76-9, Jan 1982.
[122] S. Ma, Y. Yang, D. L. Carnes, K. Kim, S. Park, S. H. Oh, and J. L. Ong, "Effects of dissolved calcium and phosphorous on osteoblast responses," *J Oral Implantol,* vol. 31, pp. 61-7, 2005.
[123] R. Marom, I. Shur, R. Solomon, and D. Benayahu, "Characterization of adhesion and differentiation markers of osteogenic marrow stromal cells," *J Cell Physiol,* vol. 202, pp. 41-8, Jan 2005.
[124] A. F. Parisi and B. L. Vallee, "Zinc metalloenzymes: characteristics and significance in biology and medicine," *Am J Clin Nutr,* vol. 22, pp. 1222-39, Sep 1969.
[125] J. Eberle, S. Schmidmayer, R. G. Erben, M. Stangassinger, and H. P. Roth, "Skeletal effects of zinc deficiency in growing rats," *J Trace Elem Med Biol,* vol. 13, pp. 21-6, Jul 1999.
[126] M. Ikeuchi, A. Ito, Y. Dohi, H. Ohgushi, H. Shimaoka, K. Yonemasu, and T. Tateishi, "Osteogenic differentiation of cultured rat and human bone marrow cells on the surface of zinc-releasing calcium phosphate ceramics," *J Biomed Mater Res A,* vol. 67, pp. 1115-22, Dec 15 2003.
[127] M. R. Kreke, W. R. Huckle, and A. S. Goldstein, "Fluid flow stimulates expression of osteopontin and bone sialoprotein by bone marrow stromal cells in a temporally dependent manner," *Bone,* vol. 36, pp. 1047-55, Jun 2005.
[128] A. S. Badami, M. R. Kreke, M. S. Thompson, J. S. Riffle, and A. S. Goldstein, "Effect of fiber diameter on spreading, proliferation, and differentiation of osteoblastic cells on electrospun poly(lactic acid) substrates," *Biomaterials,* vol. 27, pp. 596-606, Feb 2006.
[129] C. A. Gregory, W. G. Gunn, A. Peister, and D. J. Prockop, "An Alizarin red-based assay of mineralization by adherent cells in culture: comparison with cetylpyridinium chloride extraction," *Anal Biochem,* vol. 329, pp. 77-84, Jun 1 2004.
[130] M. Yamaguchi, S. Kishi, and M. Hashizume, "Effect of zinc-chelating dipeptides on osteoblastic MC3T3-E1 cells: activation of aminoacyl-tRNA synthetase," *Peptides,* vol. 15, pp. 1367-71, 1994.
[131] D. Beyersmann and H. Haase, "Functions of zinc in signaling, proliferation and differentiation of mammalian cells," *Biometals,* vol. 14, pp. 331-41, Sep-Dec 2001.

[132] M. Yamaguchi and T. Matsui, "Stimulatory effect of zinc-chelating dipeptide on deoxyribonucleic acid synthesis in osteoblastic MC3T3-E1 cells," *Peptides,* vol. 17, pp. 1207-11, 1996.
[133] Y. M. Shin, M. M. Hohman, M. P. Brenner, and G. C. Rutledge, "Experimental characterization of electrospinning: the electrically forced jet and instabilities," *Polymer,* vol. 42, pp. 9955-9967, Dec 2001.
[134] P. X. Ma, R. Zhang, G. Xiao, and R. Franceschi, "Engineering new bone tissue in vitro on highly porous poly(alpha-hydroxyl acids)/hydroxyapatite composite scaffolds," *J Biomed Mater Res,* vol. 54, pp. 284-93, Feb 2001.
[135] S. L. Hall, H. P. Dimai, and J. R. Farley, "Effects of zinc on human skeletal alkaline phosphatase activity in vitro," *Calcif Tissue Int,* vol. 64, pp. 163-72, Feb 1999.
[136] D. Chen, L. C. Waite, and W. M. Pierce, Jr., "In vitro effects of zinc on markers of bone formation," *Biol Trace Elem Res,* vol. 68, pp. 225-34, Jun 1999.
[137] M. Yamaguchi, H. Oishi, and Y. Suketa, "Stimulatory effect of zinc on bone formation in tissue culture," *Biochem Pharmacol,* vol. 36, pp. 4007-12, Nov 15 1987.
[138] N. Shimokawa and M. Yamaguchi, "Characterization of bone protein components with polyacrylamide gel electrophoresis: effects of zinc and hormones in tissue culture," *Mol Cell Biochem,* vol. 117, pp. 153-8, Nov 18 1992.
[139] E. Glasfeld, J. A. Landro, and P. Schimmel, "C-terminal zinc-containing peptide required for RNA recognition by a class I tRNA synthetase," *Biochemistry,* vol. 35, pp. 4139-45, Apr 2 1996.
[140] Z. J. Ma and M. Yamaguchi, "Stimulatory effect of zinc on deoxyribonucleic acid synthesis in bone growth of newborn rats: enhancement with zinc and insulin-like growth factor-I," *Calcif Tissue Int,* vol. 69, pp. 158-63, Sep 2001.
[141] M. Yamaguchi and M. Fukagawa, "Role of zinc in regulation of protein tyrosine phosphatase activity in osteoblastic MC3T3-E1 cells: zinc modulation of insulin-like growth factor-I's effect," *Calcif Tissue Int,* vol. 76, pp. 32-8, Jan 2005.
[142] A. Yamamoto, R. Honma, and M. Sumita, "Cytotoxicity evaluation of 43 metal salts using murine fibroblasts and osteoblastic cells," *J Biomed Mater Res,* vol. 39, pp. 331-40, Feb 1998.
[143] S. L. Ishaug, G. M. Crane, M. J. Miller, A. W. Yasko, M. J. Yaszemski, and A. G. Mikos, "Bone formation by three-dimensional stromal osteoblast culture in biodegradable polymer scaffolds," *J Biomed Mater Res,* vol. 36, pp. 17-28, Jul 1997.
[144] G. Wei and P. X. Ma, "Structure and properties of nano-hydroxyapatite/polymer composite scaffolds for bone tissue engineering," *Biomaterials,* vol. 25, pp. 4749-57, Aug 2004.
[145] H. Jeffery, "The preparation and characterisation of poly(lactide-co-glycolide) microparticles. I: Oil-in-water emulsion solvent evaporation," *International Journal of Pharmaceutics,* vol. 77, pp. 169-175, 1991.
[146] S. Gajjeraman, K. Narayanan, J. Hao, C. Qin, and A. George, "Matrix macromolecules in hard tissues control the nucleation and hierarchical assembly of hydroxyapatite," *J Biol Chem,* vol. 282, pp. 1193-204, Jan 12 2007.
[147] O. E. Petrov, E. Dyulgerova, L. Petrov, and R. Popova, "Characterization of calcium phosphate phases obtained during the preparation of sintered biphase Ca-P ceramics," *Materials Letters,* vol. 48, pp. 162-167, Apr 2001.
[148] T. Kajii, K. Suzuki, M. Yoshikawa, T. Imai, A. Matsumoto, and S. Nakamura, "Long-term effects of prostaglandin E2 on the mineralization of a clonal osteoblastic cell line (MC3T3-E1)," *Arch Oral Biol,* vol. 44, pp. 233-41, Mar 1999.

[149] R. Batzer, Y. Liu, D. L. Cochran, S. Szmuckler-Moncler, D. D. Dean, B. D. Boyan, and Z. Schwartz, "Prostaglandins mediate the effects of titanium surface roughness on MG63 osteoblast-like cells and alter cell responsiveness to 1 alpha,25-(OH)2D3," *J Biomed Mater Res,* vol. 41, pp. 489-96, Sep 5 1998.
[150] K. Nakashima, X. Zhou, G. Kunkel, Z. Zhang, J. M. Deng, R. R. Behringer, and B. de Crombrugghe, "The novel zinc finger-containing transcription factor osterix is required for osteoblast differentiation and bone formation," *Cell,* vol. 108, pp. 17-29, Jan 11 2002.
[151] Q. Tu, P. Valverde, and J. Chen, "Osterix enhances proliferation and osteogenic potential of bone marrow stromal cells," *Biochem Biophys Res Commun,* vol. 341, pp. 1257-65, Mar 24 2006.
[152] H. Sudo, H. A. Kodama, Y. Amagai, S. Yamamoto, and S. Kasai, "In vitro differentiation and calcification in a new clonal osteogenic cell line derived from newborn mouse calvaria," *J Cell Biol,* vol. 96, pp. 191-8, Jan 1983.
[153] C. A. Bashur, L. A. Dahlgren, and A. S. Goldstein, "Effect of fiber diameter and orientation on fibroblast morphology and proliferation on electrospun poly(D,L-lactic-co-glycolic acid) meshes," *Biomaterials,* vol. 27, pp. 5681-8, Nov 2006.
[154] A. S. Goldstein, "Effect of seeding osteoprogenitor cells as dense clusters on cell growth and differentiation," *Tissue Eng,* vol. 7, pp. 817-27, Dec 2001.
[155] K. D. Kavlock, T. W. Pechar, J. O. Hollinger, S. A. Guelcher, and A. S. Goldstein, "Synthesis and characterization of segmented poly(esterurethane urea) elastomers for bone tissue engineering," *Acta Biomater,* Apr 4 2007.
[156] K. J. Livak and T. D. Schmittgen, "Analysis of relative gene expression data using real-time quantitative PCR and the 2(-Delta Delta C(T)) Method," *Methods,* vol. 25, pp. 402-8, Dec 2001.
[157] M. R. Kreke, L. A. Sharp, Y. W. Lee, and A. S. Goldstein, "Effect of Intermittent Shear Stress on Mechanotransductive Signaling and Osteoblastic Differentiation of Bone Marrow Stromal Cells," *Tissue Eng Part A,* Feb 16 2008.
[158] K. K. Kaysinger and W. K. Ramp, "Extracellular pH modulates the activity of cultured human osteoblasts," *J Cell Biochem,* vol. 68, pp. 83-9, Jan 1 1998.
[159] D. H. Kohn, M. Sarmadi, J. I. Helman, and P. H. Krebsbach, "Effects of pH on human bone marrow stromal cells in vitro: implications for tissue engineering of bone," *J Biomed Mater Res,* vol. 60, pp. 292-9, May 2002.
[160] J. S. Sun, Y. H. Tsuang, C. J. Liao, H. C. Liu, Y. S. Hang, and F. H. Lin, "The effects of calcium phosphate particles on the growth of osteoblasts," *J Biomed Mater Res,* vol. 37, pp. 324-34, Dec 5 1997.
[161] C. H. Lohmann, D. D. Dean, G. Koster, D. Casasola, G. H. Buchhorn, U. Fink, Z. Schwartz, and B. D. Boyan, "Ceramic and PMMA particles differentially affect osteoblast phenotype," *Biomaterials,* vol. 23, pp. 1855-63, Apr 2002.